Doctoral Thesis

Towards an Efficient Development of High Performance Oxygenator Based CO_2 Removal

carried out for the purpose of obtaining the degree of

Doctor technicae (Dr. techn.)

submitted at TU Wien, Faculty of Mechanical and Industrial Engineering
by

Benjamin Lukitsch
Matr.Nr.: 1025868

under the supervision of
Ao.Univ.Prof. Dipl.-Ing. Dr.techn. Michael Harasek

at the
Institute of Chemical, Environmental and Bioscience Engineering
E166

reviewed by

Univ.Prof. Dipl.-Ing. Dr.techn.
Margit Gföhler
Institute of Engineering Design and Product Development
Technical University of Vienna
Getreidemarkt 9
1060 Vienna, Austria

Ao.Univ.Prof. Dr.
Roman Ullrich
Department of Anaesthesia, Intensive Care Medicine and Pain Medicine
Medical University of Vienna
Währinger Gürtel 18-20
1090 Vienna, Austria

Vienna, February 2022

_____
Benjamin Lukitsch

Die approbierte gedruckte Originalversion dieser Dissertation ist an der TU Wien Bibliothek verfügbar.
The approved original version of this doctoral thesis is available in print at TU Wien Bibliothek.

Die approbierte gedruckte Originalversion dieser Dissertation ist an der TU Wien Bibliothek verfügbar.
The approved original version of this doctoral thesis is available in print at TU Wien Bibliothek.

Examination committee

Supervisor:	Ao.Univ.Prof. Dipl.-Ing. Dr.techn. Michael Harasek
Reviewer 1:	Univ.Prof. Dipl.-Ing. Dr.techn. Margit Gföhler
Reviewer 2:	Ao.Univ.Prof. Dr. Roman Ullrich
Chairwoman:	Senior Scientist Dipl.-Ing. Dr.techn. Bettina Mihalyi

I confirm, that going to press of this thesis needs the confirmation of the examination committee.

Acknowledgement

This work was supported by Austrian Research Promotion Agency (FFG) within the framework of the project Minimal Invasive Liquid Lung (MILL). FFG project number: 857859.

Affidavit

I declare in lieu of oath, that I wrote this thesis and performed the associated research myself, using only literature cited in the volume. If text passages from sources are used literally, they are marked as such. I confirm that this work is original and has not been submitted elsewhere for any examination, nor is it currently under consideration for a thesis elsewhere.

I acknowledge that the submitted work will be checked electronically-technically using suitable and state-of-the-art means (plagiarism detection software). On the one hand, this ensures that the submitted work was prepared according to the high-quality standards within the applicable rules to ensure good scientific practice "Code of Conduct" at the TU Wien. On the other hand, a comparison with other student theses avoids violations of my personal copyright.

Vienna, February 2022

_____

Benjamin Lukitsch

Die approbierte gedruckte Originalversion dieser Dissertation ist an der TU Wien Bibliothek verfügbar.
The approved original version of this doctoral thesis is available in print at TU Wien Bibliothek.
TU Bibliothek Your knowledge hub WIEN

Die approbierte gedruckte Originalversion dieser Dissertation ist an der TU Wien Bibliothek verfügbar.
The approved original version of this doctoral thesis is available in print at TU Wien Bibliothek.

Danksagung

Mein herzlichster Dank gilt allen, die mich im Zuge meines Doktorats unterstützt haben.

Allen voran möchte ich mich bei meinem Betreuer Michael Harasek bedanken. Er wirkte als Mentor, begleitete mich auf diesem Weg und erlaubte mir durch seinen unermüdlichen Einsatz eine sorgfältige und detaillierte Auseinandersetzung mit meinem Dissertationsthema.

Großer Dank gebührt auch meinen Studien- und Arbeitskollegen Paul Ecker, Martin Elenkov und Christoph Janeczek, die mich unterstützten, bei großen Herausforderungen zuversichtlich stimmten und mich immer zum Lachen bringen konnten. Ohne euch wäre diese Arbeit nicht möglich gewesen, ich bin froh euch als enge Freunde gewonnen zu haben!

Christian Jordan, Bahram Haddadi und Markus Bösenhofer halfen mir mit ihrer umfangreichen Erfahrung und ihrem Fachwissen. Danke, dass ihr euch so entgegenkommend und selbstlos meiner angenommen habt, danke für eure Zeit und Geduld!

Ein großes Dankeschön gilt meinen Freunden, derer ich mich so zahlreich glücklich schätzen kann. Mit euch zu lachen erlaubte mir diese große Herausforderung zu bewältigen. Leider kann ich nicht alle erwähnen und möchte doch keinen missen. Bitte wisst, ich denke an jede einzelne und jeden einzelnen, während ich diese Zeilen schreibe.

Zuletzt, aber an prominentester Stelle, möchte ich mich bei meiner Familie bedanken. Besonderer Dank gilt meinem Bruder und besten Freund, der mir immer mit Rat und Tat zur Seite steht und der mich öfter zum Lachen bringt, als es mir lieb ist. Meinem Vater, der mit großer Geduld immer für mich da ist und dessen bedingungsloser Unterstützung ich mir an jedem Tag gewiss sein kann. Meiner Mutter, ohne ihrer unermüdlichen Zuwendung und ihrem selbstlosen Einsatz wäre ich niemals so weit gekommen. Sowie meinen warmherzigen Großeltern, die mir jene Geborgenheit schenkten, die ich jedem wünsche.

Danke euch allen, ohne euch wäre ich nicht dort wo ich heute stehen darf!

Die approbierte gedruckte Originalversion dieser Dissertation ist an der TU Wien Bibliothek verfügbar.
The approved original version of this doctoral thesis is available in print at TU Wien Bibliothek.

TU Bibliothek Your knowledge hub
Die approbierte gedruckte Originalversion dieser Dissertation ist an der TU Wien Bibliothek verfügbar.
The approved original version of this doctoral thesis is available in print at TU Wien Bibliothek.

Abstract

Membrane oxygenators are medical devices used to support or take over the gas exchange of the natural lung. In modern oxygenators, the gas exchange surface is provided by a hollow fiber membrane packing. While blood is pumped through the shell side of the hollow fiber packing, O_2 is used to sweep the fiber lumen. CO_2 and O_2 are exchanged through the membrane following the partial pressure gradient. Consequently, blood is enriched with O_2 and purged from CO_2.

Initially, membrane oxygenators were developed to supplement the natural lung during cardiopulmonary bypass. Here, the oxygenator has to take over the total metabolically required O_2 and CO_2 transfer. With continuous development, oxygenators were applied as lung support to manage acute respiratory distress syndrome (ARDS). Patients suffering from ARDS are often treated with lung protective ventilation (LPV). While LPV allows sufficient O_2 transfer, the CO_2 removal is limited. The limited CO_2 removal evokes serious side effects such as upcoming hypercapnia and hypercapnic acidosis. Consequently, oxygenators are increasingly used to provide additional CO_2 removal during LPV to circumvent the mentioned side effects.

This doctoral research aims to improve the development process of oxygenator-based CO_2 removal. A particular focus is placed on the initial development phase, where the work is strongly characterized by engineering challenges such as design, assembly, and first basic performance tests. The development process shall be improved in two ways. First, by designing experimental campaigns that are simple, inexpensive, and reliable. Second, by developing numerically inexpensive and accurate computational fluid dynamic (CFD) methods for in-depth insights into the CO_2 separation process.

The fundament for efficient development of oxygenator-based CO_2 removal is an accurate measurement of the CO_2 removal rate. We compared the two available CO_2 removal rate determination methods, i.e., the determination based on CO_2 concentration decrease in the blood (blood-based) and the determination based on CO_2 concentration increase in the sweep flow (sweep flow-based). Our study shows that the sweep flow-based method performed superior with a CO_2 removal measurement error of 3 % of reading. This error lies significantly ($p < 0.05$) under the CO_2 removal measurement error of the blood-based method (16 % of reading).

Furthermore, blood mimicking fluids for the determination of the CO_2 removal rate of oxygenators were evaluated. While water tests are a common method to reduce experimental effort and avoid animal tests, its application limits and reliability have never been analyzed systematically in the literature. Consequently, we compared the CO_2 removal rate of blood and water at three pathological elevated CO_2 partial pressures (50, 70, 100 mmHg) and three blood flow rates commonly applied in blood oxygenation (1000, 1300, 1600 mL/min). Our experimental data shows an average 10 % deviation between the CO_2 removal rate of blood and water. The low deviation can be attributed to the opposing influences of the material properties of the two liquids. Using CFD simulations, we could quantify the contributions of the different material properties. Compared to water, the higher CO_2 solubility of blood and the accompanied increased CO_2 removal rate (+ 125 %) is in most parts compensated by the lower CO_2 diffusion rate of blood (- 53 %), followed by the lower CO_2 permeance available with blood (- 18 %) and the higher viscosity of blood (- 10 %).

Die approbierte gedruckte Originalversion dieser Dissertation ist an der TU Wien Bibliothek verfügbar.
The approved original version of this doctoral thesis is available in print at TU Wien Bibliothek.
TU Bibliothek Your knowledge hub WIEN

While this leads to comparable macroscopic CO_2 removal rates, we could elaborate that the boundary layer built up – the main CO_2 transport resistance in oxygenators – is fundamentally different between blood and water, i.e., the two liquids do not follow the same dimensionless mass transport analogy. Hence the use of water as a blood model should be limited to the macroscopic determination of the CO_2 removal rate and not be used in studies of the boundary layer. In addition to water as a CO_2 transport model, this work investigated aqueous and animal blood models as rheological models for blood.

While experimental data is most reliable, it is mainly limited to pointwise data at easily accessible locations. Computational fluid dynamic (CFD) simulations can extend this data. However, they are numerically expensive due to the highly refined computational mesh required to resolve the diffusive CO_2 transport in the membrane packing. Consequently, in the current literature, a gap between the geometric size scales of mass transfer and hydrodynamic simulations of oxygenator membrane packings can be recorded.

In order to bridge this gap, an up-scaling method was developed. It allows scaling the transmembrane transport predicted in species transport simulations of a reduced geometry on the geometrical scales of flow simulations. This is done by calculating velocity inlet conditions of the reduced geometry based on the average velocity within the complete packing determined via CFD flow simulations. By doing so, the flow distribution in the reduced geometry is representative of the flow regime within the complete packing. This was proven by comparing experimental and numerical results. The deviation between the experimentally determined and numerically predicted CO_2 removal rate of a prototype oxygenator amounts on average to 6 % for blood and 3 % for water.

As a further novelty, our CFD model for the species transport in blood oxygenators can resolve the CO_2 transport in the membrane wall and the fiber lumen. While the membrane wall resistance is often considered negligible in literature, we could show that membrane permeance can reduce to 22 % of its original value due to plasma leakage or pervaporation. CFD simulations show that this would result in a proportional decrease of the CO_2 removal rate. This is important since numerical overprediction of the CO_2 removal rate poses a risk of incorrect validation of CFD models.

In order to guarantee high accuracy of a CFD model, suitable models for the complex material properties of blood are required. In the scope of this work, models for two of the most relevant material properties in oxygenator-based CO_2 removal, CO_2 solubility of blood and viscosity of blood, were investigated. Based on our data, we can recommend a simple and reliable CO_2 solubility model proposed in the literature. Furthermore, viscosity models for ovine, bovine, equine, and porcine blood are presented as a function of shear rate, hematocrit, and temperature. Finally, a less complex CFD model based on the calculation of local Sherwood numbers was successfully tested. It allows to qualitatively assess different microstructures of hollow fiber membranes regarding their CO_2 transport resistance in blood.

To conclude, the research conducted in this doctoral thesis offers a solid foundation for designing reliable experimental and numerical investigations of oxygenator-based CO_2 removal. Due to the experimental findings and advances in CFD modeling, oxygenator-based CO_2 removal can be efficiently developed in the future.

Die approbierte gedruckte Originalversion dieser Dissertation ist an der TU Wien Bibliothek verfügbar.
The approved original version of this doctoral thesis is available in print at TU Wien Bibliothek.
TU Bibliothek Your knowledge hub WIEN

Kurzfassung

Membranoxygenatoren sind medizinische Geräte, die den Gasaustausch der natürlichen Lunge unterstützen oder übernehmen. Bei modernen Oxygenatoren wird die Gasaustauschfläche durch Hohlfasermembranpackungen bereitgestellt. Während Blut durch die Mantelseite der Hohlfaserpackung gepumpt wird, wird das Faserlumen mit O_2 gespült. CO_2 und O_2 diffundieren dabei den Partialdruckgradienten folgend durch die Membran.

Ursprünglich wurden Membranoxygenatoren entwickelt, um die Lunge während eines kardiopulmonalen Bypasses zu ersetzen. Dabei übernimmt der Oxygenator den gesamten metabolisch erforderlichen O_2- und CO_2-Transfer. Mit kontinuierlicher Weiterentwicklung wurden Oxygenatoren als Lungenunterstützung bei der Behandlung des akuten Atemnotsyndroms (engl. Acute Respiratory Distress Syndrome, ARDS) eingesetzt. Patienten, die an ARDS leiden, werden häufig mit lungenschonender Beatmung (engl. Lung Protective Ventilation, LPV) behandelt. Während die LPV einen ausreichenden O_2-Transfer ermöglicht, ist die CO_2-Abtrennung begrenzt. Um eine ausreichende CO_2-Abtrennung zu gewährleisten, werden daher zunehmend Oxygenatoren eingesetzt.

Insofern ist es das Ziel dieser Doktorarbeit, eine effizientere Entwicklung von Oxygenator-basierter CO_2-Abtrennung zu ermöglichen. Eine effiziente Weiterentwicklung der Oxygenator-basierten CO_2-Abtrennung soll dabei auf zwei Arten bewerkstelligt werden. Erstens, durch die Reduktion der Komplexität der Versuchskampagnen bei gleichbleibender Verlässlichkeit der erhobenen Daten. Zweitens, durch die Entwicklung von weniger rechenaufwändigen, jedoch präzisen Methoden der numerischen Strömungsmechanik (engl. Computational Fluid Dynamics, CFD).

Die Grundlage für eine effiziente Entwicklung der CO_2-Abtrennung mit Oxygenatoren ist eine exakte Messung der CO_2-Abfuhrrate. Im Zuge dieser Arbeit wurden die beiden verfügbaren Methoden zur Bestimmung der CO_2-Abfuhrrate verglichen. Die erste Methode basiert auf Grundlage der Abnahme der CO_2-Konzentration im Blut (Blut-basiert). Die zweite Methode basiert auf Grundlage der Zunahme der CO_2-Konzentration im Spülgas des Oxygenators (Spülgas-basiert). Unsere Studie zeigt, dass die Spülgas-basierte Methode mit einem Messfehler von 3 % der gemessenen CO_2-Abtrennrate besser abschneidet. Dieser Fehler liegt signifikant ($p < 0{,}05$) unter dem Messfehler der Blut-basierten Methode (16 % des Messwerts).

Außerdem wurde Wasser als Blutersatz für die Bestimmung der CO_2-Abtrennrate von Oxygenatoren untersucht. Obwohl Wasser ein gängiger Blutersatz ist, um den experimentellen Aufwand und Tierleid zu verringern, wurde dessen Anwendungsgrenze und Zuverlässigkeit in der Literatur noch nicht systematisch analysiert. Daher haben wir die CO_2-Abfuhrrate von Blut und Wasser bei drei pathologisch erhöhten CO_2-Partialdrücken (50, 70, 100 mmHg) und drei Blutflussraten (1000, 1300, 1600 mL/min) verglichen. Unsere experimentellen Daten zeigen eine durchschnittliche Abweichung von 10 % zwischen der CO_2-Abfuhrrate von Blut und Wasser. Die geringe Abweichung kann auf die gegensätzlichen Einflüsse der Materialeigenschaften der beiden Flüssigkeiten zurückgeführt werden.

Mit Hilfe von CFD-Simulationen konnten wir die verschiedenen Beiträge der unterschiedlichen Materialeigenschaften quantifizieren. Die im Vergleich zu Wasser höhere CO_2-Löslichkeit von Blut und die damit einhergehende höhere CO_2-Abfuhrrate (+ 125 %) wird größtenteils durch die geringere CO_2-Diffusionsrate von Blut (- 53 %), gefolgt von

Die approbierte gedruckte Originalversion dieser Dissertation ist an der TU Wien Bibliothek verfügbar.
The approved original version of this doctoral thesis is available in print at TU Wien Bibliothek.
TU Bibliothek Your knowledge hub WIEN

der bei Blut vorliegenden geringeren CO_2-Permeanz (- 18 %) und der höheren Viskosität von Blut (- 10 %) kompensiert. Während dies zu richtigen makroskopischen CO_2-Abfuhrraten führt, konnten wir zeigen, dass die aufgebaute Grenzschicht – der größte CO_2-Transportwiderstand in Oxygenatoren – sich zwischen Blut und Wasser grundlegend unterscheidet. Die beiden Flüssigkeiten folgen insofern nicht der gleichen dimensionslosen Massentransportkorrelation. Daher sollte die Verwendung von Wasser als Blutmodell auf die makroskopische Bestimmung der CO_2-Abfuhrrate beschränkt sein und nicht für Untersuchungen der Grenzschicht verwendet werden. Neben Wasser als CO_2-Transportmodell wurden in dieser Arbeit zudem auch wässrige Lösungen und Tierblut als rheologische Modelle für Blut untersucht.

Während experimentelle Daten am zuverlässigsten sind, beschränken sie sich meist auf punktuelle Werte an leicht zugänglichen Stellen. CFD Simulationen können diese Daten erweitern, sind jedoch aufgrund des feinen Rechengitters, das zur Auflösung des diffusiven CO_2-Transports in der Membranpackung erforderlich ist, numerisch aufwendig.

Daher ist in der aktuellen Literatur eine Lücke zwischen den geometrischen Größenskalen von Stofftransportsimualtionen und hydrodynamischen Simulationen von Oxygenatormembranpackungen zu verzeichnen. Um diese Lücke zu schließen, wurde eine Up-Scaling-Methode entwickelt. Sie ermöglicht es, den transmembranen Transport, der auf Basis von Stofftransportsimulationen einer reduzierten Geometrie berechnet wurde, auf die geometrischen Größenskalen von hydrodynamischen Strömungssimulationen zu skalieren. Die durchschnittliche Abweichung zwischen experimentell ermittelter und durch die Up-Scaling-Methode numerisch vorhergesagter CO_2-Abfuhrrate eines Prototyp-Oxygenators beträgt im Mittel 6 % für Blut und 3 % für Wasser.

Als weitere Besonderheit ist unser CFD-Modell in der Lage, den CO_2-Transport in der Membranwand und dem Faserlumen aufzulösen. Während der Membranwandwiderstand in der Literatur oft als vernachlässigbar angesehen wird, konnten wir zeigen, dass die Permeanz aufgrund des Eindringens von Blutplasma auf 22 % ihres ursprünglichen Wertes sinken kann. CFD-Simulationen zeigen, dass dies zu einer direkt proportionalen Abnahme der CO_2-Abfuhrrate führen würde.

Um eine hohe Genauigkeit eines CFD-Modells zu gewährleisten, sind außerdem geeignete Modelle für die komplexen Materialeigenschaften von Blut erforderlich. Im Rahmen dieser Arbeit wurden zwei der relevantesten Materialeigenschaften, die CO_2-Löslichkeit und die Viskosität des Blutes untersucht. Auf der Grundlage unserer Daten können wir ein einfaches und zuverlässiges CO_2-Löslichkeitsmodell empfehlen. Darüber hinaus wurden Viskositätsmodelle für Schaf-, Rinder-, Pferde- und Schweineblut in Abhängigkeit von der Scherrate, dem Hämatokrit und der Temperatur entwickelt. Abschließend wurde ein CFD-Modell mit reduzierter Komplexität, das auf der Berechnung lokaler Sherwood-Zahlen basiert, erfolgreich getestet. Es erlaubte den Einsatz von mikrostrukturierten Hohlfasermembranen in Oxygenatormembranpackungen hinsichtlich des CO_2-Transportwiderstandes im Blut qualitativ zu bewerten.

Fazit: Die in dieser Dissertation durchgeführten Arbeiten stellen eine solide Grundlage für die Planung von experimentellen und numerischen Untersuchungen der CO_2-Abtrennleistung von Oxygenatoren dar. Basierend auf den experimentellen Erkenntnissen sowie den Fortschritten in der CFD-Modellierung kann in Zukunft eine erfolgreiche und effiziente Entwicklung der Oxygenator-basierten CO_2-Abtrennung erreicht werden.

Die approbierte gedruckte Originalversion dieser Dissertation ist an der TU Wien Bibliothek verfügbar.
The approved original version of this doctoral thesis is available in print at TU Wien Bibliothek.
TU Bibliothek Your knowledge hub WIEN

Contents

Danksagung iii
Abstract v
Kurzfassung vii
Contents ix
List of Appended Publications xiii
Journal Publications xiii
Reviewed Conference Publications xv
Author's Contribution xvi
Journal Publications xvi
Reviewed Conference Publications xvii
1 Introduction 1
1.1 Motivation 1
1.2 Objectives 2
1.2.1 Experimental Objectives 2
1.2.2 Computational Fluid Dynamic Objectives 3
1.3 Review State of the Art 3
1.3.1 State of the Art Oxygenator Based CO_2 Removal Devices 3
1.3.1.1 Intravascular respiratory catheter 4
1.3.1.2 Extracorporeal CO_2 removal 5
1.3.1.3 Coating and Membrane Materials 7
1.3.1.4 Microfluidic Membrane Oxygenators 8
1.3.1.5 Respirator dialysis 8
1.3.2 State of the Art Experimental Investigations 8
1.3.2.1 Determination of CO_2 Removal Rate 9
1.3.2.2 Rheological Models for Blood 11
1.3.2.3 CO_2 Transport Models for Blood 12
1.3.3 State of the Art Numerical Investigations 14
1.3.3.1 Dimensionless Sherwood Correlations 14
1.3.3.2 Computational Fluid Dynamic Methods 15
2 Methods 17
2.1 Experimental Methods 17
2.1.1 Gas Permeation Test 18
2.1.2 In Vitro Water Tests 19

Die approbierte gedruckte Originalversion dieser Dissertation ist an der TU Wien Bibliothek verfügbar.
The approved original version of this doctoral thesis is available in print at TU Wien Bibliothek.
TU Bibliothek Your knowledge hub WIEN

2.1.3 In Vitro Bovine Blood Tests 19
2.1.4 In Vivo Porcine Blood Tests 20
2.1.5 Viscosity Measurements 22
2.1.6 Assessment of the CO_2 Solubility Models for Blood 22
2.1.7 Statistical Testing 23
2.1.8 Gas Exchange Catheter Tests – Minimal Invasive Liquid Lung (MILL) 23
2.1.8.1 Flow Distribution Tests 24
2.1.8.2 Viscosity Estimation Tests 24
2.2 Computational Fluid Dynamic Methods 25
2.2.1 Governing Transport Equations 25
2.2.2 Implementation of Transmembrane Transport 26
2.2.3 Discretization Schemes 26
2.2.4 Computational Mesh 26
2.2.4.1 Computational Mesh of the Prototype Oxygenator 26
2.2.4.2 Computational Mesh of the Membrane Packing 28
2.2.5 Solver 29
2.2.6 Upscaling Method 30
2.2.7 Material Properties Blood 31
2.2.7.1 Viscosity 31
2.2.7.2 CO_2 Solubility 32
2.2.7.3 CO_2 Diffusion Coefficient 32
2.2.8 Material Properties Water 33
2.2.8.1 Viscosity 33
2.2.8.2 CO_2 Diffusion Coefficient 33
2.2.8.3 CO_2 Solubility 34
2.2.9 Material Properties Sweep Gas 34
2.2.9.1 Viscosity 34
2.2.9.2 CO_2 Diffusion Coefficient 34
2.2.9.3 CO_2 Solubility 34
2.3 Alternative Modeling Approaches – Computation of Sherwood Number 35
2.3.1 Sherwood Mass Transfer Correlation 35
2.3.2 Simplified CFD Model 35
3 Publication Summary 37
3.1 Journal Publication Summary 37
3.1.1 Journal Publication I 37

Die approbierte gedruckte Originalversion dieser Dissertation ist an der TU Wien Bibliothek verfügbar.
The approved original version of this doctoral thesis is available in print at TU Wien Bibliothek.
TU Bibliothek Your knowledge hub WIEN

3.1.2 Journal Publication II 37
3.1.3 Journal Publication III 38
3.1.4 Journal Publication IV 38
3.1.5 Journal Publication V 39
3.1.6 Journal Publication VI 39
3.1.7 Journal Publication VII 40
3.1.8 Journal Publication VIII 40
3.2 Reviewed Conference Publication Summary 41
3.2.1 Reviewed Conference Publication I 41
4 Summary and Discussion 42
4.1 Summary and Discussion of Experimental Results 42
4.1.1 Water-Based Hydrodynamic Models 42
4.1.2 Water-Based CO_2 Transport Models 44
4.1.3 Animal Blood Models for Hydrodynamic Models 44
4.1.4 Animal Blood Models for CO_2 Transport 45
4.1.5 Measurement of CO_2 Removal Performance 46
4.1.6 Measurement of CO_2 Permeance Before and After Trials 47
4.1.7 Measurement of O_2 and CO_2 for Data Validation 48
4.1.8 Thrombus Formation 48
4.2 Summary and Discussion of Computational Fluid Dynamic Results 48
4.2.1 CO_2 Solubility Model 48
4.2.2 Blood Viscosity Models for Animal Blood 50
4.2.3 Implementation of Computational Fluid Dynamic Model 50
4.2.4 Upscaling Method 52
4.2.5 Investigation of Concentration Polarization Layer 54
4.2.6 Alternative Modeling Approaches – Computation of Sherwood Number 56
5 Conclusion and Outlook 58
References 61
Appended Publications 71
Journal Publication I 72
Journal Publication II 73
Journal Publication III 74
Journal Publication IV 75
Journal Publication V 76
Journal Publication VI 77

Die approbierte gedruckte Originalversion dieser Dissertation ist an der TU Wien Bibliothek verfügbar.
The approved original version of this doctoral thesis is available in print at TU Wien Bibliothek.
TU Bibliothek Your knowledge hub WIEN

Journal Publication VII 78
Journal Publication VIII 79
Reviewed Conference Publication I 80
List of Figures 81
List of Tables 82
List of Symbols 83
List of Abbreviations 85

Die approbierte gedruckte Originalversion dieser Dissertation ist an der TU Wien Bibliothek verfügbar.
The approved original version of this doctoral thesis is available in print at TU Wien Bibliothek.
TU Bibliothek Your knowledge hub WIEN

List of Appended Publications

Journal Publications

Journal Publication I

Fully resolved computational (CFD) and experimental analysis of pressure drop and blood gas transport in a hollow fibre membrane oxygenator module.

Harasek, M., Lukitsch, B., Ecker, P., Janeczek, C., Elenkov, M., Keck, T., Haddadi, B., Jordan, C., Neudl, S., Krenn, C., Ullrich, R., & Gfoehler, M.

Chemical Engineering Transactions ***2019***, *76*, 193–198.

DOI: 10.3303/CET1976033

Journal Publication II

Computation of global and local mass transfer in hollow fiber membrane modules.

Lukitsch, B., Ecker, P., Elenkov, M., Janeczek, C., Haddadi, B., Jordan, C., Krenn, C., Ullrich, R., Gfoehler, M., Harasek, M.

Sustainability ***2020***.

DOI: 10.3390/su12062207

Journal Publication III

Estimation methods for viscosity, flow rate and pressure from pump-motor assembly parameters.

Elenkov, M., Ecker, P., Lukitsch, B., Janeczek, C., Harasek, M., Gföhler, M.

Sensors ***2020***.

DOI: 10.3390/s20051451

Journal Publication IV

Non-parametric dynamical estimation of blood flow rate, pressure difference and viscosity for a miniaturized blood pump.

Elenkov, M., Lukitsch, B., Ecker, P., Janeczek, C., Harasek, M., Gföhler, M.

International Journal of Artificial Organs ***2021***.

DOI: 10.1177/03913988211006720

Die approbierte gedruckte Originalversion dieser Dissertation ist an der TU Wien Bibliothek verfügbar.
The approved original version of this doctoral thesis is available in print at TU Wien Bibliothek.
TU Bibliothek Your knowledge hub WIEN

Journal Publication V

Microstructured hollow fiber membranes: Potential fiber shapes for extracorporeal membrane oxygenators.

Ecker, P., Pekovits, M., Yorov, T., Haddadi, B., Lukitsch, B., Elenkov, M., Janeczek, C., Jordan, C., Gfoehler, M., Harasek, M.

Membranes ***2021***.

DOI: 10.3390/membranes11050374

Journal Publication VI

Suitable CO_2 solubility models for determination of the CO_2 removal performance of oxygenators.

Lukitsch, B., Ecker, P., Elenkov, M., Janeczek, C., Jordan, C., Krenn, C.G., Ullrich, R., Gfoehler, M., Harasek, M.

Bioengineering ***2021***.

DOI: 10.3390/bioengineering8030033

Journal Publication VII

Animal blood in translational research: How to adjust animal blood viscosity to the human standard.

Ecker, P., Sparer, A., Lukitsch, B., Elenkov, M., Seltenhammer, M., Crevenna, R., Gföhler, M., Harasek, M., Windberger, U.

Physiological Reports ***2021***.

DOI: 10.14814/phy2.14880

Journal Publication VIII

Water as a blood model for determination of CO_2 removal performance of membrane oxygenators.

Lukitsch, B., Koller, R., Ecker, P., Elenkov, M., Janeczek, C., Pekovits, M., Haddadi, B., Jordan, C., Gfoehler, M., Harasek, M.

Membranes ***2021***.

DOI: 10.3390/membranes11050356

Die approbierte gedruckte Originalversion dieser Dissertation ist an der TU Wien Bibliothek verfügbar.
The approved original version of this doctoral thesis is available in print at TU Wien Bibliothek.

Reviewed Conference Publications

Reviewed Conference Publication I

Basic performance tests of the MILL intravascular CO_2 removal catheter.

Janeczek, C., Lukitsch, B., Huber-Dangl, F., Karabegovic, A., Jordan, C., Haddadi, B., Ullrich, R., Krenn, C., Gfoehler, M., Harasek, M.

*Proceedings of the Annual International Conference of the IEEE Engineering in Medicine and Biology Society, EMBS **2018**.*

DOI: 10.1109/EMBC.2018.8512522

Die approbierte gedruckte Originalversion dieser Dissertation ist an der TU Wien Bibliothek verfügbar.
The approved original version of this doctoral thesis is available in print at TU Wien Bibliothek.

Author's Contribution

Journal Publications

Journal Publication I

Benjamin Lukitsch developed the CFD model for the computation of CO_2 transport in blood, membrane, and sweep gas of oxygenators. He planned, conducted, and evaluated the in vitro blood tests in substantial parts, which were carried out to determine the CO_2 removal performance of a prototype oxygenator. He prepared and ran the flow simulations as well as validated them against the in vitro data. He wrote, reviewed, and edited the paper.

Journal Publication II

Benjamin Lukitsch developed the upscaling method, which allows the prediction of the CO_2 removal performance of oxygenators based on CO_2 transport simulations of a reduced geometry. He validated the upscaling method through in vivo experiments planned, carried out, and evaluated in substantial parts by him. He wrote, reviewed, and edited the paper.

Journal Publication III

Benjamin Lukitsch planned and conducted the in vitro water/glycerol tests in substantial parts. He reviewed and edited the paper.

Journal Publication IV

Benjamin Lukitsch planned and conducted the in vitro blood tests in substantial parts. He reviewed and edited the paper.

Journal Publication V

Benjamin Lukitsch advised on how to implement and assess the Sherwood number-based CFD method for the prediction of the CO_2 removal performance of oxygenators. Furthermore, he provided a highly accurate computational mesh to validate CFD flow simulations with micro-particle image velocimetry data. He reviewed and edited the paper.

Die approbierte gedruckte Originalversion dieser Dissertation ist an der TU Wien Bibliothek verfügbar.
The approved original version of this doctoral thesis is available in print at TU Wien Bibliothek.
TU Bibliothek Your knowledge hub WIEN

Journal Publication VI

Benjamin Lukitsch planned and conducted the in vitro and in vivo blood tests and the in vitro water tests in substantial parts. Furthermore, he played an essential role in the curation and analysis of the experimental data. He compared and discussed the performance of the different CO_2 solubility models for blood. He wrote, reviewed, and edited the paper.

Journal Publication VII

Benjamin Lukitsch advised on the development of the blood viscosity models, which allow considering the dependency of blood flow behavior on hematocrit, temperature, and shear rate. He reviewed and edited the paper.

Journal Publication VIII

Benjamin Lukitsch planned and conducted the in vitro water tests in substantial parts. He advised regarding the CFD model, which allows resolving the CO_2 concentration polarization at the oxygenator membrane in water and blood. He compared and analyzed experimental and computational findings. He developed the presented guidelines for using water as a blood substitute in the development of oxygenators. He wrote, reviewed, and edited the paper.

Reviewed Conference Publications

Reviewed Conference Publication I

Benjamin Lukitsch planned and carried out the in vitro water tests in substantial parts. He conducted the CFD for a further flow analysis of the developed CO_2 removal catheter. Furthermore, he played an essential role in the curation and analysis of the experimental data. He wrote, reviewed, and edited the paper in significant parts.

Die approbierte gedruckte Originalversion dieser Dissertation ist an der TU Wien Bibliothek verfügbar.
The approved original version of this doctoral thesis is available in print at TU Wien Bibliothek.

Die approbierte gedruckte Originalversion dieser Dissertation ist an der TU Wien Bibliothek verfügbar.
The approved original version of this doctoral thesis is available in print at TU Wien Bibliothek.

1 Introduction

1.1 Motivation[1]

Membrane oxygenators are medical devices that support or take over the gas exchange of the natural lung. While in the natural lung, the gas exchange surface is provided by the alveolar membrane [1], modern oxygenators use hollow fiber membrane packings. Here blood is pumped along the shell side of the hollow fiber packing, while the fiber lumen are swept with O_2. According to the CO_2 partial pressure gradients, CO_2 and O_2 are exchanged via the hollow fiber wall serving as a membrane. Consequently, the blood passing along the membrane is enriched with O_2 provided from the sweep flow in the lumen while depleting parts of its CO_2 content. While the oxygenated blood is returned to the patient, the purged CO_2 is discharged to the ambient via the sweep flow [2].

Initially, membrane oxygenators were developed as lung supplements in the cardiopulmonary bypass (e.g., during heart surgery). Here, blood is pumped from the inferior or superior vena cava, via a centrifugal pump, through the oxygenator and back into the ascending aorta. In cardiopulmonary bypass, the oxygenator has to take over the total metabolically required O_2 and CO_2 transfer of 250 and 200 mL/min, respectively [3].

The continuous development of oxygenators allowed an increase in gas transfer rates with a simultaneous reduction in bleeding complications. This was the basis for the application of oxygenators for partial lung support in the treatment of acute respiratory distress syndrome (ARDS) [4]. Patients suffering from ARDS are often treated with lung-protective ventilation (LPV). This ventilation method uses limited tidal volumes and decreased airway pressures to prevent lung damage [5] induced by exceeding transpulmonary pressure (barotrauma), overextension of alveoli (volutrauma), or increased shear stresses in pneumatic accessible but atelectatic alveoli (atelectrauma) [6]. Due to the pneumatic limitation of LPV, the lower gas transfer rates can only be increased by increasing the driving force (partial pressure difference) between respiration gas and blood. For a sufficiently high O_2 transfer rate, O_2 concentration (i.e., partial pressure) in the respiration gas can be increased. In contrast, an increase in the CO_2 partial pressure difference between blood and respiration gas, which breaks down to a reduction of the CO_2 concentration in the respiration gas, is only possible to a small extent. Hence, CO_2 removal via LPV is limited. This can evoke serious side effects such as upcoming hypercapnia and hypercapnic acidosis. To circumvent these side effects, oxygenators are used to provide additional CO_2 removal [7].

The CO_2 concentration of venous blood with approximately 500 mL CO_2/L is high. Hence, the total metabolic CO_2 production (200 mL/min) can be potentially eliminated by removing a 500 mL/min venous blood flow of its CO_2 content [8]. Due to the relatively low blood flow rates required for this potential total CO_2 removal, various vascular access points are applicable [9].

Depending on the used blood flow rates and incorporated membrane area of the oxygenator, total or partial CO_2 removal can be established. In order to strive for minimally invasive methods, intracorporal CO_2 removal catheters are under research [10].

[1] Due to the thematic proximity of this cumulative dissertation and the publications included therein, this section is based on the review of **Publication VI** and **Publication VIII**.

Die approbierte gedruckte Originalversion dieser Dissertation ist an der TU Wien Bibliothek verfügbar.
The approved original version of this doctoral thesis is available in print at TU Wien Bibliothek.
TU Bibliothek Your knowledge hub WIEN

Despite significant efforts to increase the biocompatibility of the oxygenator circuits [11], serious side effects are still occurring due to the extensive contact of blood with the polymer surfaces. These side effects lead to an activation of the immune response, including the complement pathways, neutrophils, and the fibrinolytic cascade. These reactions ultimately reduce platelet function and survival and prolonged bleeding times after perfusion [12]. Due to the severe side effects of the large artificial surfaces, current research focuses on increasing gas transfer rates while simultaneously decreasing membrane area and priming volume [13]. Here, oxygenator-based CO_2 removal is of particular interest due to the wide variety of applications such as arteriovenous, venovenous, total, partial, extracorporeal, and intracorporeal CO_2 removal.

1.2 Objectives

This doctoral research aims to enable more efficient development of oxygenators regarding their CO_2 separation performance. A particular focus is placed on the initial development phase, in which the work is strongly characterized by engineering challenges such as design, assembly, and first basic performance tests. This is to be achieved in two ways. First, by investigating how to design experimental campaigns to be simple but reliable. Second, by developing less numerical expensive but accurate computational fluid dynamic (CFD) methods for detailed insights into the CO_2 separation process.

1.2.1 Experimental Objectives

The following objectives were set to reduce complexity and improve the reliability of experimental methods:

i. Water-based rheological models for human blood shall be evaluated for assessment of the hydrodynamic performance of oxygenator prototypes [**Journal Publication III**].
ii. Water-based CO_2 transport models for human blood shall be evaluated to assess the CO_2 removal performance of oxygenator prototypes [**Journal Publication VIII**].
iii. Animal blood of different species shall be evaluated regarding their suitability as a rheologic model for human blood [**Journal Publication VII**].
iv. Animal blood of different species shall be evaluated regarding their suitability as a CO_2 transport model for human blood.
v. The two available methods for determining the CO_2 removal performance of oxygenators (blood-based and sweep flow-based method – Section 1.3.2.1) shall be compared and evaluated regarding their accuracy [**Journal Publication VI**].
vi. A possible decrease in CO_2 transport performance of the oxygenator membrane due to deposition of blood residues on the membrane surface or wetting of the membrane pores shall be investigated.

Die approbierte gedruckte Originalversion dieser Dissertation ist an der TU Wien Bibliothek verfügbar.
The approved original version of this doctoral thesis is available in print at TU Wien Bibliothek.
TU Bibliothek Your knowledge hub WIEN

1.2.2 Computational Fluid Dynamic Objectives

The following objectives were set to reduce numerical costs and improve the accuracy of computational fluid dynamic (CFD) methods:

i. CO_2 solubility models for blood shall be evaluated regarding their accuracy and suitability for CFD models [**Journal Publication VI**].
ii. Blood viscosity models of different animal species shall be derived for more accurate validation of CFD models using animal trials [**Journal Publication VII**].
iii. A CFD model shall be developed that fully resolves the blood side, membrane wall, and lumen of an oxygenator membrane packing. The common assumption that gas transport resistance in the membrane of an oxygenator can be neglected in CFD shall be investigated [**Journal Publication I**].
iv. An upscaling method that substantially reduces the computational effort of CFD mass transport simulations of oxygenators shall be developed [**Journal Publication II**].
v. The main transport resistance – the concentration polarization layer – shall be numerically investigated since it can not be resolved experimentally. CO_2 concentration polarization of blood and water shall be compared to establish application limits for water as a CO_2 transport model for blood [**Journal Publication VIII**].
vi. A less complex CFD model omitting gas transport in membrane wall and lumen shall be tested. Blood side gas transport resistance shall be qualitatively predicted based on local Sherwood numbers [**Journal Publication V**].

1.3 Review State of the Art[2]

This section reviews the state of the art in the development of oxygenator-based CO_2 removal. First, recent research on new prototype devices is presented. Second, the main concepts and approaches of experimental and numerical methods for developing oxygenator-based CO_2 removal are reviewed.

1.3.1 State of the Art Oxygenator Based CO_2 Removal Devices

This section gives an overview (Figure 1.1) on intravascular, para-, and extracorporeal devices for oxygenator-based CO_2 removal that have been developed or are under development. For further details on the single devices, we recommend Federspiel et al. [3], [10], Kaushik et al. [8], and the references given in Table 1.1, Table 1.2, and Table 1.3.

[2] Due to the thematic proximity of this cumulative dissertation and the publications included therein, this section is based on the review of **Publication I**, **Publication II**, **Publication VI** and **Publication VIII**.

Die approbierte gedruckte Originalversion dieser Dissertation ist an der TU Wien Bibliothek verfügbar.
The approved original version of this doctoral thesis is available in print at TU Wien Bibliothek.
TU Bibliothek Your knowledge hub WIEN

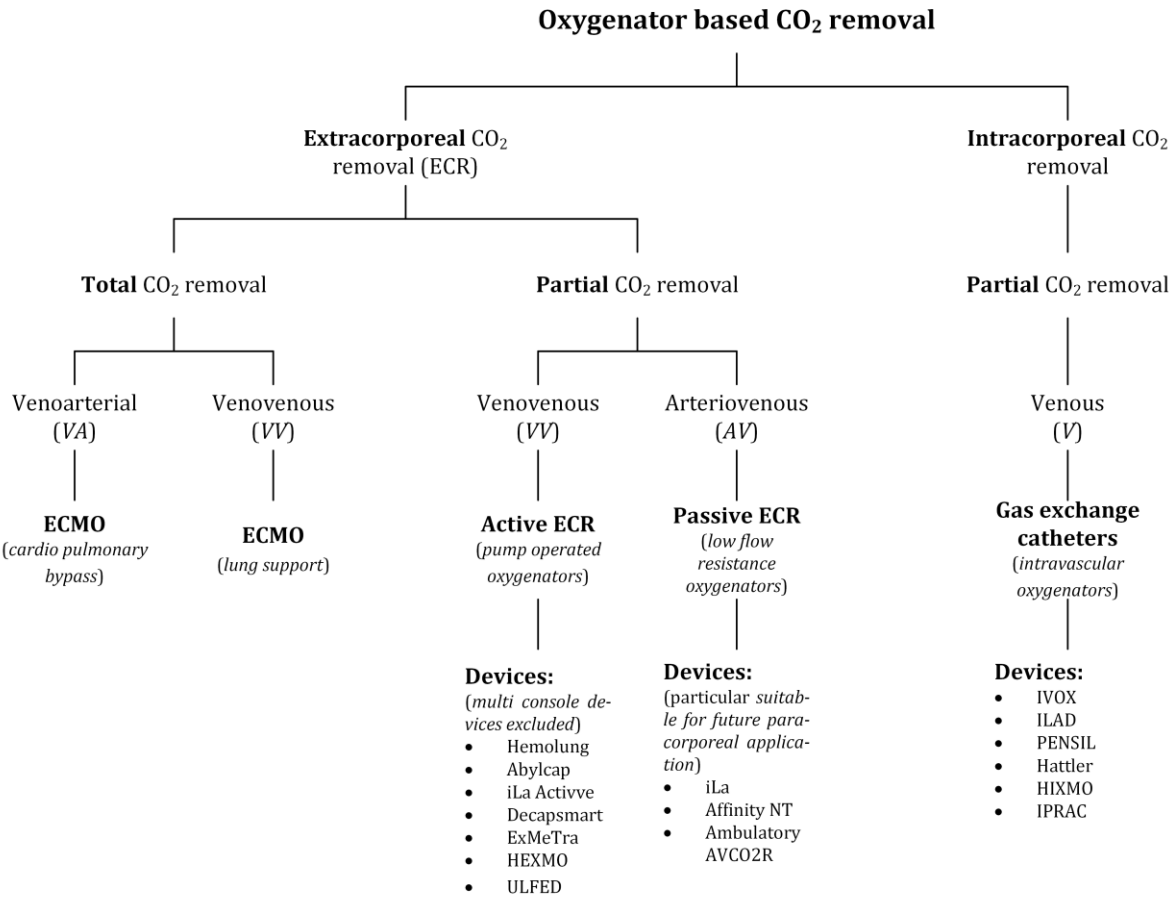

Figure 1.1. Schematic overview of devices for oxygenator based CO_2 removal adapted from [8].

1.3.1.1 Intravascular respiratory catheter

Research on the development of intravascular respiratory catheters has been conducted since the 1980s. An overview is given in Table 1.1. Intravascular respiratory catheters aim for partial lung support during LPV. However, the final goal is to develop a wearable and mobile device [10]. Up today, only one catheter (IVOX) was tested in clinical trials. It consists of a fiber module inserted into the vena cava. Crimped fibers ensure equal spacing between fibers. It is ambiguous whether the IVOX provided sufficient gas exchange to allow the reduction of mechanical ventilation [14]–[17].

The IVOX was further augmented by introducing a pulsating balloon into the packing (Hattler catheter). Pulsation of the balloon provided active mixing and a reduction of the concentration polarization layer. An increase of CO_2 exchange by a factor of 3 was achieved when compared to the IVOX. However, the development of the Hattler catheter never went past in vivo trials [18]–[20]. In the latest development step (IPRAC), the balloon of the Hattler catheter is substituted by a rotating impeller. The best performing prototype achieved a satisfactory specific CO_2 removal of 573 mL/min/m² in in vitro water tests [21], [22].

Further catheter prototypes of other research groups are ILAD, PENSIL, and HIXMO. The ILAD consists of a membrane module resembling a bottle brush. Hollow fiber membranes short in length are attached on both ends to a central shaft forming a loop. In the longitudinal direction, these fiber loops are positioned in a helix structure. The shaft is then rotated in order to disturb the built-up of concentration polarization layer and to

Die approbierte gedruckte Originalversion dieser Dissertation ist an der TU Wien Bibliothek verfügbar.
The approved original version of this doctoral thesis is available in print at TU Wien Bibliothek.
TU Bibliothek Your knowledge hub WIEN

assist blood transport in the vena cava [23]–[25]. While rotation of the membrane module allowed increased gas exchange in in vitro trials, it remains unclear whether a rotating membrane module is feasible in the vena cava without causing harm to the patient [10].

The PENSIL is a respiratory gas exchange catheter that, similar to IVOX and ILAD, only consists of a membrane module. In contrast to the other devices, the fiber lumen of the PENSIL have a dead-end. In order to increase gas transport in the lumen, pulsating sweep gas flow was applied. However, the PENSIL achieved relatively low specific CO_2 removal rates of 25 mL/min/m² [26]–[28].

The membrane module of the HIXMO consists of several disc-shaped fiber bundles. They can be expanded after the insertion of the catheter into the vena cava. This positions the hollow fibers in crossflow mode, favorable for a reduction of concentration polarization layer. In addition to a membrane module, the HIXMO catheter incorporates a miniature pump. The pump compensates for the increased flow resistance generated by the expanded fiber bundle [29]–[31].

Table 1.1. Overview of the intravascular respiratory catheter.

Device	Design Characteristics	Membrane Area [m²]	CO_2 Flux [mL/min/m²]	Status	Ref.
IVOX (CardioPulmonics, Inc., Salt Lake City, UT, USA)	crimped fiber module in vena cava	0.25	200	halted after first clinical trials	[14]–[17]
ILAD (Northwestern University, Evanston, IL; USA)	fiber module (resembling a bottle brush) rotating in vena cava	0.29	172	halted after in vitro bovine blood trials	[23]–[25]
PENSIL (Penn State University, State College, PA, USA)	fiber module (resembling a bottle brush) with dead-end fibers in vena cava, pulsating sweep gas	0.38	25	halted after in vitro trials	[26]–[28]
Hattler (McGowan Institute for Regenerative Medicine, Pittsburgh, PA, USA)	membrane module with central pulsating pump	0.38	350	halted after in vivo trials	[18]–[20]
HIXMO (RWTH Aachen University, Aachen, Germany)	series of disc-shaped fiber bundles in crossflow configuration, miniature pump to provide blood flow	not defined at the current stage	only O_2 transfer available	in vitro porcine blood tests of a single bundle	[29]–[31]
IPRAC (McGowan Institute for Regenerative Medicine, Pittsburgh, PA, USA)	membrane module with central impeller	0.07	573	in vitro water trials	[21], [22]

1.3.1.2 Extracorporeal CO_2 removal

Extracorporeal CO_2 removal (ECR) can be implemented via various vascular access routes. The venoarterial route (VA) is commonly used for total cardiopulmonary support during cardiopulmonary bypass. It poses high risks due to the access of major arteries. Furthermore, there is a lack of pulmonary perfusion, a decreased cardiac output due to a higher afterload, and an increased risk of neurological events caused by thrombi traveling from the ECMO to the brain [3].

Due to the arteriovenous pressure gradient, arteriovenous (AV) ECR allows for the use of membrane oxygenators without applying a blood pump. This reduces the aperitive complexity of the circuit. However, the blood flow rate through the oxygenator is defined

Die approbierte gedruckte Originalversion dieser Dissertation ist an der TU Wien Bibliothek verfügbar.
The approved original version of this doctoral thesis is available in print at TU Wien Bibliothek.
TU Bibliothek Your knowledge hub WIEN

by the arteriovenous pressure gradient and the flow resistance of the membrane oxygenator. Hence, oxygenators with low flow resistance and the absence of cardiac impairments are required. While adequate CO_2 removal can be achieved by increasing the sweep gas flow rates, only mild oxygenation occurs due to the limited blood flow rates [10].

Venovenous (VV) ECR poses multiple advantages over VA-ECR. Pulsatility of the blood flow and lung perfusion can be sustained. No major artery must be cannulated, and neurological events can be circumvented since thrombi can be captured in the natural lung before traveling into the brain [3].

Table 1.2 and Table 1.3 provide an overview of ECR devices currently under research. Besides VA-ECR devices (Table 1.2) with low flow resistance, which require no pump (iLa, Affinity NT), it can be differentiated between single- and multi-console VV-ECR devices (Table 1.3). Since multi-console VV-ECR can be implemented via normal commercially available extracorporeal membrane oxygenators (ECMO) combined with a commercial blood pump, only VV single-console devices are included in Table 1.3.

VV single-console devices can be differentiated regarding the integration of the blood pump. Single-console devices where blood pump and membrane module are connected in series (iLA Activve) pose no advantage to VV multi-console devices other than reduced complexity in the handling of the circuit. In comparison, the centrifugal pump of the HEXMO is positioned close to the membrane packing and can substantially characterize the flow distribution between fibers. In the ExMeTra device, silicone tubes are incorporated into the packing. Pneumatic pulsation of the silicon tubes in combination with automatic blood valves provides blood flow rates of up to 500 mL/min and promotes mixing inside the membrane packing.

Table 1.2. Overview of arteriovenous (AV) paracorporeal CO_2 removal devices.

Device	Design Characteristics	Membrane Area [m^2]	CO_2 Flux [$mL/min/m^2$]	Status	Ref.
iLA (Novalung GmbH, Hechingen, Germany)	membrane packing with low flow resistance, no pump required (no cardiac disorders)	1.3	154	commercially available	[32], [33]
Affinity NT (Medtronic, Minneapolis, Minn., USA)	membrane packing with low flow resistance, no pump required (no cardiac disorders)	2.5	60	commercially available	[34]
Ambulatory-AVCO2R (University of Texas Medical Branch, Galveston, TX, USA supported by MC3 Cardiopulmonary, Dexter, MI, USA)	ambulatory CO_2 removal for COPD patients	2.0	53	ex vivo trials with sheep	[35]

Die approbierte gedruckte Originalversion dieser Dissertation ist an der TU Wien Bibliothek verfügbar.
The approved original version of this doctoral thesis is available in print at TU Wien Bibliothek.
TU Bibliothek Your knowledge hub WIEN

Table 1.3. Overview of venovenous (VV) extracorporeal CO_2 removal (ECR) devices.

Device	Design Characteristics	Membrane Area [m^2]	CO_2 Flux [mL/min/m^2]	Status	Ref.
Hemolung (ALung Technologies, Inc., Pittsburg, PA, USA)	membrane module with integrated centrifugal pump	0.53	189	FDA Emergency Use Authorization 2020	[36]
Abylcap (BELLCO, Italy – now Medtronic)	single console-device	0.67	-	First clinical studies	[37]
iLa Activve (Novalung GmbH, Hechingen, Germany)	centrifugal blood pump and membrane module in series (3 times higher flows than iLa)	1.3	-	commercially available	[38]
Decapsmart (Hemodec, Salerno, Italy)	modified renal replacement circuit incorporating a peristaltic pump and a neonatal ECMO coupled in series with a hemofilter	0.33	-	commercially available	[39], [40]
ExMeTra (RWTH Aachen University, Aachen, Germany)	low flow membrane module with pulsatile pump incorporated in the packing	0.24	129	porcine blood in vitro trials	[41], [42]
HEXMO (RWTH Aachen University, Aachen, Germany and supported by Novalung GmbH, Hechingen, Germany)	membrane module with low priming volume and integrated pump	0.9	166	in vivo porcine blood trials	[43]
ULFED (Department of Critical Care Medicine, University of Pittsburgh Medical Center, Pittsburgh, PA, USA supported by ALung Technologies, Inc., Pittsburg, PA, USA)	low flow membrane module with integrated central impeller	0.42	179	in vitro bovine blood	[44]

1.3.1.3 Coating and Membrane Materials

In order to improve gas transfer, reduce side effects caused by the blood-surface interaction, and prevent plasma leakage, different membrane coating materials are investigated. Wang et al. [45] tested a perfluorocopolymer coated membrane oxygenator for arteriovenous CO_2 removal. CO_2 exchange of the coated membranes exceeded the CO_2 exchange of the uncoated fibers by 16 %. Analogously, Arazawa et al. [46] coated hollow fiber membranes by immobilizing carbonic anhydrase on the surface. A 36 % increase was recorded for the modified fibers.

Anti-thrombogenic surface coatings can be differentiated between biopassive and bioactive coatings. Biopassive coatings minimize the interaction between blood and the artificial surface by suppressing protein absorption via uncharged or zwitterionic hydrophilic polymers. Alternatively, they prevent surface wetting by utilizing particular hydrophobic polymer surfaces. Bioactive coatings such as heparin coatings and nitric oxide (NO) releasing coatings inhibit coagulation factors. While biopassive coatings show less effective hemocompatibility, they are more stable than bioactive coatings, prone to degradation of their active components. In general, stable coatings that do not impede the gas transfer represent the major challenge in developing future oxygenator coatings [47].

Die approbierte gedruckte Originalversion dieser Dissertation ist an der TU Wien Bibliothek verfügbar.
The approved original version of this doctoral thesis is available in print at TU Wien Bibliothek.
TU Bibliothek Your knowledge hub WIEN

Besides developing membrane coatings, current research aims to replace the common membrane materials in oxygenators such as Poly(methylpentene) (PMP) and Poly(propylene) (PP) [48] with new materials. Here silicone membranes show promising potential due to their high gas exchange performance and good hemocompatibility. Nakata et al. [49] could demonstrate that a prototype oxygenator with a silicone membrane showed comparable CO_2 removal performance to a commercially available oxygenator with a twice larger membrane surface.

1.3.1.4 Microfluidic Membrane Oxygenators

The latest development efforts are focusing on microfluidic oxygenators. Here, molds are used to produce microfluidic structures consisting of silicone with low priming volume, low flow resistance, and efficient gas exchange [50]–[52].

1.3.1.5 Respirator dialysis

Since CO_2 is predominately transported in the blood as bicarbonate, dialytic separation of CO_2 via the removal of bicarbonate is an attractive option [53], [54]. However, respiratory dialysis is restricted due to limited measures to compensate for shifts in the electrolyte concentrations and pH, which are induced by bicarbonate removal [8]. Approaches to allow long-term use by substituting bicarbonate with sodium hydroxide, tromethamine (THAM), and organic anions failed due to serious side effects such as fluid gain, hyperchloremic acidosis, hemolysis, cardiac arrhythmias, and acid-base derangements [55].

1.3.2 State of the Art Experimental Investigations

Experimental investigation methods are the most reliable methods for the development of oxygenator-based CO_2 removal. Procedures for the determination of the gas transfer, blood cell damage, and heat exchanger performance are described in the ISO standard 7199 [56]. The planning, conduction, postprocessing, and interpretation of measurement data are excessive. Furthermore, experimental studies are expensive.

Consequently, experimental studies are adapted to the developmental progress of the investigated prototype devices. In vitro tests with blood models are used for a first assessment of flow distribution [57] and CO_2 removal performance [58]. In vitro tests with blood are necessary if – besides the gas transfer performance – factors such as hemocompatibility, hemolysis, and thrombus formation and deposition are of interest [59]–[61]. In vivo or ex vivo experiments are conducted when the effect of the blood-contacting device on health parameters such as liver and renal function [62] or cardiac output [63] is studied. Finally, clinical trials are used to prove the positive effect on the patient (e.g., the effect of surface coated oxygenator systems [64]) or to revise therapeutic strategies [65].

In the scope of this work, the main focus is on the initial development phase, i.e., the design of in vitro tests for evaluation of the CO_2 removal performance and blood distribution of prototype oxygenators. In the following section, the critical issues for a successful experimental design of these in vitro campaigns are reviewed.

Die approbierte gedruckte Originalversion dieser Dissertation ist an der TU Wien Bibliothek verfügbar.
The approved original version of this doctoral thesis is available in print at TU Wien Bibliothek.
TU Bibliothek Your knowledge hub WIEN

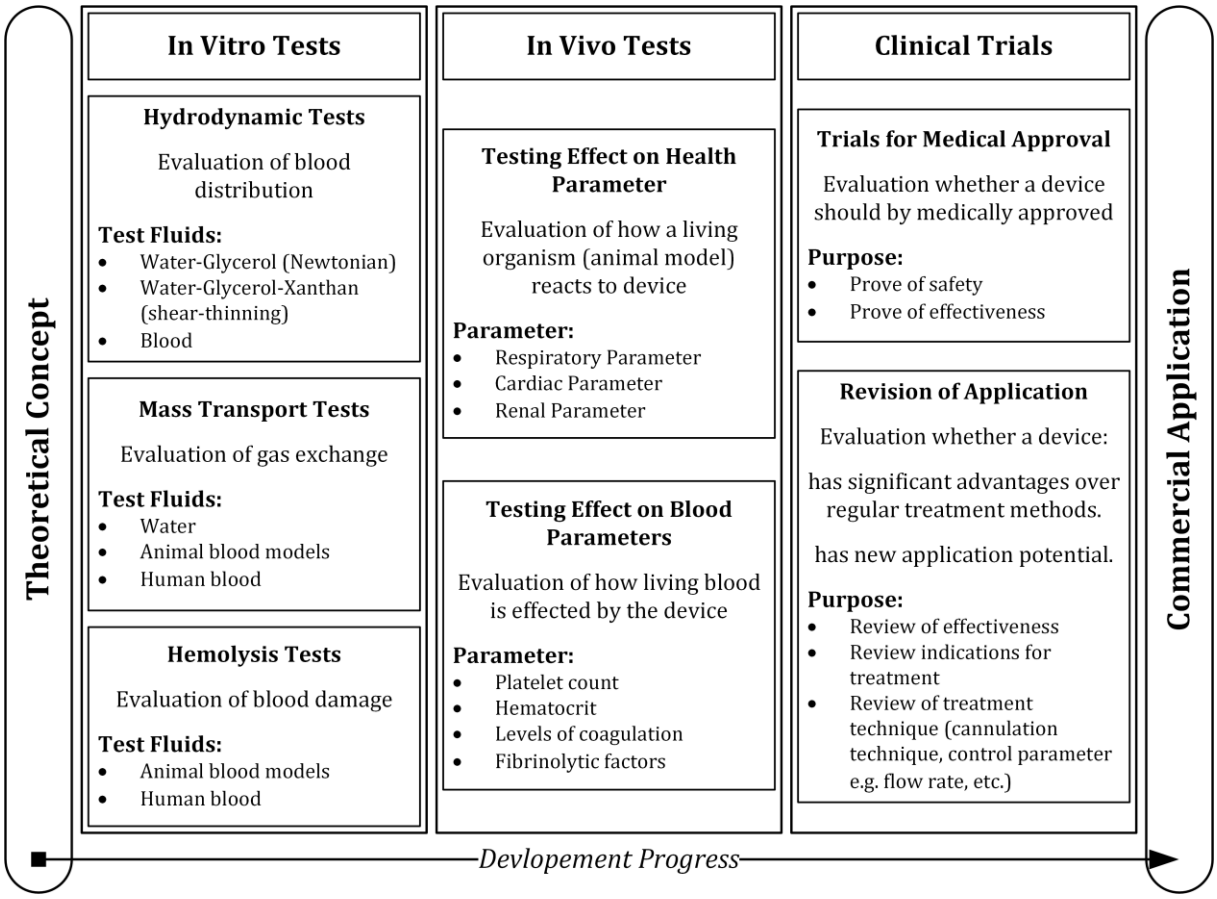

Figure 1.2. Overview of experimental methods used for the development of oxygenators.

1.3.2.1 Determination of CO_2 Removal Rate[3]

For future research and development of oxygenator-based CO_2 removal, accurate and reliable measurement of CO_2 removal rate is a fundamental requirement. There are two options for the measurement of the CO_2 removal rate (Figure 1.3). First, by measuring the flow rate and CO_2 concentration decrease of blood across the membrane packing – blood-based method. This is done via an ultrasound flow probe, a blood gas analyzer (BGA), and a CO_2 solubility model. Second, by measuring the flow rate and the CO_2 concentration increase of sweep gas across the membrane packing – sweep flow-based method. This is done via volumetric piston stroke or thermal conductivity sensor and an infrared-based CO_2 sensor (e.g., NDIR). In order to monitor and control the oxygenator test, BGA and blood flow rate measurement is required in both methods.

Consequently, the sweep flow-based method requires additional measurement equipment but shows high accuracy due to the reliable infrared measurement principle. In contrast, the accuracy of the blood-based method is dependent on the CO_2 solubility model accuracy. Furthermore, additional measurement errors are induced by the required samples at the oxygenator inlet. Both – CO_2 solubility model and measurement samples at the inlet – are not required for the sweep flow-based method [**Journal Publication VI**]. However, due to the less extensive experimental setup of the blood-based method, both CO_2 removal prediction methods are equally applied in recent research.

[3] This section is based on the review of **Publication VI**.

Die approbierte gedruckte Originalversion dieser Dissertation ist an der TU Wien Bibliothek verfügbar.
The approved original version of this doctoral thesis is available in print at TU Wien Bibliothek.
TU Bibliothek Your knowledge hub WIEN

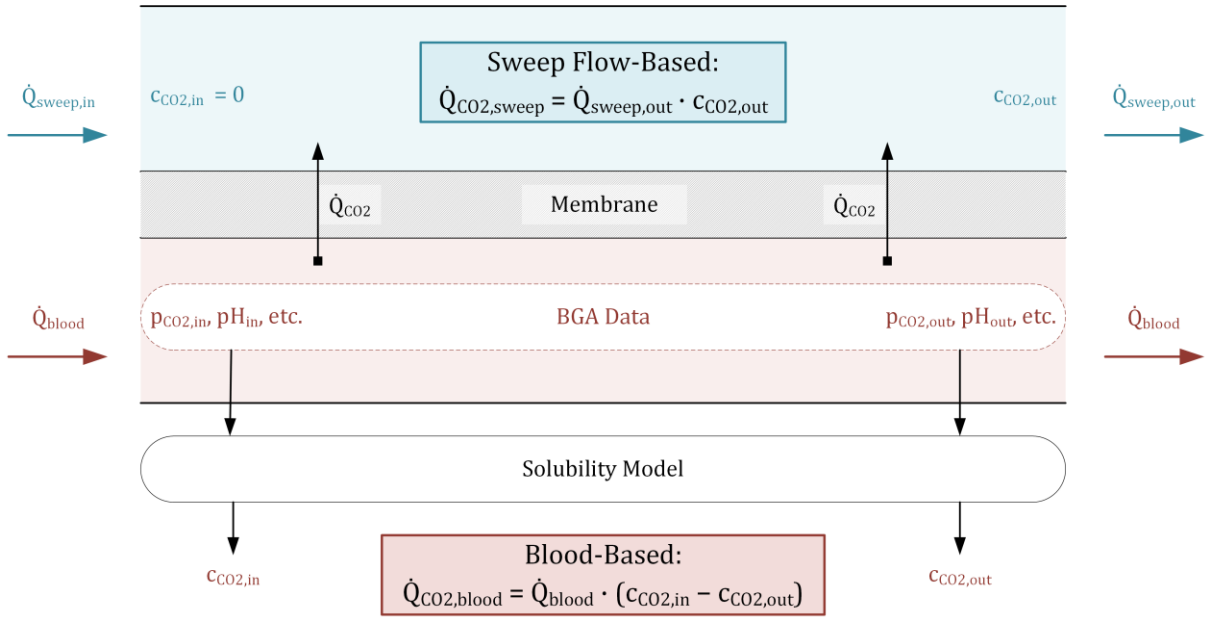

Figure 1.3. Scheme for sweep flow- and blood-based CO_2 removal rate prediction method.

Due to the lower sensitivity on model and measurement errors and the simple measurement principle, the sweep flow-based method has been used in various studies investigating the CO_2 removal performance of oxygenators. Arazawa et al. [46] investigated the influence of carbonic anhydrase on the CO_2 removal efficiency of hollow fiber membranes. For this purpose, the enzyme was immobilized on the shell side of the fibers. The CO_2 removal rate was measured for modified and unmodified membranes in in vitro experiments with phosphate-buffered solution (PBS) and bovine blood. In contrast to the blood-based method, the sweep gas-based method is independent of a CO_2 solubility model and allows a direct comparison of the CO_2 removal rates measured for the two liquids. Eash et al. [66] investigated the CO_2 removal performance of a respiratory catheter in in vivo experiments with sheep and calves. As the catheter was inserted into the right atrium, the sampling required for the blood-based method would not be possible due to limited accessibility. The sweep gas-based method could be used here as a reliable alternative. Mihelc et al. [57] developed a respiratory catheter with an impeller built into the membrane packing to reduce blood side CO_2 transport resistance. In vitro studies with water and in vivo studies with calves were conducted to evaluate the influence of different impeller designs on the CO_2 removal rate. Again, the sweep flow-based method allowed the comparison of CO_2 removal rate determined with the two liquids. Limited accessibility of blood-based method in in vivo studies of catheter systems was avoided. The sweep gas-based method is also used in studies with no different test liquids (e.g., blood and water) or limited accessibility. May et al. [67] measured the CO_2 removal in the sweep gas of a low flow membrane oxygenator in vitro trials using bovine blood. Analogously, Wang et al. [45] determined the gas exchange performance of a prototype oxygenator with a perfluorocopolymer coated microporous hollow fiber packing in in vivo trials, using sheep as an animal model.

The blood-based method for determining CO_2 removal performance is used for various reasons. For instance, May et al. [54] conducted studies on respiratory dialysis. Here, CO_2 is removed in the form of bicarbonate utilizing standard hemodialysis membrane modules. In contrast to membrane oxygenation, where O_2 is used as a sweep fluid, liquid

Die approbierte gedruckte Originalversion dieser Dissertation ist an der TU Wien Bibliothek verfügbar.
The approved original version of this doctoral thesis is available in print at TU Wien Bibliothek.
TU Bibliothek Your knowledge hub WIEN

dialysate is applied. Hence, the infrared-based CO_2 concentration measurement as used in the sweep gas-based method is not applicable. Consequently, the in vitro trials with bovine and porcine blood by May et al. [54] were evaluated with the blood-based method.

Furthermore, the BGA data provided by the blood-based method gives essential information on blood parameters at the inlet and outlet of the oxygenator. This data is required to validate and set up CFD simulations. CFD simulations extend the experimental data, which is often limited regarding spatial resolution and accessibility. In order to develop a CFD model for the numerical investigation of the CO_2 removal process, Hormes et al. [68] designed a prototype oxygenator incorporating a small membrane packing with a low fiber number. The CO_2 removal performance of this miniature oxygenator was determined in in vitro porcine blood trials. The simple geometry allowed a numerically inexpensive validation of the CFD model based on the blood-based method and the required BGA measurements.

The blood-based method is also used to study the CO_2 removal performance of oxygenators when there is no particular suitability. Schraven et al. [69] investigated the potential of pulsatile blood flow to increase the CO_2 removal of oxygenators. For this purpose, in vitro tests were performed with porcine blood. Wu et al. [70] determined the gas exchange rates of a microfluidic oxygenator with a porous polycarbonate membrane in in vitro tests with human blood. Borchardt et al. [42] investigated an oxygenator with an integrated pulsating pump in in vitro tests with porcine blood.

As outlined above, both methods for determining the CO_2 removal rates are used to the same extent in recent research. However, the CO_2 removal rates obtained by the blood-based and sweep flow-based method are rarely compared. Barret et al. [71] determined the CO_2 removal performance of an extracorporeal oxygenator in vitro with human blood using both methods. The CO_2 removal rate was measured at a constant blood flow rate (400 mL/min) and varying sweep flows (0 to 1000 mL/min). The relative deviation of blood-based CO_2 removal from sweep flow-based CO_2 removal was found to be dependent on the CO_2 removal rate. It was largest (20 %) at low CO_2 removal rates (57.9 mL/min – lowest sweep flow) and lowest (6 %) at high CO_2 removal rates (94.0 mL/min – highest sweep flow). The average deviation amounted to 11 %.

[**Journal Publication VI**] compared the CO_2 removal rate predicted by blood-based and sweep flow-based method. While measurement error of sweep flow-based method was found to be low (3 % of reading), measurement error of blood-based method was significantly ($p < 0.05$) higher (16 % of reading). Furthermore, the accuracy of the blood-based method displayed a strong dependency on the chosen solubility model. Deviation in CO_2 removal rate predicted by blood and sweep flow-based method could increase to a value of 127 % when an inadequate CO_2 solubility model was chosen.

1.3.2.2 Rheological Models for Blood

In vitro tests with blood are excessive and expensive due to the limited durability and availability of blood and the associated contamination of the test circuits. Hence, for efficient and cost-effective development of oxygenator-based CO_2 removal, accurate and reliable rheological models with comparable viscosity and density are required. However, the two-phase nature of blood and the interaction between blood cells and blood plasma result in complex rheologic behavior, including shear-thinning and thixotropic effects

Die approbierte gedruckte Originalversion dieser Dissertation ist an der TU Wien Bibliothek verfügbar.
The approved original version of this doctoral thesis is available in print at TU Wien Bibliothek.
TU Bibliothek Your knowledge hub WIEN

[72]. Consequently, dependent on the flow regime, multiple fluids have been proposed as rheological blood models for hydrodynamic tests of blood-contacting devices.

Since the macroscopic viscosity of blood converges to approx. 3.5 mPa s at shear rates above 200 1/s [73], Newtonian models are applied for devices with elevated shear rates, e.g., left ventricular assist devices (LVAD). Using dimensionless analyses and an enlarged model with the ratio of 5:1, Chua and Akamatsu [74] investigated the wall shear stress in the clearance gap of a centrifugal blood pump with air as a Newtonian Model. Zhu et al. [75] used water to test an intraventricular assist device in an in vitro mock circulation. However, the most common Newtonian model for blood is a mixture of glycerol and water with a glycerol content of 40 w% (3.5 mPa s, 1100 kg/m^3) [76]–[79]. Besides viscosity and density, optical measurement systems require transparent blood models with a refractive index comparable to the flow guiding parts, i.e., PDMS models of vessels or acryl models of pumps. In order to increase the refractive index of water-glycerol mixtures, sodium iodide [80] or sodium chloride [81] is added.

Non-Newtonian blood models have been developed to match the shear-thinning behavior of blood at flow conditions with low to intermediate (< 200 1/s) shear rates. Here commonly aqueous solutions with Xanthan gum (approx. 0.05 w%) and glycerol (approx. 40 w%) are used [82]–[84]. However, Xanthan gum reduces the refractive index. This can be compensated only to a certain extent since the shear-thinning behavior of Xanthan gum solutions is sensitive to salts (e.g., sodium iodide, sodium chloride) [85].

To assess the hemolysis in blood-contacting devices, it is common practice to use animal blood models [86]. However, animal species show differences in the mechanical fragility of erythrocytes [87], resulting in deviations of the normalized indices of hemolysis between species. In a comparative study, bovine and porcine blood exhibited comparable hemolytic characteristics to human blood, while ovine blood showed increased sensitivity towards mechanical stress [88].

In general, hemorheological parameters differ between species. The most substantial deviations of whole blood viscosity of man and animal species can be recorded at low shear rates (0.7 1/s). At high shear rates (94 1/s), differences in whole blood viscosity decrease. A proper fit for the shear-thinning behavior of human blood can be recorded for porcine and equine blood [89]. In [**Journal Publication VII**], viscosity models were derived, considering the animal-specific dependency of the whole blood viscosity on shear rate, hematocrit, and temperature. These mathematical models will, in the future, provide an essential basis for the selection of the correct animal model for in vitro or in vivo tests.

1.3.2.3 CO_2 Transport Models for Blood[4]

In order to increase efficiency and reduce the cost of in vitro tests to determine the CO_2 removal rate of a prototype oxygenator, reliable and easily accessible CO_2 transport models are required. Consequently, water as a CO_2 transport model for blood was proposed early and can be traced back to research published in the 1970s [90]. Today in vitro water tests are still common practice in various studies due to the substantially reduced experimental effort compared to in vitro blood tests [**Journal Publication VIII**].

Hout et al. [91] conducted in vitro water tests with two different oxygenator models to examine the dependency of the CO_2 removal rate on the sweep flow rate. In order to

[4] This section is based on the review of **Publication VIII**.

Die approbierte gedruckte Originalversion dieser Dissertation ist an der TU Wien Bibliothek verfügbar.
The approved original version of this doctoral thesis is available in print at TU Wien Bibliothek.
TU Bibliothek Your knowledge hub WIEN

guarantee the comparability of the data obtained for the two oxygenator designs, the CO_2 removal rate was normalized by the maximum CO_2 removal rate. To a linear approximation, this makes the CO_2 removal rate independent from the specific mass transfer characteristics of an oxygenator [92] and, consequently, the test fluid (blood/water) used.

Hattler et al. [58] determined the CO_2 and O_2 transfer rates of a respiratory catheter in vitro with water and in vivo using calves as large animal models. The suitability for water as a blood model in gas exchange experiments is only discussed for O_2 to a limited extent. Furthermore, comparability of in vitro and in vivo data is not guaranteed. The catheter positioned in the vena cava close to the right atrium was exposed to different hydrodynamic conditions than the catheter in the in vitro test loop. Consequently, an in-depth investigation on the suitability of water as a blood model to determine the CO_2 removal rate of oxygenators cannot be conducted. However, Mihelc et al. [57] and Jeffries et al. [21] reported that the CO_2 removal rate of a respiratory catheter measured in vivo with calves and in vitro with water correlates within a 10 % deviation. The good agreement is attributed to opposing effects of viscosity and CO_2 solubility of blood and water on the CO_2 removal rate.

Svitek et al. [93] assume similarity between the CO_2 mass transfer mechanisms of water and blood in the context of a dimensionless analysis, i.e., water and blood follow the same Sherwood correlation when their material parameters (e.g., density, viscosity, CO_2 diffusion rate, and solubility) are considered accordingly. That allows a Sherwood correlation for predicting CO_2 removal with blood to be established based on in vitro tests with water. Svitek et al. show that the water data-based Sherwood model reasonably predicts the CO_2 removal rates of in vitro bovine blood tests for the applied range of blood flow rates. However, the Sherwood correlations of the two fluids are not compared directly, failing to prove the initial assumption of similarity in mass transfer characteristics.

Wickramasinghe et al. [94] compared the CO_2 mass transfer characteristics of Newtonian and Non-Newtonian blood models. As Newtonian models, water and water-glycerol mixtures with various glycerol fractions were investigated. As Non-Newtonian models, water-glycerol-Xanthan mixtures with various glycerol and Santhan content were investigated. Wickramasinghe et al. could show that for CO_2 mass transfer, Newtonian and Non-Newtonian blood models follow a comparable Sherwood correlation if the Non-Newtonian behavior is considered accordingly in the Reynolds and Schmidt number.

Tabesh et al. [95] determined the CO_2 removal rate of a prototype oxygenator in vitro with porcine blood and water. The CO_2 removal for blood and water was calculated based on BGA and pH sensor data, respectively. Blood was saturated with O_2 and CO_2 to match normed venous conditions. Water was set to varying CO_2 partial pressure levels by exposing it to saturation gas streams with different CO_2/N_2 ratios. The difference in CO_2 removal rates was then studied in dependency of the CO_2 partial pressure of water. Based on the acquired data, a correlation was developed, which allows minimizing the difference between the CO_2 removal rate of blood and water by adjusting the CO_2 partial pressure of water. The correlation calculates the CO_2 partial pressure based on the mean retention time and effective membrane surface. It was checked for two commercial oxygenators with comparable packaging design to the prototype oxygenator. The adjustment of the CO_2 partial pressure of water to a level given by the correlation allowed to reduce the maximum deviation between CO_2 removal rates of blood and water to 5 %. However, the authors acknowledge that this correlation could depend on the investigated membrane

Die approbierte gedruckte Originalversion dieser Dissertation ist an der TU Wien Bibliothek verfügbar.
The approved original version of this doctoral thesis is available in print at TU Wien Bibliothek.
TU Bibliothek Your knowledge hub WIEN

packing design and flow setup. Furthermore, by adjusting the CO_2 partial pressures in the water, this method distorts the driving force for transmembrane CO_2 transport. A comparison of the CO_2 removal rate of blood and water at the same inlet CO_2 partial pressures is not given.

In [**Journal Publication VI**], the CO_2 removal rate determined with blood and water was systematically compared to provide a future reference for replacing avoidable in vivo experiments with in vitro water tests. The deviation at nine measurement points – three pathological elevated CO_2 partial pressures (50, 70, 100 mmHg) and three blood flow rates (1000, 1300, 1600 mL/min) – amounted on average to 10 %. Follow-up CFD studies allowed us to attribute the low deviation in CO_2 removal rate to the opposing influences of the material properties of the two liquids. Compared to water, the higher CO_2 solubility of blood and the accompanied increased CO_2 removal rate (+ 125 %) is in most parts compensated by the lower CO_2 diffusion rate of blood (- 53 %), followed by the lower CO_2 permeance available with blood (- 18 %), and the higher viscosity of blood (- 10 %). However, dimensionless analysis of the CO_2 mass transport characteristics of blood and water strongly indicates that, in the two liquids, the built-up of CO_2 concentration polarization differs significantly. Consequently, water as a blood model should be limited to the macroscopic determination of the CO_2 removal rate and not be used in studies of the boundary layer.

1.3.3 State of the Art Numerical Investigations[5]

Numerical investigation methods are used for a wide range of applications in the development of oxygenator-based CO_2 removal, from initial evaluations of design strategies to detailed analyses and process parameter studies. They are either faster and cheaper than experimental methods or allow an extension of the experimentally obtained data.

1.3.3.1 Dimensionless Sherwood Correlations

The simplest numerical method for the prediction of the CO_2 removal performance of oxygenators are dimensionless Sherwood correlations. Sherwood correlations for hollow fiber membrane oxygenators are commonly based on heat exchange analogies of pipe bundle heat exchangers [96]. The Sherwood number (*Sh*) is calculated via the Reynolds (*Re*) and Schmidt (*Sc*) number using a correlation of the form $Sh = a \cdot Re^b \cdot Sc^{0.33}$. The mass transfer coefficient *k* can then be calculated using *Sh*. If we assume a negligible mass transfer resistance in the membrane, average transmembrane flux can be calculated by the product of *k* and the partial pressure difference between blood and sweep bulk flow [93]. Material properties of the mass transfer system are considered via the material parameters in the Sherwood, Schmidt, and Reynolds number, i.e., density, viscosity, and diffusion rate. With the characteristic velocity *u*, *Re* allows considering different blood flow rates. However, the basic flow guidance and the geometry of the hollow fiber bundle must be considered over the empirical fitting parameters *a* and *b* [97]. Consequently, design adaptions cannot be evaluated based on Sherwood correlations since they would require a modification of the empirical parameters to a value apriorily not known.

[5] This section is based on the review of **Publication I** and **Publication II**.

Die approbierte gedruckte Originalversion dieser Dissertation ist an der TU Wien Bibliothek verfügbar.
The approved original version of this doctoral thesis is available in print at TU Wien Bibliothek.
TU Bibliothek Your knowledge hub WIEN

1.3.3.2 Computational Fluid Dynamic Methods

Computational fluid dynamics (CFD) models are highly complex but provide a flexible platform for investigating membrane separation processes [98]. Here, the membrane module geometry is discretized into a computational grid consisting of finite volume cells. The relevant transport equations (Section 2.2.1) are then solved for each cell of this grid. Consequently, CFD directly considers the flow guidance and geometry in its computations. Therefore, information on process parameters can be provided in the spatial resolution of the computational grid. However, phenomena scaling below this resolution cannot be computed directly but must be modeled [99].

In order to resolve the narrow distances between the individual fibers of a membrane packing, a high number of relatively small computational cells and thus a high computational effort is necessary. Consequently, CFD simulations of oxygenators can be divided into homogenous models – CFD models that do not resolve the packing and heterogenous models – CFD models that resolve the membrane packing [100].

In homogenous models, the membrane packing is considered a homogenous porous medium. Darcy's law is applied to model the flow resistance of the packing via a source term in the momentum equation. This inexpensive computational method can study the flow distribution in the complete geometry of an oxygenator [101]–[103]. Furthermore, it was proposed to estimate the gas exchange performance within the packing based on Sherwood correlations [104], [105]. However, these correlations must be determined experimentally for different packing densities and flow arrangements [97].

In heterogeneous models, the membrane packing is resolved by the computational grid. While commonly computer models of ideal fiber packings are investigated, D'Onofrio et al. [106] proposed a method to acquire a realistic three-dimensional model of a blood oxygenator by reconstructing micro-CT scans. While heterogeneous models are less dependent on empirical models, they are computational more expensive. In addition to the fine geometric features of membrane packings, high Schmidt numbers are present in mass transfer problems. These result in steep concentration gradients of the permeating species in the laminar boundary layer [107]. For an adequate resolution of this diffusive transport resistance, an additional cell refinement of the computational grid perpendicular to the membrane surface is required [108].

This additional mesh refinement for mass transfer simulations is accompanied by a significant increase in computational effort [**Journal Publication II**]. Consequently, heterogeneous flow simulations are feasible on macroscopic scales – e.g., membrane modules [109], representative parts of fiber packings [100] – while heterogenous mass transport simulations are limited to microscopic scales – e.g., single fibers, periodic fiber arrangements [97] or smaller parts of packings [110].

In order to overcome this gap in geometrical size scale, an upscaling method was proposed [**Journal Publication II**]. It allows using CFD mass transport simulations of smaller packings to predict the total CO_2 removal performance of oxygenators. The latter is achieved by deducing inlet velocity boundary conditions of the mass transport simulations from macroscopic CFD flow simulations.

While blood is considered a single phase in most heterogenous CFD models, Kaesler et al. [111] used an Eulerian-Eulerian approach to describe two phases, red blood cells

Die approbierte gedruckte Originalversion dieser Dissertation ist an der TU Wien Bibliothek verfügbar.
The approved original version of this doctoral thesis is available in print at TU Wien Bibliothek.
TU Bibliothek Your knowledge hub WIEN

and blood plasma. This allowed considering the influence of the heterogeneous distribution of red blood cells and consequently hemoglobin on the O_2 transfer of a prototype oxygenator.

Commonly, heterogenous CFD models only include the blood side in the simulation domain, as the concentration polarization layer in the blood is the main transport resistance [3]. Therefore, CO_2 and O_2 partial pressure at the membrane surface is set to a uniform constant value [112], [**Journal Publication V**]. However, in studies of the oxygen transport in a prototype oxygenator, Taskin et al. [113] additionally resolved the membrane wall and showed that neglection of the membrane resistance leads to an overprediction of O_2 transfer. This approach was extended in [**Journal Publication I**], and the hollow fiber lumen was included. While this is numerically complex due to the required multi-region solver, the approach allows considering the gas side decrease in driving force over the length of the fibers.

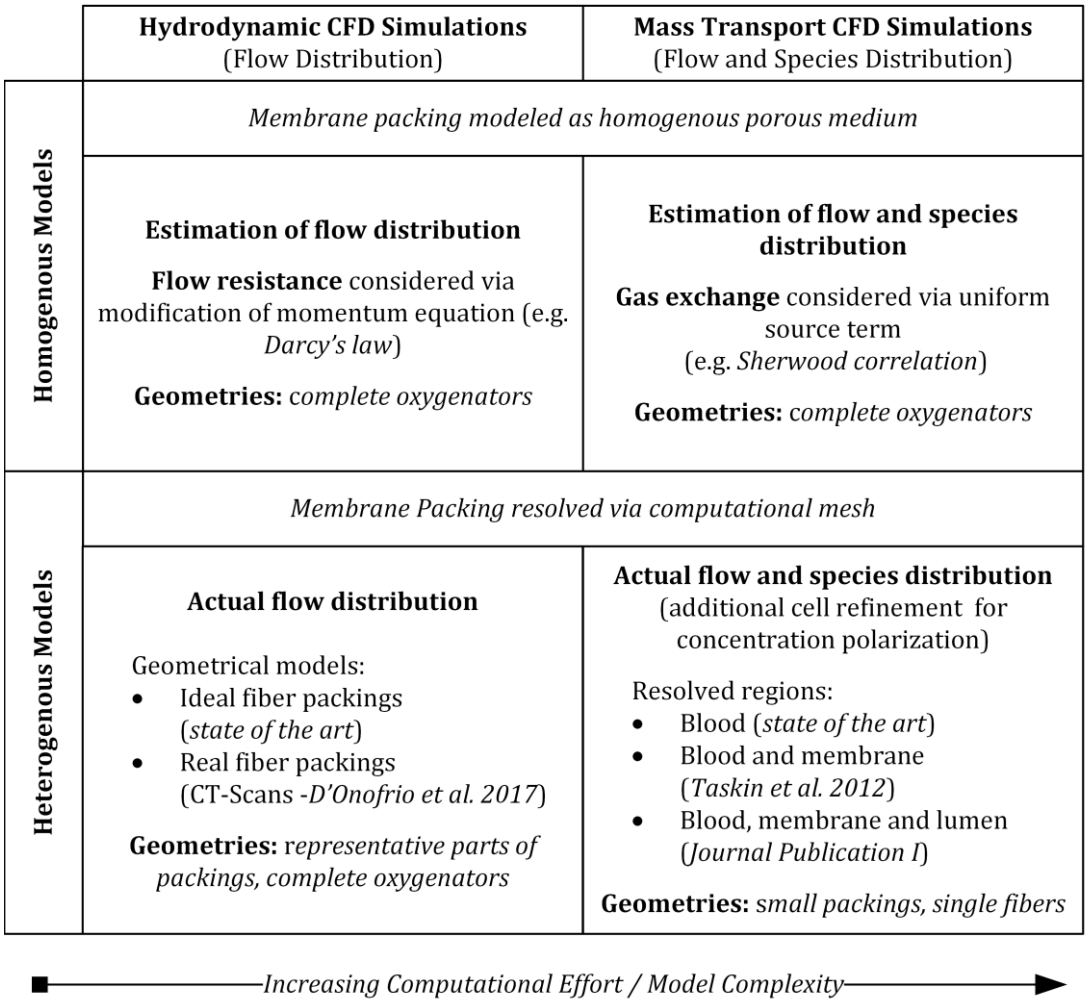

Figure 1.4. Overview of CFD models used for the development of oxygenators.

Die approbierte gedruckte Originalversion dieser Dissertation ist an der TU Wien Bibliothek verfügbar.
The approved original version of this doctoral thesis is available in print at TU Wien Bibliothek.
TU Bibliothek Your knowledge hub WIEN

2 Methods[6]

In this work, existing experimental and numerical (CFD) methods for investigating the CO_2 removal performance of oxygenators were utilized, evaluated, and further developed. In this section, the used methods are described. The descriptions are intended to provide the basis for understanding the research presented in Chapter 3 (Publication Summary) and Chapter 4 (Summary and Discussion)

2.1 Experimental Methods

The CO_2 removal performance of a prototype oxygenator was determined experimentally in vitro with water and bovine blood and in vivo with porcine blood. The prototype oxygenator was developed at the Technical University of Vienna for the application as a membrane module in an intravascular CO_2-separation catheter. Elaborate tests of the prototype oxygenator were conducted at the Center for Biomedical Research of the Medical University of Vienna. Due to the extensive development effort for an intravascular gas exchange catheter, only basic performance tests of the complete catheter system (membrane module + drive unit – Section 2.1.8) were conducted. All tests were approved by the institutional ethics and animal welfare committee and the national authority (ZI. 153/115-97/98).

The prototype oxygenator is presented in Figure 2.1a. The blood flows into the coaxial cylindrical cavity within the hollow fiber membrane packing. Through a deflector in the center of the cavity (baffle), blood is guided radially through the shell side of the packing into the hollow cylindrical space between packing and module wall. From there, it flows back radially through the shell side of the packing to the centrally located outlet. The cross-flow created by the double deflection is intended to reduce the build-up of concentration polarization as much as possible. The spiral arrangement of the fibers, which is defined by the winding of a fiber mat around the inlet and outlet pipe, can be seen in Figure 2.1b. It shows the cross-section of the epoxy fiber potting, which separates the blood on the shell side and the sweep gas on the lumen side of the fibers.

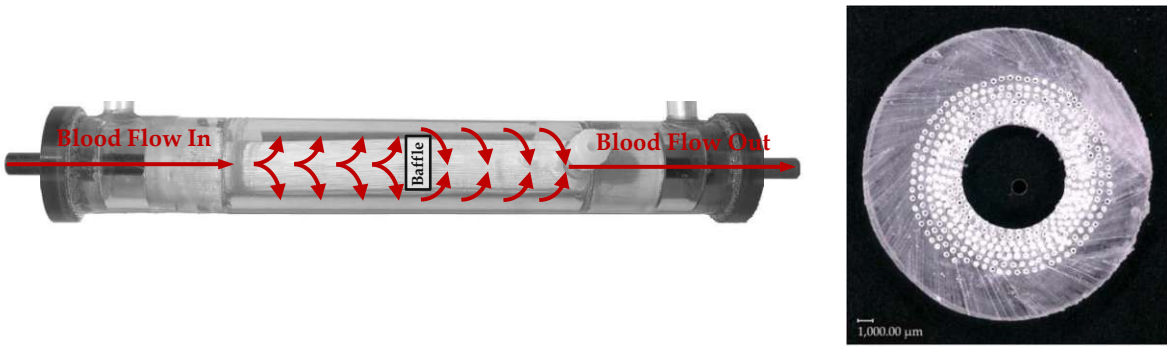

(**a**) (**b**)

Figure 2.1. Prototype oxygenator: (**a**) Principle flow guidance; (**b**) slice of fiber potting to illustrate fiber arrangement. By Lukitsch et al. [**Journal Publication II]** (CC BY 4.0).

[6] The method section is based on the method sections of the publications included in this cumulative dissertation.

Die approbierte gedruckte Originalversion dieser Dissertation ist an der TU Wien Bibliothek verfügbar.
The approved original version of this doctoral thesis is available in print at TU Wien Bibliothek.
TU Bibliothek Your knowledge hub WIEN

As sweep gas, O_2 was used. The sweep gas flows axially through the fiber lumen of the hollow fiber membranes. The respiration gases O_2 and CO_2 are then exchanged over the membrane (fiber wall) following the partial pressure gradient. Consequently, CO_2 is removed from the blood and transported from the oxygenator via the sweep gas exhaust. O_2 diffuses through the membrane into the blood, generating a higher O_2 saturation.

The hollow fiber membranes used are commercially available but were only approved for research purposes. The integrity of the hollow fibers cannot be guaranteed entirely for the construction of the prototype oxygenators.

2.1.1 Gas Permeation Test

In order to guarantee the functionality of the built prototype oxygenators, pure gas permeation tests were performed (Figure 2.2).

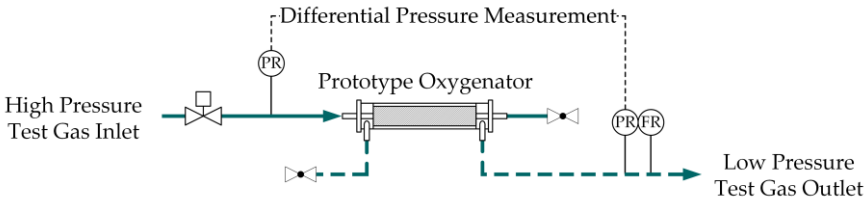

Figure 2.2. Scheme of pure gas permeation measurement. Adapted from Lukitsch et al. [**Journal Publication VI**] (CC BY 4.0).

Pure O_2, CO_2, or N_2 was applied at the shell side of the hollow fiber membranes in a dead-end configuration (stage cut of 1). The pressure difference across the membrane Δp [Pa] and permeate flow $\dot{V}$ [mL/STP/min] was measured. With an estimation of the membrane area A [m^2] based on fiber and module dimensions, the pure gas permeance P_i [mL STP/min/m^2/Pa] of species i can be determined.

$$P_i = \frac{\dot{V}}{\Delta p \cdot A} \qquad 2.12.1.1$$

The used Polymethylpentene (PMP) hollow fiber membranes (Membrana Oxyplus® 90/200 PMP, 3M) are selective to CO_2. This allows to detect leakage through the potting or the membrane since the latter would result in a reduced ideal selectivity ($S_{i,j}$ [-], e.g., of CO_2 and N_2).

$$S_{i,j} = \frac{P_i}{P_j} \qquad with\ i \neq j \qquad e.g.: S_{CO2,N2} = \frac{P_{CO2}}{P_{N2}} \qquad 2.12.1.2$$

Pure gas permeation of modules was assessed after in vitro or in vivo tests. A decrease in gas permeation performance (permeance) indicates water-filled pores in the membrane wall or blood residues on the membrane surface. Both would undercut the long-term durability and performance of a prototype oxygenator.

Die approbierte gedruckte Originalversion dieser Dissertation ist an der TU Wien Bibliothek verfügbar.
The approved original version of this doctoral thesis is available in print at TU Wien Bibliothek.
TU Bibliothek Your knowledge hub WIEN

2.1.2 In Vitro Water Tests

Figure 2.3 shows the experimental setup of the in vitro water tests to determine the CO_2 removal rate of the prototype oxygenator [**Journal Publication VI**]. Deionized water was pumped in a loop using a centrifugal blood pump (BPX- 80, Medtronic). The water flow rate was measured using an ultrasound flow probe (SONOFLOW CO.55/080). A commercial extracorporeal oxygenator (ECMO Adult, Eurosets) was used to saturate the water with CO_2. To control the CO_2 level in the water, two mass flow controllers (MFC - GF40, Brooks) were used to sweep the ECMO with a defined mixture of CO_2 and N_2. While the water loop was connected to the fiber shell side of the prototype oxygenator, the sweep fluid (pure O_2) was applied to the lumen side. Sweep flow was controlled by a third MFC (GF40, Brooks). Exhaust gas flow rates of the ECMO and the prototype oxygenator were measured via piston stroke measurement devices (Defender 510, Bios DryCal). Additionally, the CO_2 concentration in the prototype oxygenator exhaust gas was measured via NDIR (BINOS 100 M, Emerson) to assess the CO_2 removal rate. Before and after the prototype oxygenator, two sample ports (BG, Figure 2.3) were installed for offline blood gas analysis (BGA - ABL825 FLEX, Radiometer Medical A/S). The pressure was measured (PR, Figure 2.3) before and after both membrane modules (ECMO and prototype oxygenator) on the gas and waterside, using pressure transmitters (AMS 4711, Analog Microelectronics). The CO_2 removal rate was measured at three partial pressure levels (50, 70, 100 mmHg) at three blood flows each (1000, 1300, 1600 mL/min). These nine measurement points correspond to elevated pathological CO_2 partial pressure values and the intended blood flow rates of the oxygenator prototype.

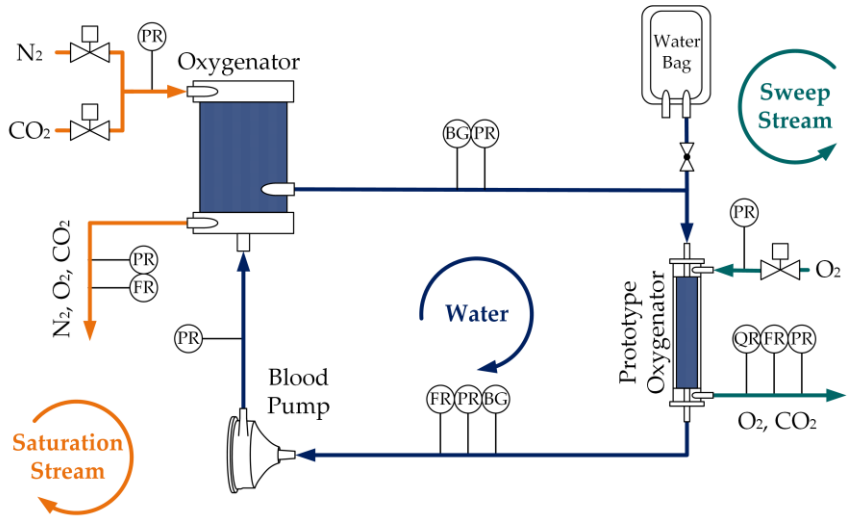

Figure 2.3. Scheme of in vitro water tests. Adapted from Lukitsch et al. [**Journal Publication VI**] (CC BY 4.0).

2.1.3 In Vitro Bovine Blood Tests

Figure 2.4 shows the experimental setup of the in vitro bovine blood tests to determine the CO_2 removal rate of the prototype oxygenator [**Journal Publication I**]. Bovine blood was provided by the Teaching and Research Farm of the University of Veterinary Medicine Vienna. The blood was pumped in a loop using a centrifugal blood pump (BPX-80, Medtronic). The blood flow rate was measured using an ultrasound flow probe (SONOFLOW CO.55/080).

Die approbierte gedruckte Originalversion dieser Dissertation ist an der TU Wien Bibliothek verfügbar.
The approved original version of this doctoral thesis is available in print at TU Wien Bibliothek.
TU Bibliothek Your knowledge hub WIEN

A commercial extracorporeal oxygenator (ECMO Adult, Eurosets) was used to set pathological relevant venous CO_2 and O_2 levels in the blood. To control the CO_2 and O_2 level, three mass flow controllers (MFC - GF40, Brooks) were used to sweep the ECMO with a defined mixture of O_2, CO_2, and N_2.

The fiber shell side of the prototype oxygenator was connected to the blood loop. The sweep fluid (pure O_2) was applied to the lumen side. Sweep flow was controlled by a fourth MFC (GF40, Brooks). Exhaust gas flow rates of the ECMO and the prototype oxygenator were measured via piston stroke measurement devices (Defender 510, Bios DryCal). Additionally, the CO_2 concentration in the prototype oxygenator exhaust gas was measured via NDIR (BINOS 100 M, Emerson) to assess the CO_2 removal rate (sweep flow-based CO_2 removal rate – **Journal Publication VI**).

Before and after the prototype oxygenator, two sample ports (BG, Figure 2.4) for offline blood gas analysis (BGA - ABL825 FLEX, Radiometer Medical A/S) were installed. The BGA data (e.g., CO_2 partial pressure) combined with a CO_2 solubility model and the blood flow rate enables a second method to determine the CO_2 removal rate (blood-based CO_2 removal rate – **Journal Publication VI**). Comparing the sweep flow-based CO_2 removal rate and blood-based CO_2 removal rate allows us to assess the accuracy of different CO_2 solubility models [**Journal Publication VI**].

The pressure was measured (PR, Figure 2.4) before and after both membrane modules (ECMO and prototype oxygenator) on the gas and blood side, using pressure transmitters (AMS 4711, Analog Microelectronics). The CO_2 removal rate was measured at three partial pressure levels (50, 70, 100 mmHg) at three blood flows each (1000, 1300, 1600 mL/min). These nine measurement points correspond to elevated pathological CO_2 partial pressure values and the intended blood flow rates of the oxygenator prototype.

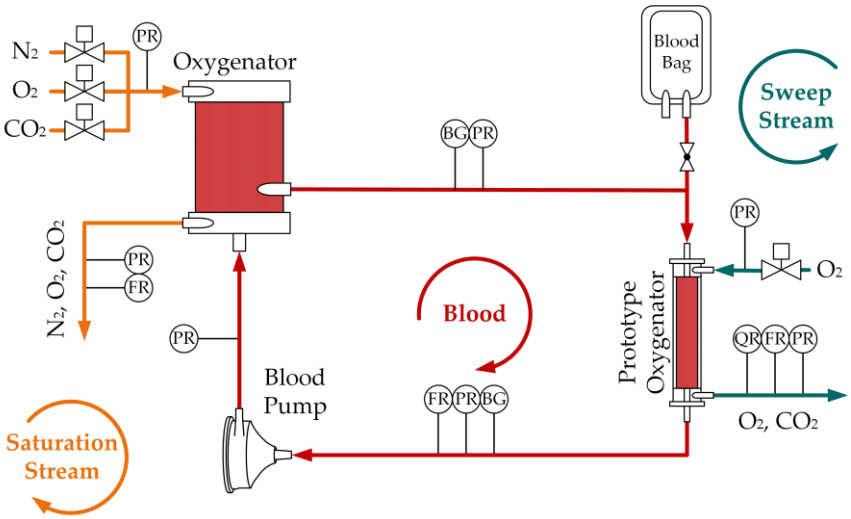

Figure 2.4. Scheme of in vitro bovine blood tests. Oxygenator. By Lukitsch et al. [**Journal Publication VI**] (CC BY 4.0).

2.1.4 In Vivo Porcine Blood Tests

Figure 2.5 shows the experimental setup of the in vivo porcine blood tests to determine the CO_2 removal rate of the prototype oxygenator [**Journal Publication II**]. Two pigs were provided by the teaching and research farm of the University of Veterinary Medicine Vienna.

Die approbierte gedruckte Originalversion dieser Dissertation ist an der TU Wien Bibliothek verfügbar.
The approved original version of this doctoral thesis is available in print at TU Wien Bibliothek.
TU Bibliothek Your knowledge hub WIEN

The animals were sedated and mechanically ventilated via an endotracheal tube. Oxygen saturation and CO_2 partial pressure were controlled via the ventilator (Servo 900C, Siemens). Ringer's solution was administered to maintain physiological blood pressure. Heparin was injected intravenously to prevent blood clotting. Blood pressure, cardiac output, body temperature (approx. 37°C), and heart rate were monitored (PiCCO plus, Pulsion Medical System).

Blood was pumped (BPX-80, Medtronic) from the pig to the prototype oxygenator via a cannula in the femoral vein. The oxygenated blood was then returned via a cannula in the jugular vein. The blood flow rate was measured using an ultrasound flow probe (SONOFLOW CO.55/080).

While the blood circuit was connected to the shell side of the fibers of the prototype oxygenator, the sweep fluid (pure O_2) was applied to the lumen side. Sweep flow was controlled by an MFC (GF40, Brooks). Exhaust gas flow rates of the ECMO and the prototype oxygenator were measured via piston stroke measurement devices (Defender 510, Bios DryCal). Additionally, the CO_2 concentration of the prototype oxygenator exhaust gas was measured via NDIR (BINOS 100 M, Emerson) to assess the CO_2 removal rate (sweep flow-based CO_2 removal rate – **Journal Publication VI**).

Before and after the prototype oxygenator, two sample ports (BG, Figure 2.5) for offline blood gas analysis (BGA - ABL825 FLEX, Radiometer Medical A/S) were installed (blood-based CO_2 removal rate – **Journal** Publication VI). Comparison of the sweep flow-based CO_2 removal rate and blood-based CO_2 removal rate allows assessing the accuracy of different CO_2 solubility models [**Journal Publication VI**].

The pressure was measured (PR, Figure 2.5) before and after both membrane modules (ECMO and prototype oxygenator) on the gas and blood side, using pressure transmitters (AMS 4711, Analog Microelectronics). The CO_2 removal rate was measured at three partial pressure levels (50, 70, 100 mmHg) at three blood flows each (1000, 1300, 1600 mL/min). These nine measurement points correspond to elevated pathological CO_2 partial pressure values and the intended blood flow rates of the oxygenator prototype.

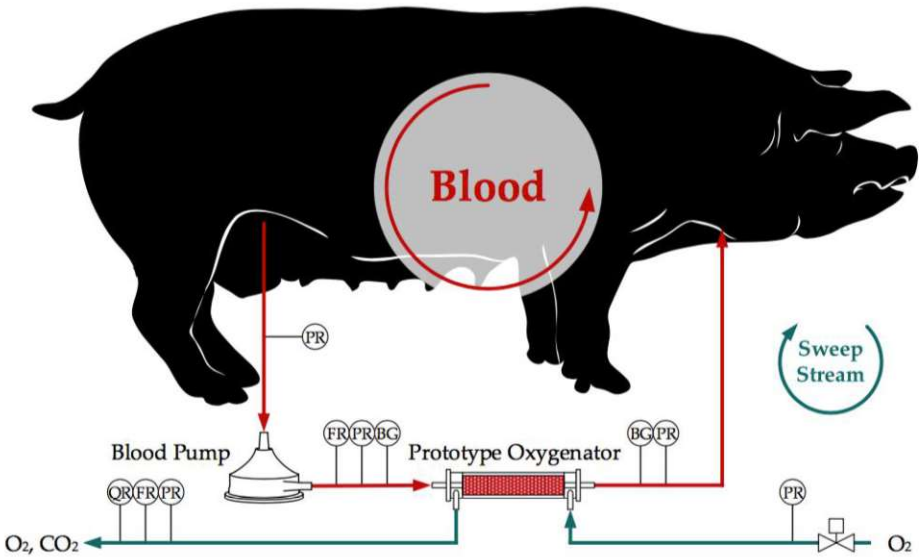

Figure 2.5. Scheme of in vivo porcine blood tests. By Lukitsch et al. [**Journal Publication II**] (CC BY 4.0).

Die approbierte gedruckte Originalversion dieser Dissertation ist an der TU Wien Bibliothek verfügbar.
The approved original version of this doctoral thesis is available in print at TU Wien Bibliothek.
TU Bibliothek Your knowledge hub WIEN

2.1.5 Viscosity Measurements

In the course of this work, bovine blood and porcine blood viscosity were measured for two reasons:

i. To gain reliable data for the viscosity models needed in the CFD simulations (Section 2.2.7.1).
ii. To provide training data for a blood viscosity estimator based on a Gaussian process regression model [**Journal Publication IV**].

Whole blood viscosity was measured with a Physica MCR301 rheometer (Anton Paar, Austria). The Rheometer was equipped with a Peltier controlled stainless steel double gap cylinder system (internal gap: 0.417mm; external gap: 0.462mm, cup length: 42mm). The whole blood viscosity was measured at logarithmically homogeneously distributed shear rates between 1 s^{-1} and 1000 s^{-1} at constant temperature (37°C) [**Journal** Publication VII].

2.1.6 Assessment of the CO_2 Solubility Models for Blood

The CO_2 removal rate was determined via two methods (Section 2.1.3 and 2.1.4). First, based on measurements in the sweep gas – sweep gas-based CO_2 removal rate ($\dot{Q}_{CO2,sweep}$ [mL STP/min]). Second, based on measurements in the blood (resp. water) – blood-based CO_2 removal rate ($\dot{Q}_{CO2,blood}$ [mL STP/min]). In both methods the CO_2 removal rate is calculated as the product between flow rate through the prototype oxygenator and the CO_2 concentration difference across the prototype oxygenator. Consequently, $\dot{Q}_{CO2,sweep}$ is calculated via the sweep flow rate $\dot{Q}_{sweep}$ [mL STP/min] and the CO_2 concentration difference in the sweep flow $\Delta c_{CO2,sweep}$ [-]. Analogously, $\dot{Q}_{CO2,blood}$ is calculated using the blood flow rate $\dot{Q}_{blood}$ [mL/min] and the CO_2 concentration difference in blood flow $\Delta c_{CO2,blood}$ [-]. In contrast to blood. The CO_2 inlet concentration of the sweep fluid can be assumed zero since medical O_2 was applied.

$$\dot{Q}_{CO2,sweep} = \left|\dot{Q}_{sweep} \cdot \Delta c_{CO2,sweep}\right| = \left|\dot{Q}_{blood} \cdot \Delta c_{CO2,blood}\right| = \dot{Q}_{CO2,blood} \qquad 2.12.1.3$$

While the CO_2 concentration in the sweep gas can be measured directly using NDIR, blood side measurement is limited to determining standard blood parameters such as CO_2 partial pressure, pH, bicarbonate concentration, hematocrit (volume fraction of red blood cells in the blood), and oxygen saturation. Using these parameters, the CO_2 concentration can be calculated via a CO_2 solubility model. Consequently, only the blood-based CO_2 removal rate is dependent on the accuracy of the CO_2 solubility model. This allows the assessment of the CO_2 solubility model error by calculating the relative deviation of the blood-based CO_2 removal rate from the sweep flow-based CO_2 removal rate (prediction error – ε [%]).

$$\varepsilon = \left|\frac{\dot{Q}_{CO2,blood} - \dot{Q}_{CO2,sweep}}{\dot{Q}_{CO2,sweep}}\right| \cdot 100 \qquad 2.12.1.4$$

However, the prediction error is only a measure for the CO_2 solubility model error. It includes measurement errors on the sweep side, measurement errors on the blood side, and propagation and amplification of BGA measurement errors via the CO_2 solubility model (propagation of uncertainty).

Die approbierte gedruckte Originalversion dieser Dissertation ist an der TU Wien Bibliothek verfügbar.
The approved original version of this doctoral thesis is available in print at TU Wien Bibliothek.
TU Bibliothek Your knowledge hub WIEN

Nevertheless, it could be shown that measurement errors of the sweep flow-based CO_2 removal rate are satisfactory (3 % of reading), and measurement errors of the blood-based CO_2 removal rate (approx. 16 % of reading) are relatively small compared to the determined prediction errors (ε of up to 125 %). We could demonstrate that a similar propagation of uncertainty is to be expected for other standard BGA devices. Consequently, ε gives a generic evaluation of the investigated blood CO_2 solubility models [**Journal Publication** VI].

2.1.7 Statistical Testing

The following statistical tests were performed to compare the performance of the individual CO_2 solubility models:

i. Levene's test [114] was applied to test for the homogeneity of variances between two groups (e.g., in vitro and in vivo data).
ii. Welch's t-test was [115] utilized to test for significance between two groups with unequal sample size and variances.
iii. Games-Howell posthoc test was used [116] to test for significance between more than two groups.

For all statistical tests, values of $p < 0.05$ were considered statistically significant [**Journal Publication** VI].

2.1.8 Gas Exchange Catheter Tests – Minimal Invasive Liquid Lung (MILL)

In this work, basic performance tests of an intravascular CO_2 removal catheter the minimal invasive liquid lung (MILL) were conducted. The MILL catheter consists of two main components, the membrane module for respiration gas exchange and a drive unit (miniature blood pump driven by an electric motor). The catheter shall be operated within the body's largest blood vessel, the inferior vena cava. Consequently, the pump must compensate for the blood flow resistance in the blood vessel generated by the inserted catheter. Furthermore, the blood pump is required to compensate for the pressure loss of the membrane packing in order to provide sufficient blood flow (approx. 1 L/min) for the targeted CO_2 exchange (40 mL STP CO_2/min – 20 % of metabolic CO_2 production [3]). Both the miniature blood pump and the membrane module were designed and assembled at the Technical University of Vienna. CO_2 removal performance tests of the membrane module, in this work generally referred to as prototype oxygenator, are described in Section 2.1.2, 2.1.3, and 2.1.4. The MILL catheter can be seen in Figure 2.6.

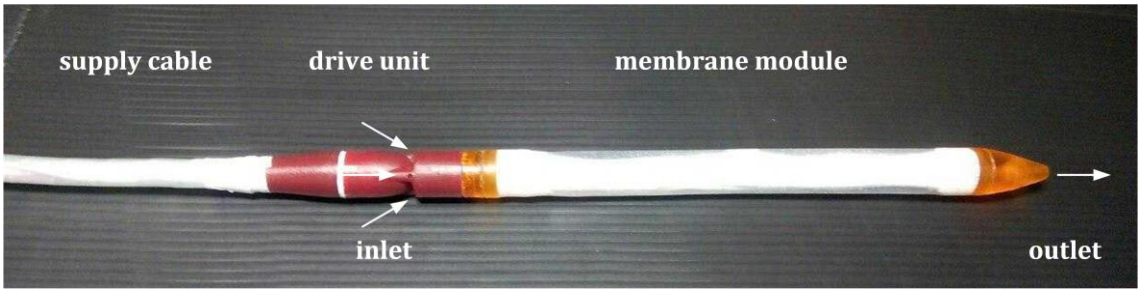

Figure 2.6. Prototype of the minimal invasive liquid lung (MILL) intravascular CO_2 removal catheter [**Reviewed Conference Publication I**].

Die approbierte gedruckte Originalversion dieser Dissertation ist an der TU Wien Bibliothek verfügbar.
The approved original version of this doctoral thesis is available in print at TU Wien Bibliothek.
TU Bibliothek Your knowledge hub WIEN

2.1.8.1 Flow Distribution Tests

In vitro tests were conducted to investigate the interaction between membrane module and catheter pump (Figure 2.7). A water-glycerol mixture (60 vol.% water and 40 vol.% glycerol) was used as a rheologic blood model. The catheter prototype was inserted into a silicone model of the inferior vena cava to produce flow conditions similar to the intended application. The pressure head of the catheter pump and pressure loss over the membrane were measured (AMS 4711, Analog Microelectronics). Flow rate (measured with an ultrasound flow probe - SONOFLOW CO.55/080) through the vena cava was set to physiological levels using a commercial centrifugal blood pump (BPX-80, Medtronic).[**Reviewed Conference Publication I**]

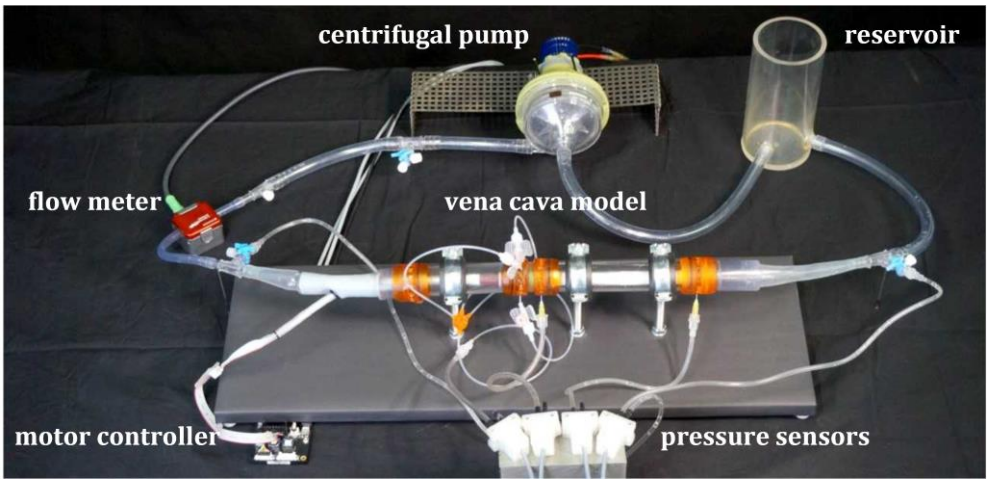

Figure 2.7. Flow distribution test setup [**Reviewed Conference Publication I**].

Based on the motor speed and pressure head of the catheter pump, the flow rate generated by the catheter pump could be estimated via the pump characteristics determined in pretests.

2.1.8.2 Viscosity Estimation Tests

Viscosity estimation tests were conducted to provide training data for a Gaussian regression model. It allows for the estimation of blood viscosity, pressure loss over the membrane packing, and blood flow rate based on motor speed and motor current. The test setup (Figure 2.8) comprises the catheter pump, a reservoir, and a throttle.

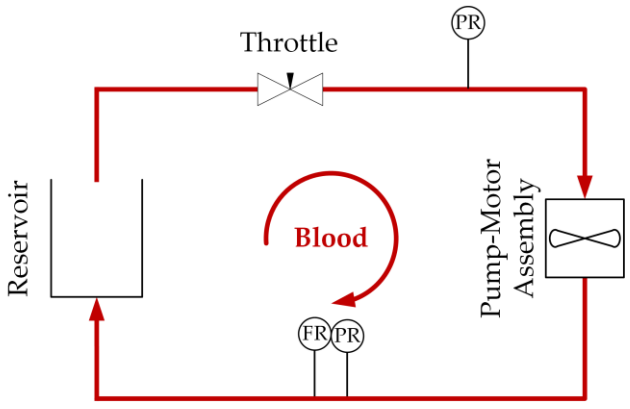

Figure 2.8. Scheme of the viscosity estimation tests.

Die approbierte gedruckte Originalversion dieser Dissertation ist an der TU Wien Bibliothek verfügbar.
The approved original version of this doctoral thesis is available in print at TU Wien Bibliothek.
TU Bibliothek Your knowledge hub WIEN

The throttle was used to set different flow resistances in the circuit. The catheter pump was driven by an ECX-8 motor (Maxon Group). Before and after the catheter pump the pressure was measured (PR - AMS 4711, Analog Microelectronics). The flow rate was measured via an ultrasound flow probe (FR - SONOFLOW CO.55/080).

The tests were conducted with water-glycerol mixtures and bovine blood provided by the Teaching and Research Farm of the University of Veterinary Medicine Vienna. The viscosity was variated either by adapting the glycerol content (water-glycerol mixture) or blood plasma content (adaption of bovine blood hematocrit) [**Journal Publication III**, **Journal Publication IV**].

2.2 Computational Fluid Dynamic Methods

The main focus of this work was the development of a Computational Fluid Dynamics (CFD) model to determine the CO_2 removal rate of a prototype oxygenator. In contrast to experiments, the CFD model allows a high temporal and spatial resolution of the flow inside the oxygenator. Therefore, through CFD, it is possible to resolve the main CO_2 transport resistance in oxygenators – the concentration polarization in the blood-side boundary layer. This allows a detailed evaluation of measures to reduce this resistance. In the following section, the main elements of the CFD model are described.

All CFD simulations were conducted using OpenFOAM® 4.1 (ESI Group).

2.2.1 Governing Transport Equations

In CFD, the governing transport equations of a flow, namely, mass (Eq. 2.2.1), momentum (Eq. 2.2.2), and energy balance (Eq. 2.2.3), are solved [117].

$$\frac{\partial \rho}{\partial t} + \nabla \cdot (\rho \boldsymbol{u}) = 0 \qquad 2.2.1$$

$$\frac{\partial \rho \boldsymbol{u}}{\partial t} + \nabla \cdot \rho \boldsymbol{u}\boldsymbol{u} = -\nabla p + \nabla \cdot \mu(\nabla \boldsymbol{u} + \nabla^T \boldsymbol{u}) \qquad 2.2.2$$

$$\frac{\partial \rho c_p T}{\partial t} + \nabla \cdot \rho c_p T \boldsymbol{u} = \nabla \cdot k(\nabla T) \qquad 2.2.3$$

Here ρ [kg/m³] denotes the density, p [Pa] pressure, μ [Pa s] dynamic viscosity, **u** [m/s] fluid velocity, T [K] temperature, k [W/(m K)] thermal conductivity, and c_p [J/(kg K)] the specific heat capacity. In order to numerically predict the CO_2 separation rate of oxygenators, the partial mass balances (specie balances) are required [97], [110]

$$\frac{\partial \rho Y_i}{\partial t} + \nabla \cdot \rho Y_i \boldsymbol{u} = \nabla \cdot D_i(\nabla Y_i) \qquad 2.2.4$$

with Y_i [kg/kg] the mass fraction of species i and D_i [m²/s] the corresponding diffusion coefficient.

The moderate velocities (approx. 0.1 m/s) within the packing, the small spacing between fibers (approx. 200 μm) [**Journal Publication II**], and the whole blood viscosity of approx. 2.3 10^{-6} m²/s [89] produce Re numbers of approx. 10. Hence, additional transport equations for turbulence modeling are mainly not required.

The governing transport equations are formulated via the conservative finite volume method. Hence the differential equations are integrated over the control volume.

Die approbierte gedruckte Originalversion dieser Dissertation ist an der TU Wien Bibliothek verfügbar.
The approved original version of this doctoral thesis is available in print at TU Wien Bibliothek.
TU Bibliothek Your knowledge hub WIEN

2.2.2 Implementation of Transmembrane Transport

The transmembrane transport was implemented as a volumetric source term added to the governing transport equations (Eq. 2.2.1- 2.2.4).

$$\frac{\partial \rho}{\partial t} + \nabla \cdot (\rho \boldsymbol{u}) = S_m = \sum S_{m,i} \quad 2.2.5$$

$$\frac{\partial \rho \boldsymbol{u}}{\partial t} + \nabla \cdot \rho \boldsymbol{u}\boldsymbol{u} = -\nabla p + \nabla \cdot \mu(\nabla \boldsymbol{u} + \nabla^T \boldsymbol{u}) + S_m \boldsymbol{u} \quad 2.2.6$$

$$\frac{\partial \rho c_p T}{\partial t} + \nabla \cdot \rho c_p T \boldsymbol{u} = \nabla \cdot k(\nabla T) + \sum S_{m,i}\, c_{p,i} T + \sum S_{m,i}\, \Delta h_{cond,i} = \nabla \cdot k(\nabla T) \quad 2.2.7$$

$$\frac{\partial \rho Y_i}{\partial t} + \nabla \cdot \rho Y_i \boldsymbol{u} = \nabla \cdot D_i(\nabla Y_i) + S_{m,i} \quad 2.2.8$$

With S_m [kg/(m³ s)] the sum of all transmembrane species fluxes $S_{m,i}$ [kg/(m³ s)], $c_{p,i}$ [J/(kg K)] the specific heat capacity and $\Delta h_{cond,i}$ [J/(kg)] the specific condensation enthalpy of species i.

Transmembrane specie flux $S_{m,i}$ is calculated for every computational cell adjacent to the membrane based on specie permeance P_i [kg/(m² s Pa)] and partial pressure difference Δp_i [Pa] between the one cell (e.g., in the blood region) and the neighboring cell on the other side of the membrane (e.g., in the sweep flow region).

$$S_{m,i} = P_i \, \mathrm{A} \, \Delta p_i / V \quad 2.2\ 2.2.9$$

With A [m²], the membrane surface shared by the cells of the two different regions, and V [m³], the cell volume of the cell to which the source term is applied.

2.2.3 Discretization Schemes

Since in technically relevant problems, the finite volume formulation of the governing transport equations cannot be solved analytically, they are discretized spatially and temporally and are then numerically solved. Hence, discretization of the transport equations requires various discretization schemes for the spatial and temporal derivatives. Only stationary flow problems were investigated in this work, omitting the necessity for highly accurate time discretization schemes. For spatial discretization, the second-order unbound Van Leer scheme was applied to increase the accuracy of the solution [118].

2.2.4 Computational Mesh

2.2.4.1 Computational Mesh of the Prototype Oxygenator

The spatial discretization of the geometry has to be provided as a computational mesh. Mesh resolution must be fine enough to resolve the physical processes of interest but low enough to limit computational costs to an acceptable amount [119].

Figure 2.9 shows the geometry and computational mesh of the prototype oxygenator investigated. Due to the complexity of the geometry, the effort to produce a computational mesh is extensive.

Die approbierte gedruckte Originalversion dieser Dissertation ist an der TU Wien Bibliothek verfügbar.
The approved original version of this doctoral thesis is available in print at TU Wien Bibliothek.
TU Bibliothek Your knowledge hub WIEN

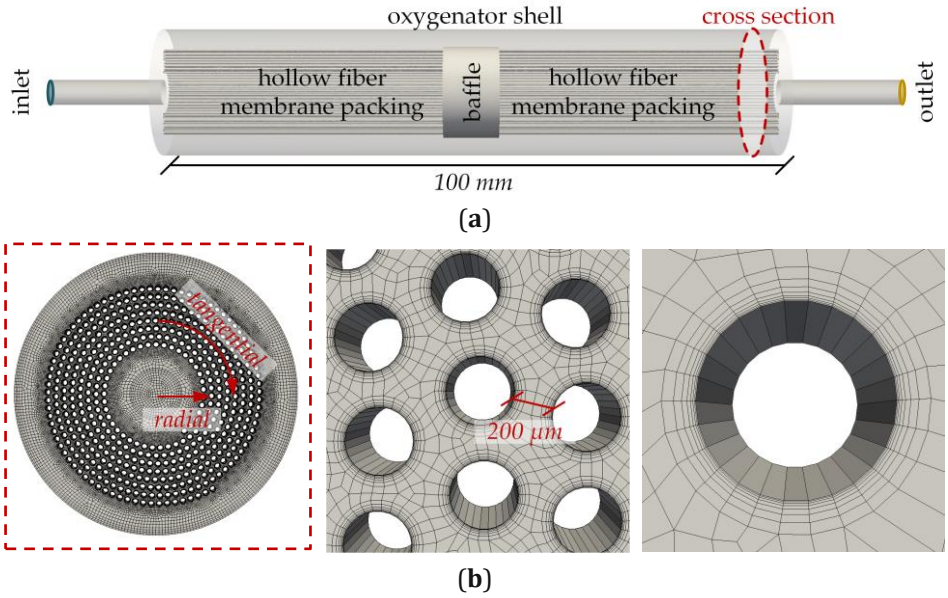

Figure 2.9. The geometry of the prototype oxygenator investigated: (**a**) Cross-section in side view; (**b**) Cross-section of the fiber packing with close up on the boundary layer mesh of the fibers. Adapted from Lukitsch et al. [**Journal Publication VIII**] (CC BY 4.0)

A relatively fine mesh is needed to resolve the narrow spacings in the fiber packing (approx. 200 µm, Figure 2.9b center). Consequently, cell size in the radial and tangential direction (Figure 2.9b left) variated from 87 µm (cells in the packing) to 175 µm (cells outside the packing, Figure 2.9b left). The resolution must be further increased to resolve the steep CO_2 concentration gradients towards the membrane wall. Therefore, ten cell layers were applied (Figure 2.9b right). The cell layer thickness decreases successively towards the membrane wall. The ratio of the most outer layer thickness to the most inner layer thickness equals 1:5. The thickness of the most inner layer measured 1.4 µm.

In the longitudinal direction, this high resolution is not needed due to the parallel arrangement of the fibers. However, to limit the numerically relevant aspect ratio of the computational cells [120], a longitudinal cell length of 350 µm was chosen. Due to the fiber length of 100 mm (Figure 2.9a) the total cell number amounts to 32 Mio. cells, inducing significant computational effort to the CFD computations.

In order to guarantee a high mesh quality of the computational grid, the commercial meshing software Gambit 2.4.6 (ANSYS) was utilized [**Journal Publication I**]. While Gambit comes with significantly higher manual effort than other automatic meshing algorithms, it provides a high level of cell refinement and cell size control. Furthermore, the automatic algorithms tested (SnappyHexMesh – OpenFOAM® 4.1, ESI Group; cfMesh 1.1, Creative Fields Holding LTD) could not generate the required cell layers at the membrane. Gambit allowed to discretize the geometry using only hexahedron cells. Hence, the complex geometry could be discretized as a mesh showing only low un-orthogonality. Since Gambit could not handle the complete cell number, the mesh produced by Gambit was later longitudinally refined in axial direction using *OpenFOAM*®.

Die approbierte gedruckte Originalversion dieser Dissertation ist an der TU Wien Bibliothek verfügbar.
The approved original version of this doctoral thesis is available in print at TU Wien Bibliothek.
TU Bibliothek Your knowledge hub WIEN

2.2.4.2 Computational Mesh of the Membrane Packing

Due to the high number of cells necessary to adequately resolve the geometry of the prototype oxygenator, CFD CO_2 transport simulations were conducted on a packing segment. The smaller mesh size allowed to reduce the computational effort and could be used for:

i. Mesh independency studies for the cell boundary layer at the membrane.
ii. Plausibility studies to test the chosen material models for blood and sweep fluid.
iii. Testing of the numerical setup in regards to stability and convergence.

A fully parameterized computational grid for a single fiber was developed for the mesh dependency study based on the OpenFOAM® utility BlockMesh [**Journal Publication I**]. This allows an exact definition of the grid resolution at precisely defined areas and generation of meshes consisting only of hexahedron cells. Figure 2.10 shows three grids generated for the mesh dependency study with different resolutions (coarse, medium, fine). In addition, the calculated Grid Convergence Index (GCI) is shown. It estimates the error of the numerical solution due to the chosen mesh [121]. Based on the GCI, it can be deduced that a suitable computational grid should have at least the medium resolution in the boundary layer area.

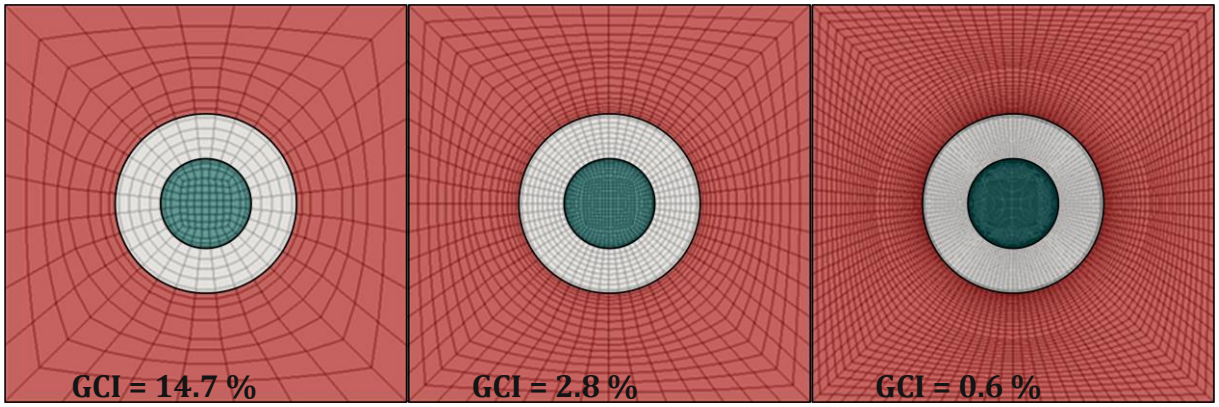

Figure 2.10. Coarse, medium, and fine computational mesh of a single hollow fiber membrane including shell side (red), membrane wall (grey), and lumen (green).

A python script was written for the meshing of a membrane packing [**Journal Publication I**]. The script takes the mesh of a single fiber and uses it to assemble the mesh of a packing. The fiber length, -diameter, -wall thickness, and spacing can be varied and the number of fibers and their arrangement (staggered, non-staggered) can be defined. This allowed producing high-quality grids (Figure 2.11). They were utilized to validate the flow fields determined with CFD simulations via µPIV measurements [**Journal Publication V**].

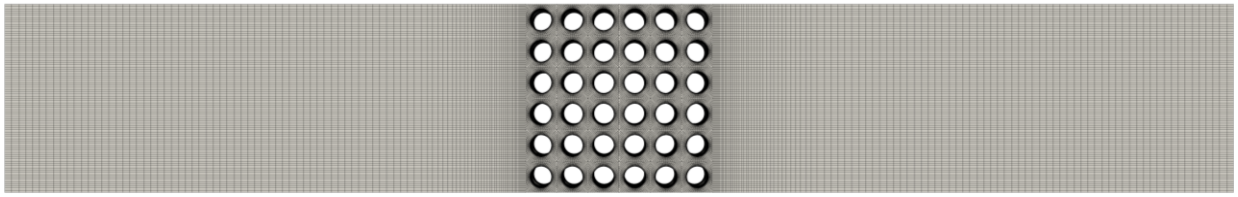

Figure 2.11. Mesh for validation of the flow field via µPIV-Measurement data. The packing segment was assembled from computational grids of a single fiber (Figure 2.10).

Die approbierte gedruckte Originalversion dieser Dissertation ist an der TU Wien Bibliothek verfügbar.
The approved original version of this doctoral thesis is available in print at TU Wien Bibliothek.
TU Bibliothek Your knowledge hub WIEN

2.2.5 Solver

In order to consider the transmembrane transport, an in-house developed multi-region solver (membraneFOAM) was utilized and adapted to the separation problem investigated in this work. The solver solves the transport equations of the single regions, which are divided by the membrane independently. However, the different regions are coupled by transmembrane transport. The latter is implemented as a volumetric source term in the transport equations for all cells attached to the membrane surface (Section 2.2.2).

Transmembrane transport is calculated based on the driving force across the membrane. While the solver can handle different driving forces, the partial pressure difference between the computational cell and its neighbor cell on the other side of the membrane is utilized in this work. If there is no direct neighbor cell (non-conformal mesh between the regions), the partial pressure can be interpolated based on nearby values using various schemes. This is possible since the partial pressure boundary field is mapped to the neighbor region. In Figure 2.12 the basic structure of the solution algorithm is illustrated.

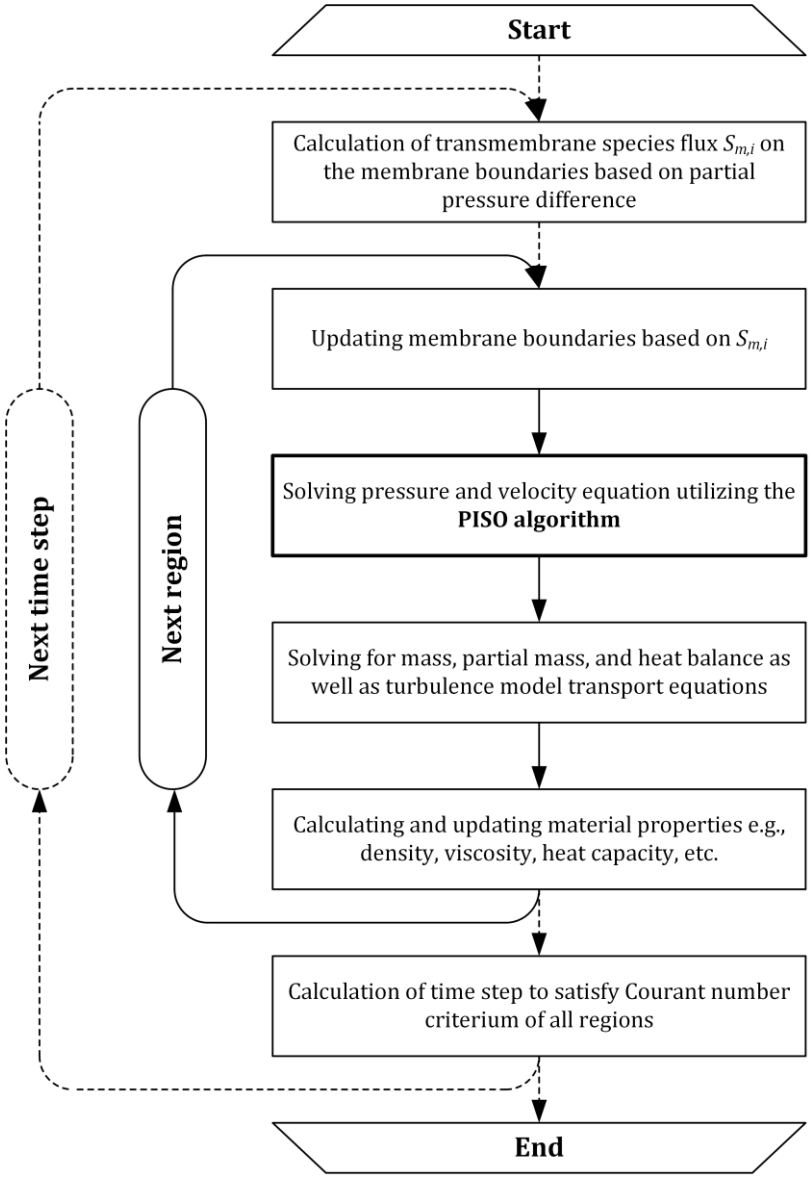

Figure 2.12. Workflow of the solving algorithm adapted from [98].

Die approbierte gedruckte Originalversion dieser Dissertation ist an der TU Wien Bibliothek verfügbar.
The approved original version of this doctoral thesis is available in print at TU Wien Bibliothek.
TU Bibliothek Your knowledge hub WIEN

At the beginning of the computation of each timestep, the transmembrane flux is calculated. Then for every region, the transmembrane flux is applied as a volumetric source term to the computed fields. Subsequently, velocity and pressure equations (deductions of the mass and momentum balances) are solved using the PISO algorithm to gain the velocity and pressure fields [122]. Afterward, the equations of the mass fractions and temperature are solved. Finally, the material properties are updated. After this is done for every region, the computation of the next time step starts.

2.2.6 Upscaling Method

Due to the complexity of the applied solver (membraneFoam) and the high number of computational cells necessary to adequately resolve the whole prototype oxygenator, an upscaling method was developed [**Journal Publication II**].

The upscaling method uses CFD flow simulations of a complete or representative part of a hollow fiber module (Figure 2.9a) and samples the velocities within this packing (Figure 2.13a,b). Flow simulations are significantly less expensive than species transport simulations due to three reasons. First, the required solvers are less complex and hence faster. Second, the concentration polarization towards the membrane must not be resolved, reducing the cell count significantly. Third, mass transport in the membrane and sweep flow region can be neglected.

The sampled velocities are then used to calculate an average velocity that can be used to calculate the inlet velocity boundary condition of the reduced geometry (Figure 2.13c). In this way, the method allows the flow conditions in the reduced geometry to represent the flow regime in the complete fiber packing. CO_2 transport simulations of the reduced geometry can then provide an accurate prediction of the average transmembrane flux of the whole geometry. Figure 2.14 shows the workflow of this upscaling method.

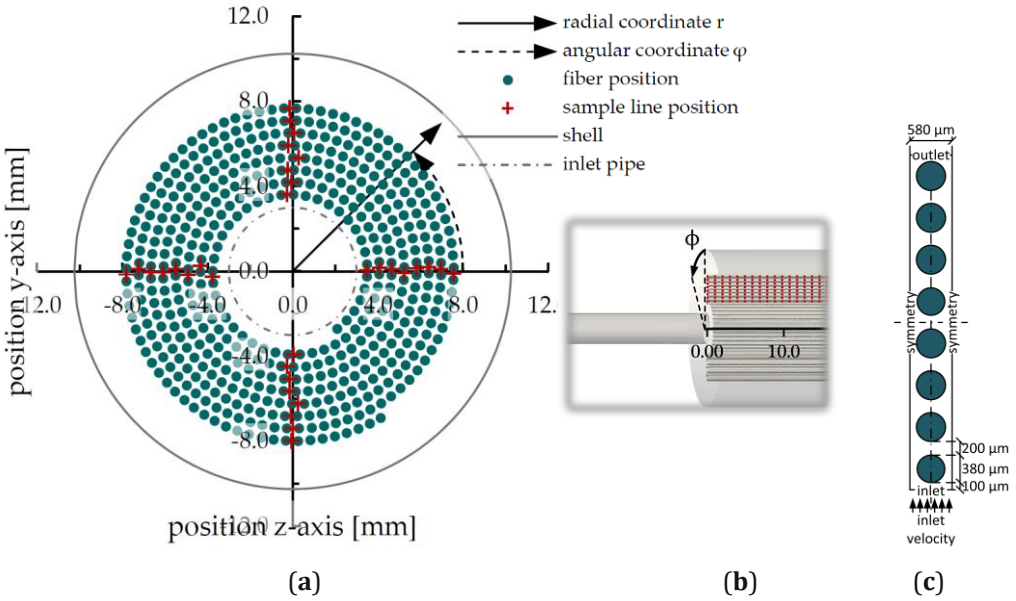

Figure 2.13. Packing geometry: (**a**) Scheme of the prototype oxygenator fiber arrangement including sampling line positions; (**b**) Longitudinal distribution of sample points; (**c**) Scheme of reduced geometry for CO_2 transport simulations. Adapted from Lukitsch et al. [**Journal Publication II**] (CC BY 4.0)

Die approbierte gedruckte Originalversion dieser Dissertation ist an der TU Wien Bibliothek verfügbar.
The approved original version of this doctoral thesis is available in print at TU Wien Bibliothek.
TU Bibliothek Your knowledge hub WIEN

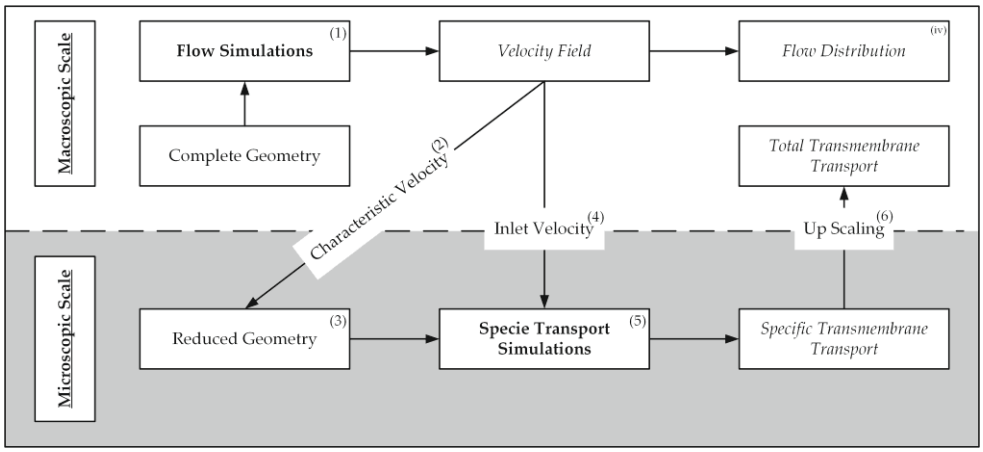

Figure 2.14. Workflow of the upscaling method. By Lukitsch et al. [**Journal Publication II**] (CC BY 4.0).

The described upscaling method was validated for the CO_2 removal performance of the prototype oxygenator for blood [**Journal Publication II**] and water [**Journal Publication VIII**].

2.2.7 Material Properties Blood

Examining the transport equations (Section 2.2.2), the essential material properties can be identified. These are:

i. The Viscosity, which influences the flow distribution significantly.
ii. The CO_2 solubility, which is needed to calculate the partial pressure (driving force for transmembrane flux) based on the mass fractions.
iii. The CO_2 diffusion coefficient, since it characterizes the main transport resistance, the CO_2 concentration polarization located in the boundary layer.

Thermal material properties play only a minor role due to the isothermal conditions ensured by the heat exchanger installed in the oxygenator.

2.2.7.1 Viscosity

Blood viscosity results from multiple characteristics like the viscosity of blood plasma, red blood cell (RBC) aggregation, RBC deformation, and the interaction between plasma and RBC. Due to these features, blood generally shows shear thinning properties [89]. The typical shear thinning behavior can be seen in Figure 2.15.

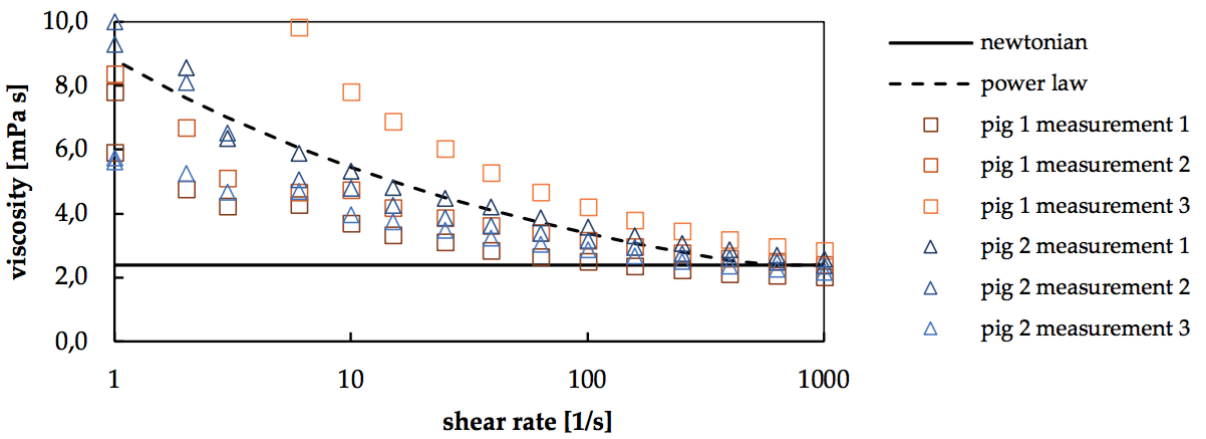

Figure 2.15. Shear rate dependency of the whole blood viscosity of porcine blood. By Lukitsch et al. [**Journal Publication II**] (CC BY 4.0).

Die approbierte gedruckte Originalversion dieser Dissertation ist an der TU Wien Bibliothek verfügbar.
The approved original version of this doctoral thesis is available in print at TU Wien Bibliothek.
TU Bibliothek Your knowledge hub WIEN

Numerous models have been proposed for the whole blood viscosity of human blood [123]. However, to validate CFD models or to extend experimental data with CFD, blood viscosity models of animals are of interest since in vitro and in vivo tests are primarily conducted with animal blood. In the course of this research, data supplied by the Medical University of Vienna was used to derive mathematical models which describe the influence of hematocrit, temperature, and shear rate on the whole blood viscosity of humans, pigs, sheep, and horses [**Journal Publication VII**].

Additionally, whole blood viscosity of the blood used in in vitro and in vivo tests was measured (Section 2.1.5) to minimize errors induced by the viscosity model during validation of the CFD methods. For the CFD simulations, the following simple but accurate power-law model was applied.

$$\mu = \max(\mu_{min}, \min(\mu_{max}, \mu_0 \cdot \dot{\gamma}^{n-1})) \qquad 2.2\ 2.2.10$$

Here μ is the dynamic whole blood viscosity [Pa s], μ_{min} represents the Newtonian viscosity at high shear rates (Figure 2.15), μ_{max} can be considered as a numerical limiter to improve stability at the initial phase of the computations, μ_0 and n are empirical parameters, and $\dot{\gamma}$ is the shear rate [1/s]μ_{min} (2.38 mPa), μ_0 (8.81 mPa), and n (0.792) were determined via regression of the measurement data (Section 2.1.5).

2.2.7.2 CO_2 Solubility

The CO_2 solubility model is used to calculate the blood side driving force for transmembrane flux, the CO_2 partial pressure. Hence, a suitable selection of the CO_2 solubility model is crucial to predict the transmembrane flux via CFD accurately.

In the course of this work, four CO_2 solubility models commonly used for human blood were investigated regarding their suitability for bovine and porcine blood (Section 2.1.6 [**Journal Publication VI**]). This allowed to reduce errors induced by the CO_2 solubility model during validation of the CFD methods. The data shows that the simplest model proposed by Loeppky [124] gives the most accurate results.

$$c_{CO2,total} = q \cdot p_{CO2}^{t} \qquad 2.2.11$$

Here q (0.128 mL STP CO_2/mL/mmHg$^{0.369}$), t (0.369 [-]) are empirical parameters, p_{CO2} denotes the CO_2 partial pressure [mmHg], and $c_{CO2,total}$ the total CO_2 concentration [mL STP CO_2/mL] which can be derived from CO_2 mass fractions. An adaption of the empirical parameters to either porcine or bovine blood gives no significant reduction of the solubility model error.

2.2.7.3 CO_2 Diffusion Coefficient

As the partial pressure was calculated based on the total CO_2 concentration in blood (Section 2.2.7.3), the different CO_2 species – physically dissolved CO_2, bicarbonate, and carbaminohemoglobin – were not considered explicitly but summarized as one total CO_2 species.

Die approbierte gedruckte Originalversion dieser Dissertation ist an der TU Wien Bibliothek verfügbar.
The approved original version of this doctoral thesis is available in print at TU Wien Bibliothek.
TU Bibliothek Your knowledge hub WIEN

Hence the corresponding total CO_2 diffusion coefficient has to consider the contribution of physically dissolved CO_2 and bicarbonate to the total diffusive CO_2 transport. The diffusion of carbaminohemoglobin can be neglected since CO_2 is bound to the relatively large hemoglobin molecule located in the RBC. Consequently, the total diffusive CO_2 transport can be written as

$$-D_{CO2,total}\nabla c_{CO2,total} = -D_{CO2}\nabla c_{CO2} - D_{HCO3^-}\nabla c_{HCO3^-} \quad 2.2.12$$

with $D_{CO2,total}$ the total CO_2 diffusion coefficient of all CO_2 species [m^2/s], D_{CO2} the diffusion coefficient of physically dissolved CO_2 [m^2/s], D_{HCO3^-} the diffusion coefficient of bicarbonate [m^2/s], $c_{CO2,total}$ the total CO_2 concentration [-], c_{CO2} the concentration of physical dissolved CO_2 [-], and c_{HCO3^-} the concentration of bicarbonate [-].

The derivation of the total CO_2 concentration by the partial pressure (λ_{CO2} [1/mmHg]) can be approximated as constant at elevated, clinically relevant CO_2 partial pressure levels. Hence, the following relationship can be derived [**Journal Publication I**]

$$D_{CO2,total} = D_{HCO3^-} + (D_{CO2} - D_{HCO3^-})\ \frac{\alpha_{CO2}}{\lambda_{CO2}} \quad 2.2.13$$

when utilizing α_{CO2} the solubility of physically dissolved CO_2 in blood plasma [1/mmHg]. The values for the different parameters can be taken from Table 2.1.

Table 2.1. Summary of material parameters required for the total diffusion coefficient ($D_{CO2,total}$). [93]

Symbol	Description	Units	Value
α_{CO2}	solubility of CO_2 in blood	mL CO_2 STP/mL/mmHg	6.62 E-04
D_{CO2}	diffusivity of CO_2 in blood	m^2/s	4.62 E-10
D_{HCO3^-}	diffusivity of HCO_3^- in blood	m^2/s	7.39 E-10
λ_{CO2}	slope of CO_2 dissociation curve	mL CO_2 STP/mL/mmHg	4.25 E-03

2.2.8 Material Properties Water

Reliable data for the material properties of water can be found in the NIST webbook [125]. Consequently, the material properties of water were taken from literature without any additional experimental investigations. A summary of the required material parameters can be found in Table 2.2.

Table 2.2. Summary of water material properties. [125]

Symbol	Description	Units	Value
$H_{CO2,w}$	Henry´s law constant for CO_2 in water	mL CO_2 /mL/mmHg	8.27 E-4 [126]
$D_{CO2,w}$	diffusivity of CO_2 in water	m^2/s	2.38 E-9 [127]
ρ_w	density of water	kg/m^3	993.33 [128]
μ_w	dynamic viscosity of water	Pa s	6.91 E-04 [129]

2.2.8.1 Viscosity

Constant values for viscosity and density of water at 37 °C were taken from Wagner et al. [130] and Kestin et al. [131], respectively.

2.2.8.2 CO_2 Diffusion Coefficient

The CO_2 Diffusion coefficient was taken from Himmelblau [127].

Die approbierte gedruckte Originalversion dieser Dissertation ist an der TU Wien Bibliothek verfügbar.
The approved original version of this doctoral thesis is available in print at TU Wien Bibliothek.
TU Bibliothek Your knowledge hub WIEN

2.2.8.3 CO_2 Solubility

The driving force for transmembrane flux (partial pressure p_i [mmHg]) was calculated based on Henry's law

$$c_i = H_i \cdot p_i \quad 2.2.14$$

with H_i the Henry coefficient (solubility) [mL STP/mL/mmHg] and c_i the concentration of species i [mL STP/mL] [126].

2.2.9 Material Properties Sweep Gas

Material Properties of the sweep gas underly fewer complex phenomena than blood. Therefore, minor variations in the material properties of the investigated gasses can be expected. Consequently, the material properties of the gases were taken from literature without any additional experimental investigations. Furthermore, the findings of **Journal Publication I** indicate, that the gas side CO_2 transport resistance has limited influence on the overall transmembrane CO_2 flux under the investigated conditions. Hence, the gas side was neglected in the subsequent studies to save computational costs, omitting gas material properties.

2.2.9.1 Viscosity

Dynamic viscosity for each species (μ_i [Pa s]) considered in the gas phase (CO_2, O_2, N_2) was determined using Sutherland's formula

$$\mu_i = A_s \frac{\sqrt{T}}{1+T_s/T} \quad 2.2.15$$

with T the Temperature [K], and A_s (1.458 E-6 $K^{-0.5}$), T_s (110.4 K) empirical parameters for air [132].

2.2.9.2 CO_2 Diffusion Coefficient

The diffusion coefficient of CO_2 in O_2 (2.02 E-5 m^2/s) was taken from literature by Marrero and Mason [133].

2.2.9.3 CO_2 Solubility

The driving force for transmembrane flux (partial pressure – p_i [mmHg]) was calculated based on the assumption of an ideal gas mixture

$$p_i = p \cdot x_i \quad 2.2.16$$

with p the total pressure [mmHg], and x_i the mole fraction [-] of species i (Dalton's law).

Die approbierte gedruckte Originalversion dieser Dissertation ist an der TU Wien Bibliothek verfügbar.
The approved original version of this doctoral thesis is available in print at TU Wien Bibliothek.
TU Bibliothek Your knowledge hub WIEN

2.3 Alternative Modeling Approaches – Computation of Sherwood Number

2.3.1 Sherwood Mass Transfer Correlation

An alternative to complex and numerical expensive CFD species transport simulations are dimensionless Sherwood correlations. They allow to predict transmembrane flux based on the dimensionless Sherwood (Sh [-]), Reynold (Re [-]), and Schmidt (Sc) number. The mass transfer analogy for crossflow within a hollow fiber membrane packing then takes the form of

$$Sh = a \cdot Re^{b} \cdot Sc^{0.33} \tag{2.3.1}$$

with the empirical parameters a and b [96]. In order to account for the diffusion of bicarbonate and physically dissolved CO_2 in the blood, [93] proposed the following definitions for Sh and Sc:

$$Sh = \frac{k_{CO_2} \cdot d_{fiber}}{\alpha_{CO_2} \cdot D_f} \tag{2.3.2}$$

$$Sc = \frac{\nu_{blood}}{D_{eff}} \tag{2.3.3}$$

With the CO_2 mass transfer coefficient k_{CO2} [m/Pa/s], fiber diameter d_{fiber} [m], CO_2 solubility in blood α_{CO2} [1/Pa], facilitated diffusion D_f of CO_2 in blood [m^2/s], Newtonian kinematic viscosity of blood ν_{blood} [m^2/s], and effective diffusion D_{eff} of CO_2 in blood [m^2/s].

Definitions of D_f and D_{eff} are non-trivial and ambiguous. A popular proposal for D_f and D_{eff} was given by [93]. Sh and Sc for water can be calculated analogously to the definitions above by substituting D_f and D_{eff} with the diffusivity of CO_2 in water (Section 2.2.8).

Average transmembrane CO_2 flux j_{CO2} [m/Pa/s] can then be calculated utilizing the mass transfer coefficient k_{CO2} and the CO_2 partial pressure difference Δp_{CO2} [Pa] between water/blood bulk flow and sweep gas.

$$j_{CO_2} = k_{CO_2} \cdot \Delta p_{CO_2} \tag{2.3.4}$$

The empirical parameters a and b are a priori not known since they are dependent on the mass transfer characteristics, the hollow fiber packing arrangement, and flow guidance [97]. Consequently, for an accurate prediction of transmembrane flux, a and b must be determined experimentally. This poses the most significant disadvantage compared to CFD simulations, which can deal with differing geometries and flow guidance.

2.3.2 Simplified CFD Model

Modeling the CO_2 transport within the blood flow as a passive scalar allows omitting the empirical parameters a and b. Here, a transport equation of a passive scalar representing the CO_2 concentration (c_{CO2} [-]) is added to the mass, momentum, and energy balance (Eq. 2.2.1-2.2.3). This requires a significantly less complex solver architecture compared to the solver described in Section 2.2.5.

$$\frac{\partial c_{CO_2}}{\partial t} + \nabla\left(\boldsymbol{u} c_{CO_2}\right) = \nabla^2\left(D_{CO_2} c_{CO_2}\right) \tag{2.3.5}$$

Die approbierte gedruckte Originalversion dieser Dissertation ist an der TU Wien Bibliothek verfügbar.
The approved original version of this doctoral thesis is available in print at TU Wien Bibliothek.
TU Bibliothek Your knowledge hub WIEN

For reliable results, a suitable diffusion coefficient D_{CO2} [m^2/s] must be chosen, which adequately models the diffusion rate of CO_2 in blood [**Journal Publication V**]. The CO_2 transfer coefficient k_{CO2} [m/s] can then be estimated, assuming a value of zero for c_{CO2} at the membrane wall.

$$k_{CO_2} = -\frac{D_{CO_2}}{C_{CO_2,b}} \frac{\partial c_{CO_2}}{\partial n} \quad 2.3.6$$

Here $c_{CO2,b}$ [-] denotes the bulk flow value of c_{CO2} and n [m] the orthogonal vector component of the membrane wall. The CO_2 transfer coefficient allows the calculation of a local Sherwood number Sh [-] using a characteristic length d [m].

$$Sh = \frac{k_{CO_2} d}{D_{CO_2}} \quad 2.3.7$$

While this model has advantages due to the lower complexity compared to the proposed CFD model (Section 2.2.5) and the independence of empirical parameters required by the Sherwood correlation, it only allows for a qualitative assessment of transmembrane flux since the membrane resistance is neglected and a total CO_2 removal is assumed at the membrane wall (c_{CO2} of zero at the membrane wall).

Die approbierte gedruckte Originalversion dieser Dissertation ist an der TU Wien Bibliothek verfügbar.
The approved original version of this doctoral thesis is available in print at TU Wien Bibliothek.
TU Bibliothek Your knowledge hub WIEN

3 Publication Summary

3.1 Journal Publication Summary

3.1.1 Journal Publication I

Title: *Fully resolved computational (CFD) and experimental analysis of pressure drop and blood gas transport in a hollow fibre membrane oxygenator module.*

In this paper, a CFD model which allows to resolve the CO_2 transport within a hollow fiber membrane packing of an oxygenator is presented. The model – membraneFOAM – is implemented in OpenFOAM an open-source CFD code that offers excellent flexibility and a solid fundament for efficient numerical optimization of oxygenators. Similar to comparable codes in literature, membraneFOAM resolves the blood region within the membrane packing. In addition, the membrane wall and the sweep gas region in the fiber lumen can be resolved.

The CFD simulations show that the decrease in CO_2 partial pressure (the driving force of transmembrane CO_2 flux) is strongest in the boundary layer of the blood flow (35 mmHg), followed by the drop across the selective membrane surface (12 mmHg) and the membrane wall (2 mmHg). No partial pressure gradient in the radial direction of the hollow fiber membranes can be observed in the lumen.

Besides computational analysis, in vitro experiments with bovine blood were conducted (Section 2.1.3) to determine the CO_2 removal performance of a prototype oxygenator. While it was possible to conduct flow simulations of the complete prototype oxygenator, the numerically expensive CO_2 transport simulations were limited to a small packing segment. Therefore, only the flow simulations were validated. Only a rough comparison between the numerically and experimentally determined CO_2 removal rate could be made.

The limitations of species transport simulations to small packings pointed out the necessity to find an upscaling method that allows transferring the findings of the CO_2 transport simulations (packing segments) on the scale of flow simulations (whole packings).

3.1.2 Journal Publication II

Title: *Computation of global and local mass transfer in hollow fiber membrane modules.*

In this publication, an upscaling method (Section 2.2.6) is presented that predicts the total CO_2 removal rate of oxygenators using CFD CO_2 transport simulations of a reduced geometry. First, CFD flow simulations of a complete or representative part of an oxygenator membrane packing are conducted. Then the velocities within this packing are sampled. The velocity samples are afterward used to calculate an average velocity. Based on the average velocity, inlet velocity boundary conditions of the reduced geometry are deduced. In doing so, the upscaling method ensures that the flow condition in the reduced geometry is representative of the flow regime within the complete packing. Consequently, CO_2 transport simulations of the reduced geometry give an accurate prediction of the average transmembrane flux.

Die approbierte gedruckte Originalversion dieser Dissertation ist an der TU Wien Bibliothek verfügbar.
The approved original version of this doctoral thesis is available in print at TU Wien Bibliothek.
TU Bibliothek Your knowledge hub WIEN

In order to validate the upscaling method, in vivo trials (Section 2.1.4) were conducted. In the experiments, the CO_2 removal rate of a prototype oxygenator was determined at nine measuring points (three CO_2 partial pressures at three blood flow rates). A maximum deviation of 7 % between experimental and numerically determined CO_2 removal was recorded. Since the CFD simulations could predict the influence of the CO_2 partial pressure and the blood flow rate on the CO_2 removal rate, it was possible to validate both the upscaling method and the CFD CO_2 transport model presented in **Journal Publication** I.

3.1.3 Journal Publication III

Title: *Estimation methods for viscosity, flow rate and pressure from pump-motor assembly parameters.*

This work presents an estimation method based on Gaussian process regression models. It allows estimating important control variables which cannot be measured directly since currently available sensors do not meet the spatial restrictions and long-term stability required in intracorporal medical assist devices. By estimating blood flow rate, whole blood viscosity, and pressure loss over the membrane (e.g., within oxygenators, dialysis systems), the reliability and accuracy of blood pump control systems in intracorporal medical assist devices can be improved.

In vitro tests with a prototype gas exchange catheter consisting of a miniature blood pump and a membrane packing were conducted (Section 2.1.8.2) to validate the estimation method. Different water–glycerol mixtures were used to model variations in the viscosity of blood. Additionally, flow rate and pressure loss over the membrane were measured. The viscosity, flow rate, and pressure loss were estimated from motor current and motor speed measurements. The presented method can be used to accurately (coefficient of determination approx. 0.98) predict blood flow rate, pressure, and viscosity online.

3.1.4 Journal Publication IV

Title: *Non-parametric dynamical estimation of blood flow rate, pressure difference and viscosity for a miniaturized blood*.

This work presents an estimation method based on Gaussian process regression models for intracorporal gas exchange catheter systems. The gas exchange catheter comprises two main components: a membrane packing for the gas exchange and a miniature blood pump to compensate for the pressure loss induced by the membrane packing and the catheter itself. The method estimates whole blood viscosity, blood flow rate, and pressure loss over the membrane packing based on motor current and motor speed measurement. While the proof of concept has been delivered in previous work for water-glycerol as a blood model (Newtonian fluid) [**Journal Publication III**], this work aims to validate the estimation method for an animal blood model (shear-thinning fluid).

Consequently, in vitro trials with bovine blood were conducted (Section 2.1.8.2). In the course of the tests, hematocrit was adjusted to 11 different levels in order to vary whole blood viscosity. Additionally, the flow rate through and pressure loss across the membrane of the gas exchange catheter was measured. The results suggest that this method can estimate essential hydrodynamic parameters with high accuracy (coefficient of determination approx. 1) online.

Die approbierte gedruckte Originalversion dieser Dissertation ist an der TU Wien Bibliothek verfügbar.
The approved original version of this doctoral thesis is available in print at TU Wien Bibliothek.
TU Bibliothek Your knowledge hub WIEN

3.1.5 Journal Publication V

Title: *Microstructured hollow fiber membranes: Potential fiber shapes for extracorporeal membrane oxygenators.*

In this paper, a Sherwood number-based CFD model was used (Section 2.3.2) to estimate the influence of microstructured hollow fiber membranes on the CO_2 removal performance of oxygenators. While the CFD model is not capable of considering the CO_2 transport resistance induced by the membrane [**Journal Publication I**], it is less computationally expensive and allows for a qualitative assessment of different fiber geometries regarding CO_2 removal performance. In order to validate the numerically determined flow field, micro-particle image velocimetry experiments were conducted.

The CFD simulation showed that an increase in surface area to volume ratio leads to increased areas with low flow. In addition to an increased formation of concentration polarization, this also leads to an increased risk of thrombus formation. Therefore, increasing the specific surface area by modifying the membrane profile does not automatically lead to improved oxygenator performance. However, suitable fiber geometries allow for a 48 % increase in CO_2 flux compared to the conventional circular geometry.

3.1.6 Journal Publication VI

Title: *Suitable CO_2 solubility models for determination of the CO_2 removal performance of oxygenators.*

In this work, the general performance of the CO_2 removal determination based on blood side measurements (blood-based method) is evaluated and discussed. Furthermore, model prediction errors of four different CO_2 solubility models were quantified (Section 2.1.6). Therefore, the CO_2 removal of a prototype oxygenator was determined using the sweep flow-based and the blood-based method (Section 2.1.3 and 2.1.4). The predictions of both methods were compared. This was done for in vitro trials using bovine blood (Section 2.1.3) and in vivo trials using porcine blood (Section 2.1.4).

The results show that the simplest CO_2 solubility model (Loeppky [124]) is more robust and performs better than the more complex models. Evaluation of the obtained data suggests that the original parameters of this model can be considered generic and suitable for bovine and porcine blood. Compared to the simplest model, the more complex models show a significantly better performance for in vitro bovine blood data than in vivo porcine blood data. However, these models are susceptible to pH as an input parameter, making them prone to high variations in their prediction performance. For the best performing model (Loeppky), the average deviation of the blood-based CO_2 removal rate from the sweep flow-based CO_2 removal rate is 31 % for in vitro bovine blood data and 23 % for in vivo porcine blood data.

Die approbierte gedruckte Originalversion dieser Dissertation ist an der TU Wien Bibliothek verfügbar.
The approved original version of this doctoral thesis is available in print at TU Wien Bibliothek.
TU Bibliothek Your knowledge hub WIEN

3.1.7 Journal Publication VII

Title: *Animal blood in translational research: How to adjust animal blood viscosity to the human standard.*

This work conducted viscosity measurements of human, porcine, equine, and ovine blood at different hematocrit, temperatures, and shear rates (Section 2.1.5). Based on a multi-linear regression approach, viscosity models were derived for each species. They reflect the dependence of hematocrit, temperature, and shear rate on blood viscosity.

Adequate consideration of blood viscosity is crucial for the reliability of performance tests of blood-contacting biomedical devices. Since the dependence of blood viscosity on hematocrit, temperature and shear rate differs significantly between animal species, the above-mentioned mathematical models are an essential basis for selecting the correct animal model for in vitro or in vivo tests. Furthermore, suitable viscosity models are necessary to extent experimental data with CFD simulation results (Section 2.2.7.1).

This study shows that porcine blood cannot be recommended for experiments at low flow conditions, although the erythrocyte properties are similar in pigs and humans. However, porcine blood mimics human blood excellently at high flow conditions. Horse blood consistently exhibited increased blood viscosity and is unsuitable as an experimental model in this regard. Under several conditions tested, sheep blood came closest to human blood viscosity of all species tested.

3.1.8 Journal Publication VIII

Title: *Water as a blood model for determination of CO_2 removal performance of membrane oxygenators.*

In this paper, the suitability of water as a blood model for predicting the CO_2 removal performance of oxygenators is evaluated. For this purpose, the CO_2 removal performance of a prototype oxygenator was determined in vitro using water as a blood substitute (Section 2.1.2). The results are compared to in vivo studies using porcine blood (Section 2.1.4). In general, the CO_2 removal rate of porcine blood and water is comparable despite differing fluid properties (CO_2 diffusion rate, CO_2 solubility, and viscosity). The deviation of the CO_2 removal rate determined with porcine blood from that of water amounts to approximately 10 %. This deviation agrees well with data found in recent literature.

To better understand this remaining difference and to assess the application limits of in vitro water tests, CFD simulations were conducted and validated based on the experimental results [**Journal Publication I**, **Journal Publication II**]. The CFD simulations quantify the partly opposing influences of the differing fluid properties of blood and water on the CO_2 removal rate. Our data indicate that the difference in CO_2 solubility between blood and water has the strongest effect on CO_2 removal rate, followed by the difference in CO_2 diffusion rate, and the difference in viscosity. Furthermore, the CFD simulations resolve the main CO_2 transport resistance in membrane oxygenators, the diffusional boundary layer attached to the membrane surface. The results suggest that the diffusional boundary layer generally behaves differently in blood and water. Hence, examinations of the CO_2 boundary layer (micro-scale) should preferably be conducted with blood. However, for the accurate determination of the total CO_2 removal performance of oxygenators (macro-scale), water tests can be considered suitable.

Die approbierte gedruckte Originalversion dieser Dissertation ist an der TU Wien Bibliothek verfügbar.
The approved original version of this doctoral thesis is available in print at TU Wien Bibliothek.
TU Bibliothek Your knowledge hub WIEN

3.2 Reviewed Conference Publication Summary

3.2.1 Reviewed Conference Publication I

Title: *Basic performance tests of the MILL intravascular CO_2 removal catheter.*

In this work, basic performance tests of the MILL intravascular CO_2 removal catheter were conducted (Section 2.1.8.1). The two main components of the catheter, the membrane module, and the miniature blood pump, were manufactured in-house. The in vitro tests utilizing a water-glycerol mixture as a blood model aimed to investigate the interaction between membrane module and pump. Therefore, the catheter prototype was inserted into a silicone model of the inferior vena cava.

In order to better understand the flow distribution in the vena cava, CFD simulations were conducted. To reduce CFD model complexity, flow through the pump and the membrane module was neglected by adding additional boundary conditions. While this decreased the computational costs, it also introduced model errors. Consequently, validation with the experimental data was only possible to a limited extent.

The tests showed that the miniature pump provides the membrane module with the required 1 L/min blood flow. However, the data suggest that catheter insertion could increase total pressure at the entrance of the right atrium. This pressure increase cannot be omitted by the miniature pump. CFD simulations also indicated a high-velocity jet at the outlet of the catheter and provided an impetus for future design revisions.

Die approbierte gedruckte Originalversion dieser Dissertation ist an der TU Wien Bibliothek verfügbar.
The approved original version of this doctoral thesis is available in print at TU Wien Bibliothek.
TU Bibliothek Your knowledge hub WIEN

4 Summary and Discussion

This work aims to assess and improve experimental and numerical (CFD) methods for investigating the CO_2 removal performance of oxygenators. Particular focus is placed on the initial development phase, in which the work is strongly characterized by engineering challenges such as design, assembly, and basic performance tests. Therefore, in this section, research results that collectively improve the development of oxygenator-based CO_2 removal are presented.

4.1 Summary and Discussion of Experimental Results

Reliable but simple experiments are essential for the efficient optimization of oxygenators. The use of human blood or animal blood models increases the experimental effort significantly [**Journal Publication VIII**]:

i. The use of blood is accompanied by animal suffering.
ii. The use of blood is not permitted in all technical laboratories.
iii. Test circuits get contaminated and must be rebuilt due to blood deposits.
iv. Additional logistical challenges arise due to the limited durability of blood.
v. An ethics committee approval must be obtained.

Consequently, water-based blood models can be used to reduce the experimental effort in earlier stages of oxygenator development.

4.1.1 Water-Based Hydrodynamic Models

Water-glycerol mixtures are commonly used in literature as hydrodynamic models of blood [85]. In contrast to blood, water-glycerol shows no shear thinning behavior. Consequently, the Newtonian viscosity of the mixture is commonly matched to the constant viscosity of blood at high shear rates via the glycerol content. Despite this simplification, it was demonstrated [**Journal Publication III**], [**Journal Publication IV**] that water-glycerol can be used to develop complex control algorithms for respiratory catheters. The investigated control algorithms show improved performance due to the estimation of viscosity, flow rate, and pressure loss across the membrane packing.

Substituting blood with water-glycerol decreased the experimental effort significantly since experiments with variating viscosities were required for algorithm training. Different levels of viscosity could be achieved relatively simply by changing the glycerol content. Compared to water-glycerol, an adaption of the blood viscosity via modification of the hematocrit was experimentally more extensive. First, the RBC were separated from blood plasma using a blood centrifuge. Then RBC and blood plasma were mixed in the required ratios.

The root mean square errors (RMSE) of the estimation algorithm for blood and water-glycerol are comparable, i.e., the deviations between the predicted and actual value of viscosity, flow rate, and pressure loss of the two liquids are in the same range (Table 4.1).

Die approbierte gedruckte Originalversion dieser Dissertation ist an der TU Wien Bibliothek verfügbar.
The approved original version of this doctoral thesis is available in print at TU Wien Bibliothek.
TU Bibliothek Your knowledge hub WIEN

Table 4.1. Comparison of root mean square errors (RMSE) of the estimated parameters for water-glycerol and bovine blood [**Journal Publication III**, **Journal Publication IV**].

Variable	Water-Glycerol [Journal Publication III]	Bovine Blood [Journal Publication IV]
Viscosity	0.049 mPa s	0.31 mPa s
Flow rate	46 mL/min	0.31 mL/min
Pressure loss	8.7 mmHg	0.09 mmHg

When comparing the RMSE of flow rate and pressure loss, it can be observed that the estimation method, which initially was tested for water-glycerol, performs even better for bovine blood (shows lower RMSE at comparable experimental conditions). Only RMSE of viscosity is increased for bovine blood by one order of magnitude. The elevated RMSE of bovine blood viscosity probably originates from its complex shear-thinning rheologic behavior. However, an RMSE of 0.31 mPa s can be considered reasonable at a mean viscosity of approx. 3.3 mPa s.

Water-glycerol also allowed to investigate the coupling of the catheter pump and the membrane module, providing critical information in the initial development of the respiratory catheter [**Reviewed Conference Publication I**].

A comparison of the pump characteristics measured for water-glycerol and bovine blood can be seen in Figure 4.1. The pump characteristics determined with water-glycerol and bovine blood match reasonable. However, the curve for water-glycerol is elevated, i.e., higher pressure heads occur at lower flow rates. The latter is due to the higher viscosity of the water-glycerol mixture used, which was matched to model human blood. Compared to bovine blood used, human blood is more viscous.

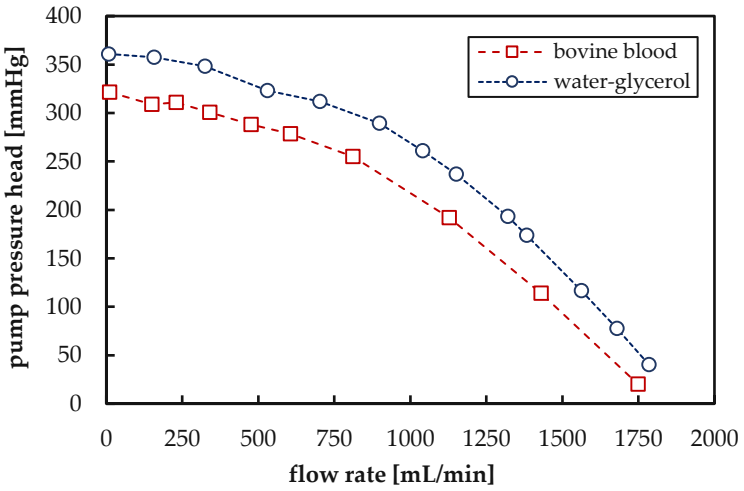

Figure 4.1. Comparison of pump characteristics measured with water-glycerol and bovine blood.

The suitability of water-glycerol mixtures in both test series can be attributed to the high rotational speed of the catheter pump and the associated high shear rates above 200 1/s (Section 2.2.7.1) [**Journal Publication VII**]. CFD studies have shown that this benchmark is also commonly exceeded in membrane packings [104]. At shear rates above 200 1/s, blood can be considered a Newtonian fluid [**Journal Publication VII**]. After thorough investigation, water-based rheological models for human blood can be considered suitable for hydrodynamic performance tests of oxygenators (**Experimental Objective I**).

Die approbierte gedruckte Originalversion dieser Dissertation ist an der TU Wien Bibliothek verfügbar.
The approved original version of this doctoral thesis is available in print at TU Wien Bibliothek.
TU Bibliothek Your knowledge hub WIEN

4.1.2 Water-Based CO_2 Transport Models

As discussed in [**Journal Publication VI**], water is commonly used in in vitro tests to determine the CO_2 removal of prototype oxygenators. However, in contrast to previous work, [**Journal Publication VI**] systematically quantifies the difference between the CO_2 removal rate determined with water and the CO_2 removal rate determined with blood. An average difference in CO_2 removal of approx. 10 % can be expected. Figure 4.2 compares the CO_2 removal rate measured for porcine blood and water at three different (blood/water) flow rates and three different CO_2 partial pressures.

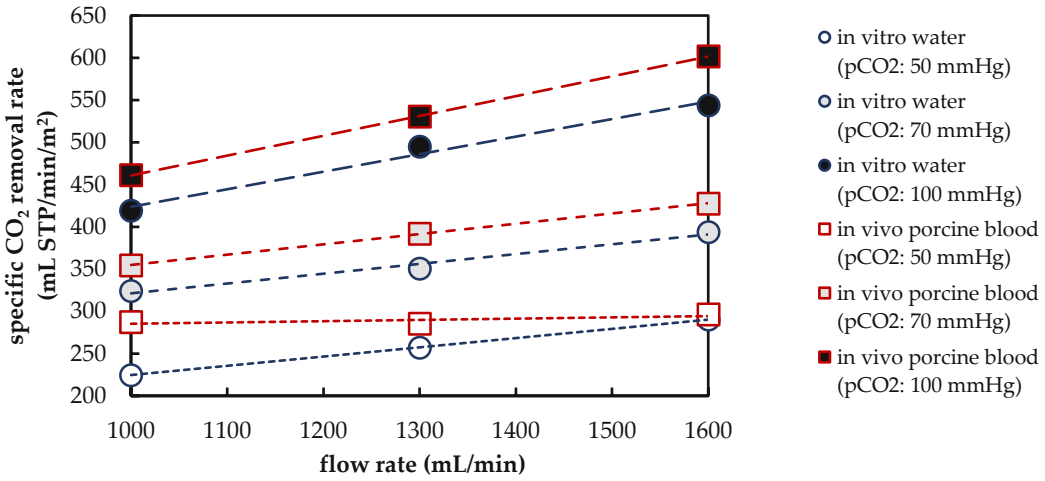

Figure 4.2. Comparison of experimentally determined CO_2 removal. Red squares: in vivo studies with porcine blood; blue circles: in vitro studies with water. By Lukitsch et al. [**Journal Publication VIII**] (CC BY 4.0).

Water can reasonably model the influence of the (blood/water) flow rate and CO_2 partial pressure on CO_2 removal (Figure 4.2). Consequently, water-based CO_2 transport models for human blood can be considered suitable to determine the macroscopic CO_2 removal rate of oxygenators (**Experimental Objective II**). However, it could be shown that the diffusive boundary layer – the main CO_2 transport resistance – behaves differently for blood and water (Section 4.2.5), limiting in vitro water tests to the macroscopic prediction of the CO_2 removal rate [**Journal Publication VI**].

4.1.3 Animal Blood Models for Hydrodynamic Models

While there are studies on the rheologic behavior of human blood [134], [135], literature that investigates and compares the whole blood viscosity of standard animal models to the whole blood viscosity of human blood is scarce. In the future, [**Journal Publication VII**] will provide a solid decision-making basis for selecting an appropriate animal model (**Experimental Objective III**). The study shows that the suitability of animal blood models is dependent on the biomedical application investigated. The differing dependency between whole blood viscosity (WBV) and shear rate of different animal species substantially characterizes the outcome of these experimental investigations. A comparison of WBV at three different shear rates for human, porcine, ovine, and equine blood is given in Figure 4.3. WBV was measured at physiological conditions with a packed cell volume (PCV) of 40 % and 37 °C.

Die approbierte gedruckte Originalversion dieser Dissertation ist an der TU Wien Bibliothek verfügbar.
The approved original version of this doctoral thesis is available in print at TU Wien Bibliothek.
TU Bibliothek Your knowledge hub WIEN

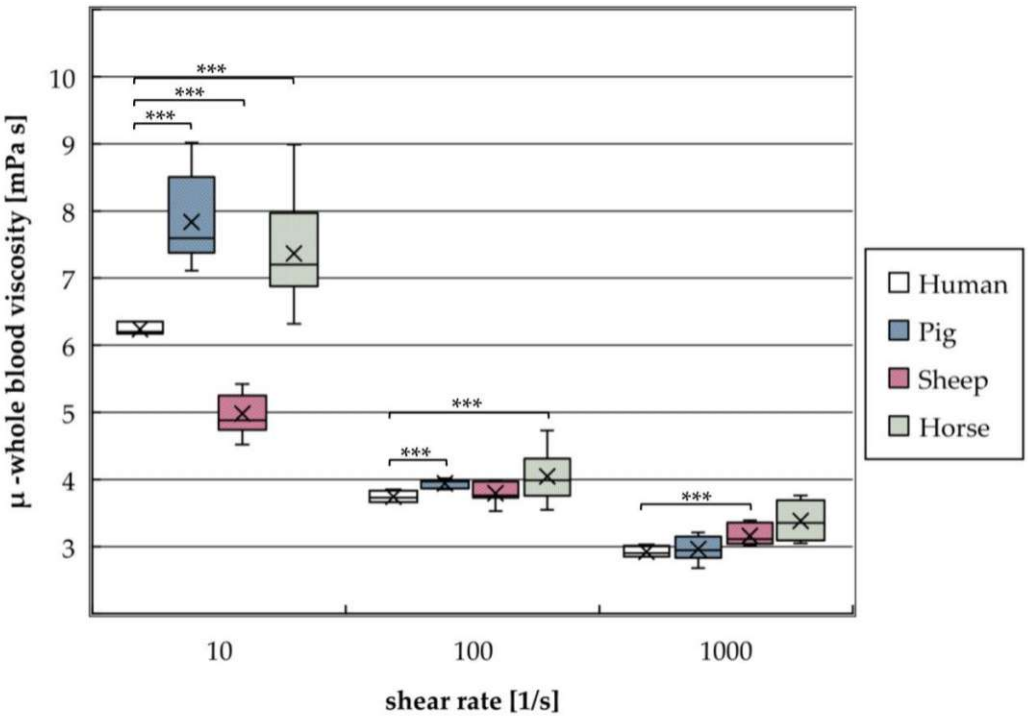

Figure 4.3. Shear rate dependency of whole blood viscosity (WBV) at physiological conditions: packed cell volume (PCV) 40 %, temperature 37 °C, for human, porcine, ovine, and equine blood. Brackets indicate significant differences (**p < 0.05, ***p < 0.01) between human and other species. adapted from [**Journal Publication VII**]

At low shear rates (10 1/s), the whole blood viscosity (WBV) of human blood differs significantly from all other investigated species. At intermediate shear rates (100 1/s), only human and ovine blood shows no significant difference in WBV. At elevated shear rates (1000 1/s), the WBV of porcine blood best matches that of human blood [**Journal Publication VII**].

While there is a significant difference of WBV between human and sheep blood at low and elevated shear rates, sheep blood provides the closest match to human blood over the investigated range of shear rates.

4.1.4 Animal Blood Models for CO_2 Transport

In this work, the CO_2 removal performance of oxygenators was not determined with human blood. Therefore, it cannot be quantified which animal blood model best fits human blood regarding CO_2 removal performance. However, in vitro experiments with bovine blood and in vivo experiments with porcine blood give comparable CO_2 removal rates for the investigated prototype oxygenator (Figure 4.4).

The average relative deviation between bovine blood and porcine blood CO_2 removal rate amounts to 14 %. The deviation increases with increasing CO_2 partial pressure from 10 % at 50 mmHg to 20 % at 100 mmHg. Furthermore, the deviation decreases with increasing blood flow rate from 17 % at 1000 mL/min to 12 % at 1600 mL/min.

Die approbierte gedruckte Originalversion dieser Dissertation ist an der TU Wien Bibliothek verfügbar.
The approved original version of this doctoral thesis is available in print at TU Wien Bibliothek.
TU Bibliothek Your knowledge hub WIEN

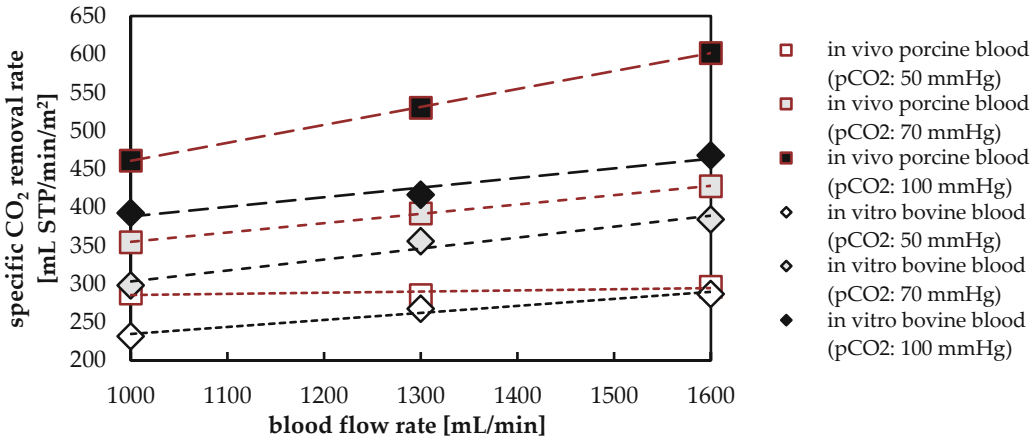

Figure 4.4. Comparison of experimentally determined CO_2 removal rate measured at three CO_2 partial pressures and blood flow rates. Red squares in vivo studies with porcine blood; black rhombuses in vitro studies with bovine blood.

The overall difference between the CO_2 removal rates measured for these two species is reasonable and lies within 22 %. This reasonable deviation in CO_2 removal rate for porcine and bovine blood, as well as the slight deviation in CO_2 removal rate between porcine blood and water (Section 4.1.2), indicates that the macroscopic CO_2 removal rate of bovine or porcine blood allows a reasonable estimate of the CO_2 removal rate of human blood. However, for a thorough evaluation of the suitability of animal blood as a CO_2 transport model for human blood (**Experimental Objective IV**), in vitro studies with human blood must have been conducted. To the author's best knowledge, a direct comparison of the CO_2 removal rate measured for animal and human blood is not available in the literature. Consequently, the deviation between the CO_2 removal rate in animal and human blood trials can not be specified.

4.1.5 Measurement of CO_2 Removal Performance

The CO_2 removal performance of an oxygenator can be determined by two methods. First, by measuring the CO_2 removal rate on the blood side (blood-based prediction method) and second, by measuring the CO_2 removal rate on the sweep gas side (sweep gas-based prediction method – Section 2.1.6). In literature, both methods are equally used [**Journal Publication VI**].

However, it could be shown that the CO_2 removal rate of an oxygenator can be measured more accurately on the sweep gas side (**Experimental Objective V)**. The CO_2 removal rate measurement error amounts to 3 % of reading. In contrast, the CO_2 removal rate measured at the blood side underlies measurement errors of approx. 16 % of reading. Since the measurement of the CO_2 removal rate on the blood side requires a CO_2 solubility model (Section 4.2.1), this error can be increased significantly, leading to unacceptably high measurement errors of up to 127 % [**Journal Publication VI**].

However, although generally inferior, the blood-based method is used commonly in literature since with higher CO_2 removal performances of oxygenators, lower measurement error of the blood-based CO_2 removal prediction method can be expected [**Journal Publication VI**]. At the investigated ratios of CO_2 removal rate and blood flow rate < 0.14, the measurement errors of the blood-based method (16 %) determined in [**Journal Publication VI**] are comparable to literature (20 %) [71].

Die approbierte gedruckte Originalversion dieser Dissertation ist an der TU Wien Bibliothek verfügbar.
The approved original version of this doctoral thesis is available in print at TU Wien Bibliothek.
TU Bibliothek Your knowledge hub WIEN

4.1.6 Measurement of CO_2 Permeance Before and After Trials

The main CO_2 transport resistance of oxygenators is located in the blood side boundary layer. It builds up due to the concentration polarization of permeating species close to the membrane surface. Since the CO_2 transport resistance of unused fibers is significantly lower than the blood side resistance, the blood side transport resistance is considered dominant and characterizing for the CO_2 transport performance of an oxygenator. Consequently, membrane resistance is often neglected in investigations of CO_2 transport [3].

However, membrane fouling due to wetting of pores or blood residues on the membrane surface could increase the CO_2 transport resistance in the membrane to a level where it would substantially influence the CO_2 transport characteristics of an oxygenator. Literature studying how membrane fouling influences the CO_2 transport performance of oxygenators is not available. Current studies on membrane fouling are limited to evaluating new membrane materials regarding their reduced hydrophily (water contact angle) and platelet adhesion [136].

This work aims to investigate whether a reduction of the membrane gas exchange performance occurs during the application of an oxygenator (**Experimental Objective VI**). Consequently, the CO_2 permeances of our prototype oxygenator were measured before and after in vitro and in vivo tests (Section 2.1.1). Our data indicates a significant decrease in CO_2 permeance after testing. However, an accurate measurement of the CO_2 permeance decrease is unfeasible due to residual moisture in the oxygenator. The latter leads to a successive increase of CO_2 permeance during the follow-up tests due to the drying mechanism induced by the measurement gas (Figure 4.5) [**Journal Publication VIII**].

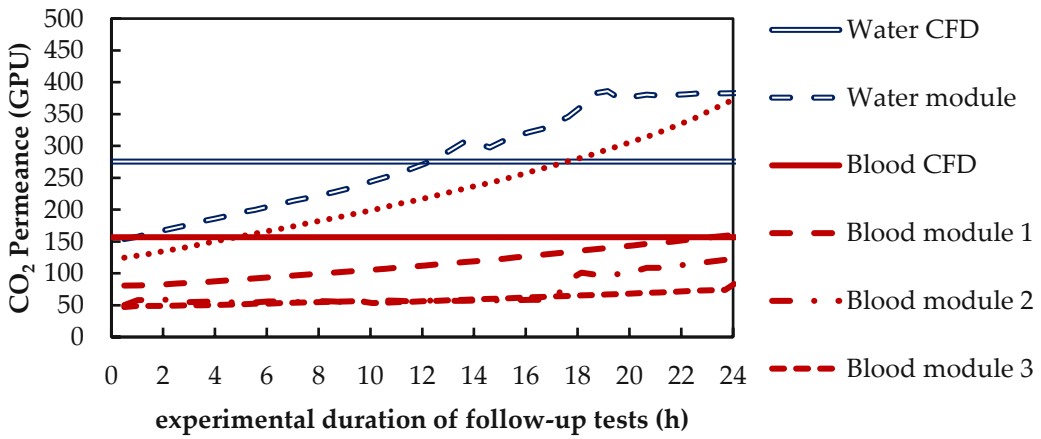

Figure 4.5. Increase in CO_2 permeance during the follow-up gas permeation measurements. Continuous lines: selected values for CFD CO_2 transport simulations. By Lukitsch et al. [**Journal Publication VIII**] (CC BY 4.0).

Based on CFD simulations, it can be estimated that the CO_2 permeance of the membrane is reduced by 78 % when used with blood. This decrease is lower if the membrane was used with water (62 %). Lower permeances of fibers used with blood could originate from blood residues detected on the membrane surface, leading to an increased membrane resistance [**Journal Publication VIII**]. Furthermore, CFD simulations indicate that a reduction in permeance reduces the CO_2 removal rate in a comparable magnitude (Section 4.2.3).

Die approbierte gedruckte Originalversion dieser Dissertation ist an der TU Wien Bibliothek verfügbar.
The approved original version of this doctoral thesis is available in print at TU Wien Bibliothek.
TU Bibliothek Your knowledge hub WIEN

For the investigated membranes, the high reduction in CO_2 permeance and the associated increase in CO_2 transport resistance in the membrane wall requires the CFD simulation to consider the membrane resistance (Section 2.2.2).

The determined reduction in CO_2 permeance is also plausible for other prototype or commercial devices. However, we must emphasize that the hollow fiber membranes built in the prototype oxygenators were only approved for research purposes. Furthermore, the integrity of the hollow fibers cannot be guaranteed entirely for the construction of the prototype oxygenators.

Consequently, similar tests as in [**Journal Publication VIII**] should be conducted with commercial oxygenators to quantify a possible CO_2 permeance reduction of oxygenators due to their contact with blood or water.

4.1.7 Measurement of O_2 and CO_2 for Data Validation

In this work, the CO_2 concentration was measured exclusively in the prototype oxygenator sweep gas. An additional measurement of the CO_2 and O_2 concentration in the sweep gas of the prototype oxygenator and the oxygenator used for CO_2 and O_2 level control of blood (Section 2.1.3) would have allowed a complete validation of the measurement data. The additional instrumental effort, which is low compared to the experimental effort, would also have allowed investigations of the O_2 transfer rate or O_2 solubility models.

4.1.8 Thrombus Formation

Since the main CO_2 transport resistance of oxygenators – the CO_2 concentration polarization – is located on the blood side, measures intended to counteract this resistance mainly concern the flow guidance of the blood. However, in addition to the resulting improvement in gas transfer rates, the formation and deposition of thrombi should be considered during the assessment of the flow guidance adaptation since they are essential factors for the service life of an oxygenator [137].

While current research investigates the influence of flow guidance [138] and membrane materials [139] on thrombus formation in oxygenators, the experimental test campaigns of this work are mainly limited to feasibility studies regarding the realization of a CO_2 transfer rate of 40 mL STP/min with restricted dimensions of the membrane module (Section 2.1.8).

4.2 Summary and Discussion of Computational Fluid Dynamic Results

4.2.1 CO_2 Solubility Model

While a numerical comparison of different blood viscosity models has been conducted [123], no recommendation for a suitable CO_2 solubility model for blood can be found in the literature. In the course of this work, the suitabilities of four different CO_2 solubility models with different levels of complexity were studied experimentally (Section 2.1.6). However, the results are summarized here since suitable CO_2 solubility models are crucial for reliable CFD-based oxygenator development (**CFD Objective I**).

Die approbierte gedruckte Originalversion dieser Dissertation ist an der TU Wien Bibliothek verfügbar.
The approved original version of this doctoral thesis is available in print at TU Wien Bibliothek.
TU Bibliothek Your knowledge hub WIEN

In [**Journal Publication VI**], CO_2 solubility models were assessed by determining the relative difference between blood-based and sweep fluid-based CO_2 removal rate prediction (prediction error ε [%] – Section 2.1.6). Prediction errors of the four investigated CO_2 solubility models are illustrated in Figure 4.6 for the in vitro trials with bovine blood and water and the in vivo trials with porcine blood.

Games-Howell test gives that the simplest model (Loeppky et al. [124]) performs significantly better than the other models. The average prediction error ($\bar{\varepsilon}$ [%]) amounts to 31 % for bovine blood tests and 23 % for porcine blood tests. The performance of the Loeppky model for porcine blood is comparable to that of the Henry model for water ($\bar{\varepsilon}$ = 16 %). Welch's *t*-test gives that for the Loeppky model, no significant difference in prediction error can be found between bovine and porcine blood tests [**Journal Publication VI**].

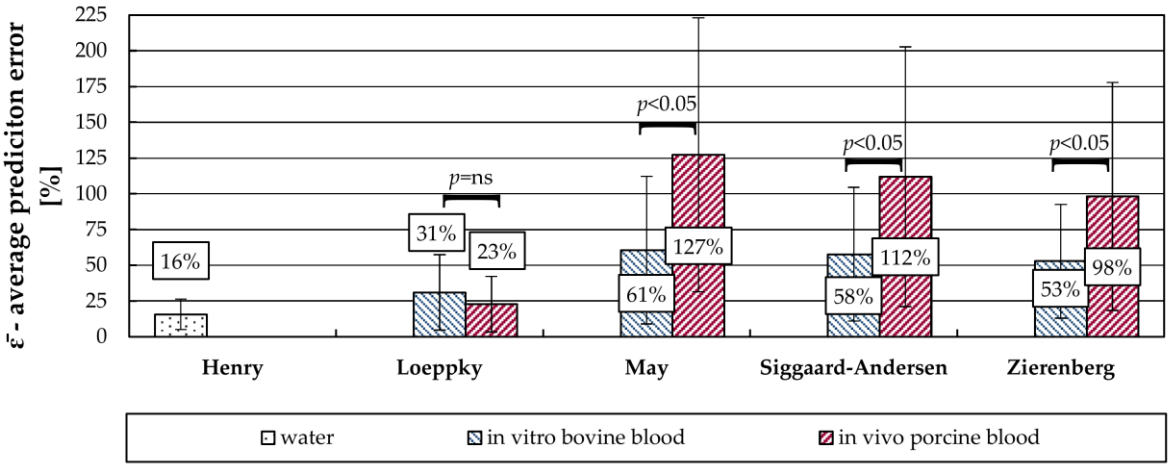

Figure 4.6. Average prediction error of the different CO_2 solubility models for in vitro tests with water and bovine blood and in vivo tests with porcine blood. The error bars show the standard deviation. Difference of average prediction error between test series was tested for significance with Welch's *t*-test. By Lukitsch et al. [**Journal Publication VI**] (CC BY 4.0).

The models with additional complexity, May [54], Siggaard-Andersen [140], and Zierenberg [141], show elevated average prediction errors and prediction error variations. These models calculate the bicarbonate concentration based on the Henderson-Hasselbalch equation [**Journal Publication VI**]. Welch's *t*-test gives that May, Siggaard-Andersen, and Zierenberg perform significantly better for the bovine blood tests than for the porcine blood tests [**Journal Publication VI**].

By omitting the calculation of the bicarbonate concentration, prediction error variation can be reduced significantly (Levene's test *p*-value < 0.05 – Figure 4.7). This simplification leads to a significant increase in average prediction error only for bovine blood tests when using the Siggaard-Anderson and Zierenberg model (Welch's test *p*-value < 0.05) [**Journal Publication VI**].

Die approbierte gedruckte Originalversion dieser Dissertation ist an der TU Wien Bibliothek verfügbar.
The approved original version of this doctoral thesis is available in print at TU Wien Bibliothek.
TU Bibliothek Your knowledge hub WIEN

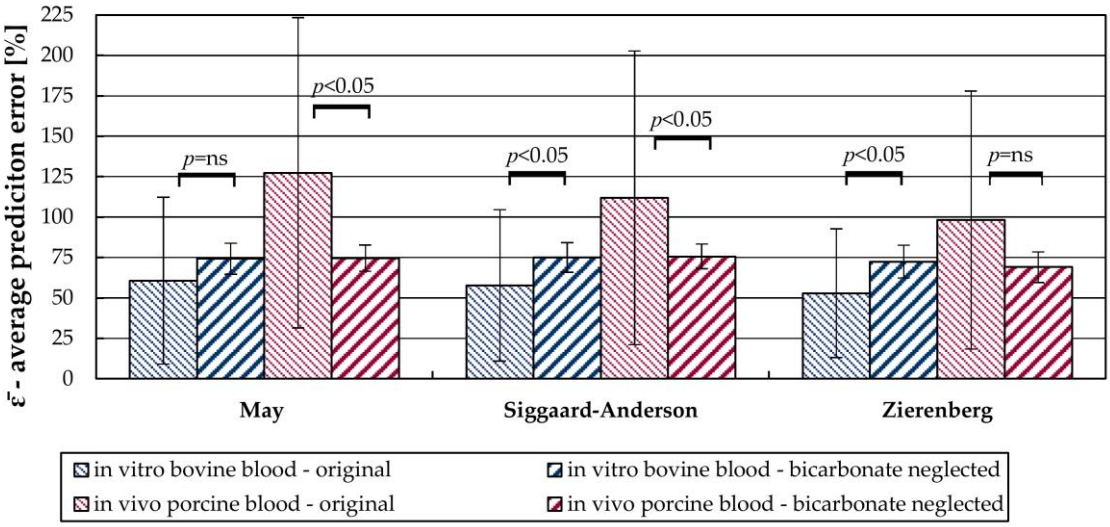

Figure 4.7. Average prediction error of the different solubility models when including (original) and neglecting the calculation of the bicarbonate content in blood. The error bars show the standard deviation. Difference of average prediction error between original model and model with neglected bicarbonate calculation was tested for significance with Welch's *t*-test. By Lukitsch et al. [**Journal Publication VI**] (CC BY 4.0).

Adapting the empirical parameters of the Loeppky model to the different test procedures and animal species allowed for no significant improvement of the Loeppky model prediction performance (Welch's test *p*-value > 0.05) [**Journal Publication VI**].

To conclude, the Loeppky model is a simple to use and generic CO_2 solubility model for blood. Compared to the more complex models, it demonstrated superior accuracy and robustness. Consequently, we recommend the Loeppky model for the blood-based CO_2 removal prediction method (Section 2.1.6) and application in CFD CO_2 transport simulations (Section 2.2.7.2).

4.2.2 Blood Viscosity Models for Animal Blood

Since in vitro and in vivo tests are commonly conducted with animal blood, accurate blood viscosity models for different animal species are required for correct CFD model validation (**CFD Objective II**). In [**Journal Publication VII**], blood viscosity models for porcine, ovine, and sheep blood were developed based on multi-linear regression. The models consider the dependency of whole blood viscosity from shear rate, hematocrit, and temperature. Due to the lack of data, a comparable model for cows – another standard animal model – was not developed.

4.2.3 Implementation of Computational Fluid Dynamic Model

In this work, a CFD model which allows resolving the CO_2 transport within a hollow fiber membrane packing of an oxygenator is presented [**Journal Publication** I]. The model is based on an in-house CFD solver for transmembrane mass transport (membraneFOAM – Section 2.2.5). The solver is implemented in OpenFOAM an open-source CFD code that offers excellent flexibility and a solid fundament for efficient numerical optimization of oxygenators. Similar to comparable codes in literature, membraneFOAM resolves the blood region within the membrane packing. In addition, the membrane wall and the sweep gas region in the fiber lumen can be resolved (**CFD Objective III**).

Die approbierte gedruckte Originalversion dieser Dissertation ist an der TU Wien Bibliothek verfügbar.
The approved original version of this doctoral thesis is available in print at TU Wien Bibliothek.
TU Bibliothek Your knowledge hub WIEN

CFD mass transport simulations of a simplified geometry (Section 2.2.6, Figure 2.13c) were conducted to analyze the fundamental phenomena of CO_2 transport in oxygenator membrane packings. To compare the CO_2 transport resistance of the blood side, membrane wall, and lumen, the drop in CO_2 partial pressure – the driving force of transmembrane flux – was investigated (Figure 4.8).

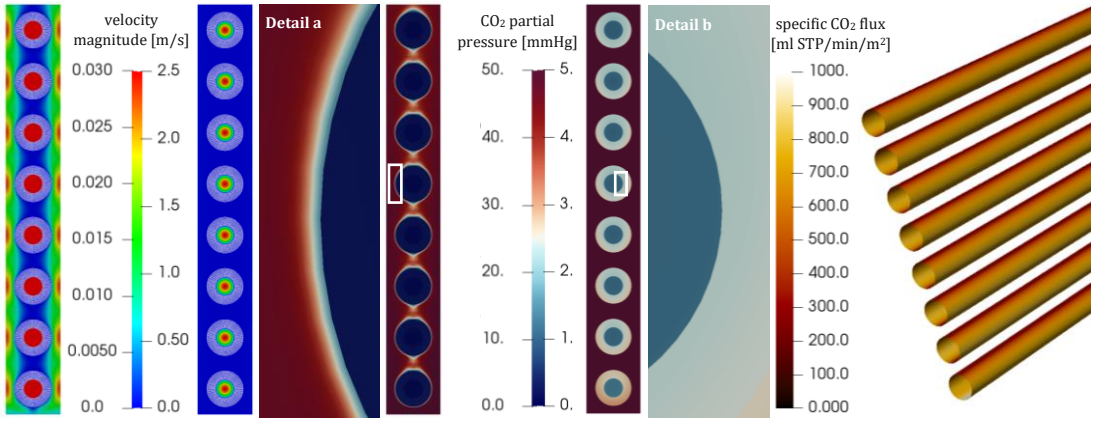

Figure 4.8. CFD mass transport simulations of a simplified geometry: (**a**) Velocity distribution; (**b**) CO_2 partial pressure distribution; (**c**) CO_2 flux on blood side membrane surface. [**Journal Publication** I]

CO_2 partial pressure in the blood decreases from 50 mmHg in the bulk flow to 15 mmHg at the membrane surface. CO_2 partial pressure drop over the selective membrane layer amounts to 12 mmHg. An additional partial pressure drop of 2 mmHg occurs in the membrane wall. No partial pressure gradient in the radial direction can be observed in the lumen [**Journal Publication** I]. Consequently, considering the lumen in CFD mass transport simulations is unnecessary if adequate sweep flow rates are set. Sufficient sweep flow can be ensured by monitoring the CO_2 concentration of the sweep flow outlet. High sweep flow rates guarantee high partial pressure differences across the total length of the hollow fiber membrane packing and hence are an inexpensive measure to maximize the CO_2 removal rate.

As described in Section 4.1.6, an increase in membrane resistance due to contact of the oxygenator with water or blood should be assumed. In order to quantify the associated reduction in transmembrane flux, the dependence of the CO_2 removal rate on permeance was investigated using CFD simulations. This allows evaluating whether the membrane resistance must be considered in CFD mass transport models of oxygenators (**CFD Objective III**). In the investigated range, the CO_2 removal rate increases approximately linearly with permeance (Figure 4.9).

Die approbierte gedruckte Originalversion dieser Dissertation ist an der TU Wien Bibliothek verfügbar.
The approved original version of this doctoral thesis is available in print at TU Wien Bibliothek.
TU Bibliothek Your knowledge hub WIEN

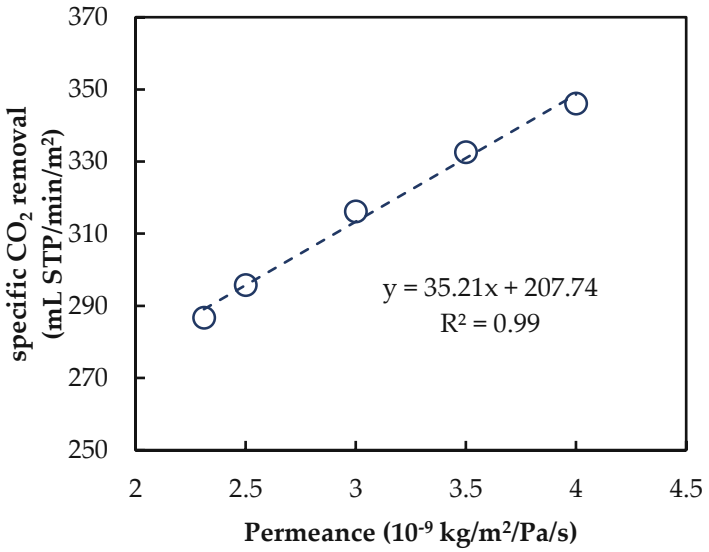

Figure 4.9. Dependency of transmembrane CO_2 flux on permeance. Determined via CFD for water. [142]

Due to the significant reduction in permeance (78 %) recorded for the prototype oxygenator, the membrane resistance must be considered to ensure an exact determination of the CO_2 removal rate using CFD. The neglection of the membrane resistance common with CFD models proposed in the literature (Section 1.3.3) would not be valid if a quantitative prediction of CO_2 removal rate is desired. If the reduction of permeance is also confirmed for commercial oxygenators, a paradigm shift towards CFD models considering membrane resistance would be required.

4.2.4 Upscaling Method

Due to the high numerical effort of CFD simulations of oxygenators, only hydrodynamic simulations of representative packing segments can be performed. In comparison, species transport simulations are limited to small parts of packings. In this work, an upscaling method was developed that predicts the total CO_2 removal rate of oxygenators based on CFD CO_2 transport simulations of small membrane packings (Section 2.2.6 – **CFD Objective IV**). In this respect, the up-scaling method bridges the gap between the geometric size scales of hydrodynamic and mass transfer simulations presently recorded in the literature (Section 1.3.3.2).

The up-scaling method was validated for both water and porcine blood [**Journal Publication VIII**]. Figure 4.10 compares the CO_2 removal rates predicted by the up-scaling method with the experimentally determined CO_2 removal rates. When combining the developed CFD model (Section 2.2.5) and the up-scaling method (Section 2.2.6), the dependence of the CO_2 removal rate on CO_2 partial pressure and blood/water flow rate can be described reasonably. The satisfactory agreement between experimental and numerical results applies to water and porcine blood [**Journal Publication VIII**].

Die approbierte gedruckte Originalversion dieser Dissertation ist an der TU Wien Bibliothek verfügbar.
The approved original version of this doctoral thesis is available in print at TU Wien Bibliothek.
TU Bibliothek Your knowledge hub WIEN

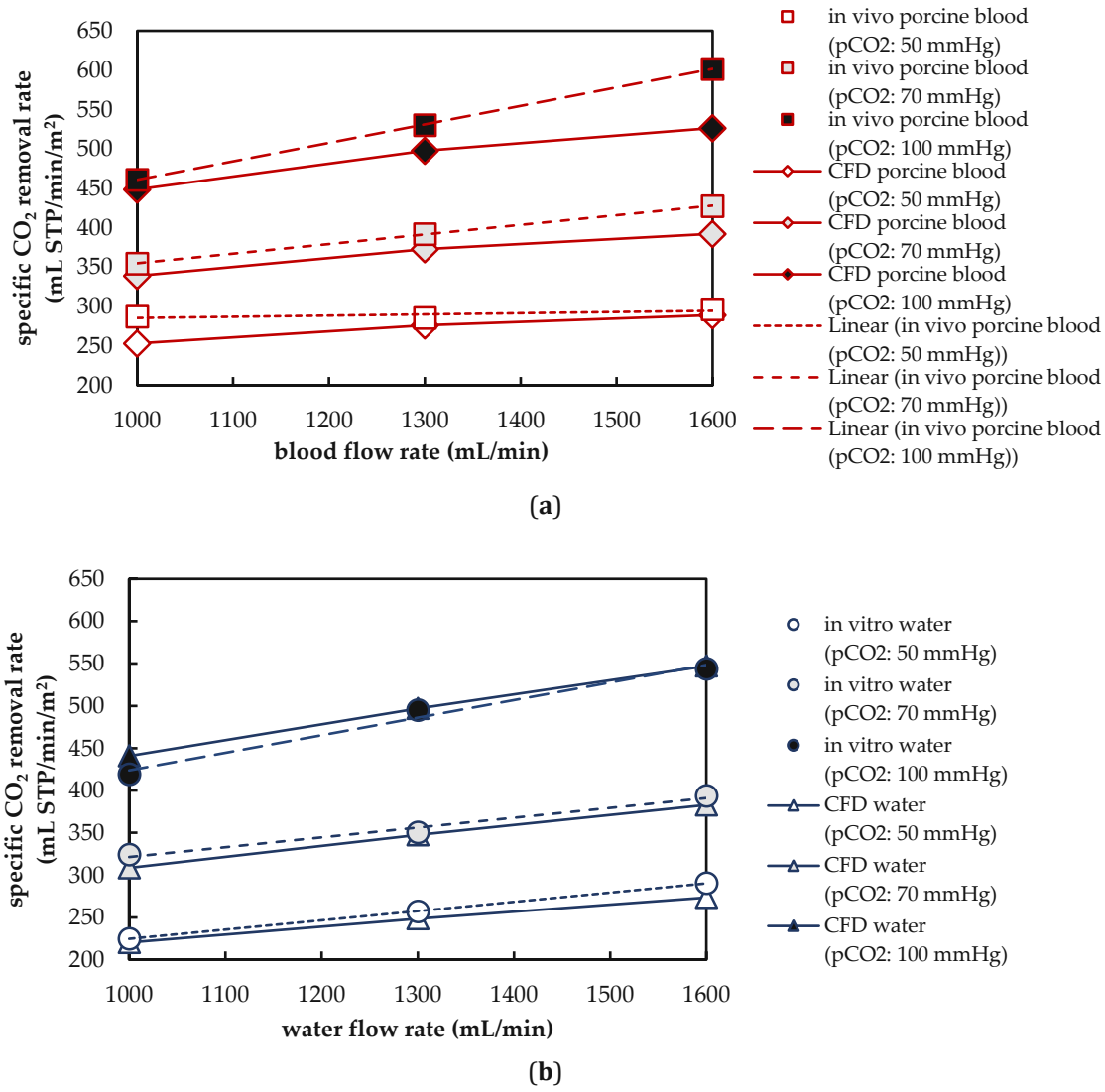

Figure 4.10. Comparison of CO_2 removal determined with experiments and CFD simulations: (**a**) in vivo porcine blood tests; (**b**) in vitro water tests. By Lukitsch et al. [**Journal Publication VIII**] (CC BY 4.0)

The mean relative deviation between numerically and experimentally determined CO_2 removal rates is 6 % for the in vivo porcine blood tests. However, higher deviations must be recorded mainly at higher CO_2 partial pressures and higher blood flow rates (13 %). For the in vitro water test, the mean relative deviation between numerically and experimentally determined CO_2 removal rate is 3 %. The CO_2 removal rate can be reproduced well for all investigated CO_2 partial pressures and water flow rates [**Journal Publication VIII**].

The up-scaling method reduces the computation time of the CFD simulations by 99.3 % (factor of 150) [**Journal Publication II**]. In contrast to Sherwood methods, no empirical fitting parameters are required (Section 2.3.1). In this respect, the up-scaling method represents a reliable, accurate, and efficient method for developing oxygenators.

Die approbierte gedruckte Originalversion dieser Dissertation ist an der TU Wien Bibliothek verfügbar.
The approved original version of this doctoral thesis is available in print at TU Wien Bibliothek.
TU Bibliothek Your knowledge hub WIEN

4.2.5 Investigation of Concentration Polarization Layer

The suitability of water for experimental prediction of the CO_2 removal performance of oxygenators was investigated. Here CFD simulations allow extending experimental data by resolving the concentration polarization in the boundary layer. By doing so, application limits for water as a CO_2 transport model can be established (**CFD Objective V**). Figure 4.11 shows exemplary p_{CO2} profiles of water and blood for a membrane packing in crossflow. As shown in Figure 4.11, the p_{CO2} boundary layer for water is thicker than that for blood. Furthermore, the p_{CO2} profiles in water show a lower slope. Both phenomena, the thicker boundary layer and the lower slope of water profiles, can be attributed to the higher diffusion rate of CO_2 in water [**Journal Publication VIII**].

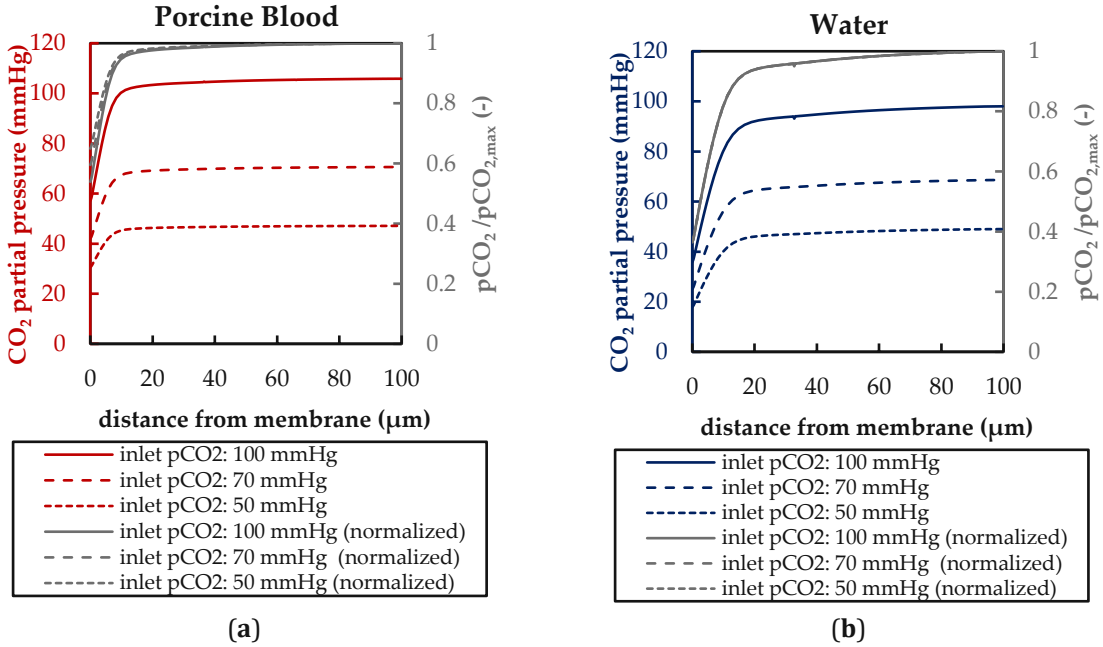

Figure 4.11. Exemplary boundary profiles of CO_2 partial pressure (pCO_2) and normalized CO_2 partial pressure (p_{CO2}'): (**a**) porcine blood (**b**) water (normalized profiles are overlapping). By Lukitsch et al. [**Journal Publication VIII**] (CC BY 4.0)

Figure 4.12 shows the influence of the flow velocity on the thickness of the p_{CO2} boundary layer profiles. The boundary layer thickness was defined as the smallest distance from the membrane wall at which 99 % of the bulk p_{CO2} is exceeded [**Journal Publication VIII**]. The boundary layer thickness is shown on the one hand as a function of the maximum velocity in the membrane packing (Figure 4.12a) and on the other hand as a function of the Reynolds number (Re [-] – Figure 4.12b). Re was calculated with the maximum velocity and fiber diameter. Due to increased shear rates (> 200 1/s), Newtonian kinematic viscosity was applied.

Die approbierte gedruckte Originalversion dieser Dissertation ist an der TU Wien Bibliothek verfügbar.
The approved original version of this doctoral thesis is available in print at TU Wien Bibliothek.
TU Bibliothek Your knowledge hub WIEN

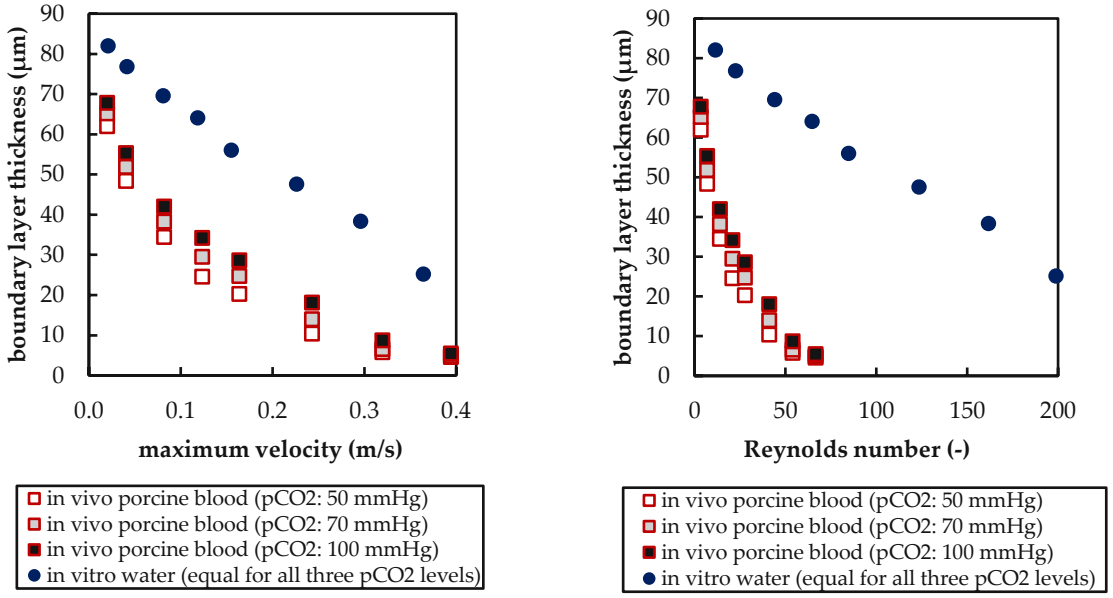

Figure 4.12. Dependency of boundary layer thickness on: (**a**) maximum velocity between fibers; (**b**) Reynolds number. By Lukitsch et al. [**Journal Publication VIII**] (CC BY 4.0)

As shown in Figure 4.12, porcine blood and water have more comparable p_{CO2} boundary layer thicknesses at the same maximum velocities than at the same Re. This indicates that at the same velocities, the lower viscosity of water leads to additional mixing and thus to a reduction of the p_{CO2} boundary layer thickness. The dependence of the boundary layer thickness on the bulk p_{CO2} recorded for blood is due to the non-linear dependence of the CO_2 partial pressure on the CO_2 concentration [**Journal Publication VIII**].

The fundamentally different behavior of the boundary layers of blood and water also becomes apparent in a dimensionless comparison of the mass transport characteristics of the two media. For this purpose, the mass transport analogy described in Section 2.3.1 was applied.

As shown in Figure 4.13, the empirical parameter b of the mass transfer analogy differs in particular. Hence, in the context of a dimensionless analysis, similarity cannot be assumed regarding the mass transfer mechanisms [**Journal Publication VIII**].

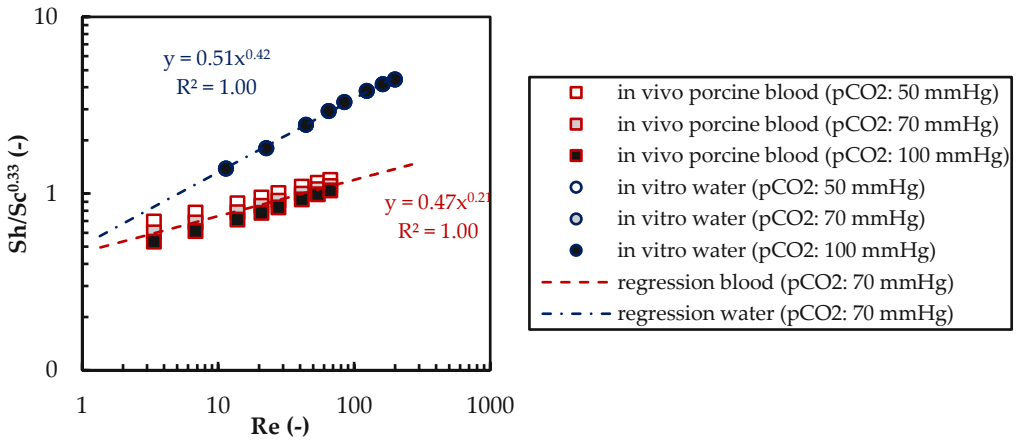

Figure 4.13. Sherwood correlations for porcine blood and water determined via the CFD results. Adapted from Lukitsch et al. [**Journal Publication VIII**] (CC BY 4.0).

Die approbierte gedruckte Originalversion dieser Dissertation ist an der TU Wien Bibliothek verfügbar.
The approved original version of this doctoral thesis is available in print at TU Wien Bibliothek.
TU Bibliothek Your knowledge hub WIEN

Despite the different mass transport characteristics, water and blood show comparable macroscopic CO_2 removal rates. This observation was investigated in more detail with additional CFD simulations. For this purpose, a material property of water was hypothetically changed to one of blood in order to individually investigate the influence of this material property on the transmembrane flux. As shown in Figure 4.13, the lower CO_2 diffusion rate of blood, followed by the lower CO_2 permeance available with blood and the higher viscosity of blood, leads to a reduction of the CO_2 removal rate. Only the higher CO_2 solubility of blood leads to an increase in the CO_2 removal rate [**Journal Publication VIII**].

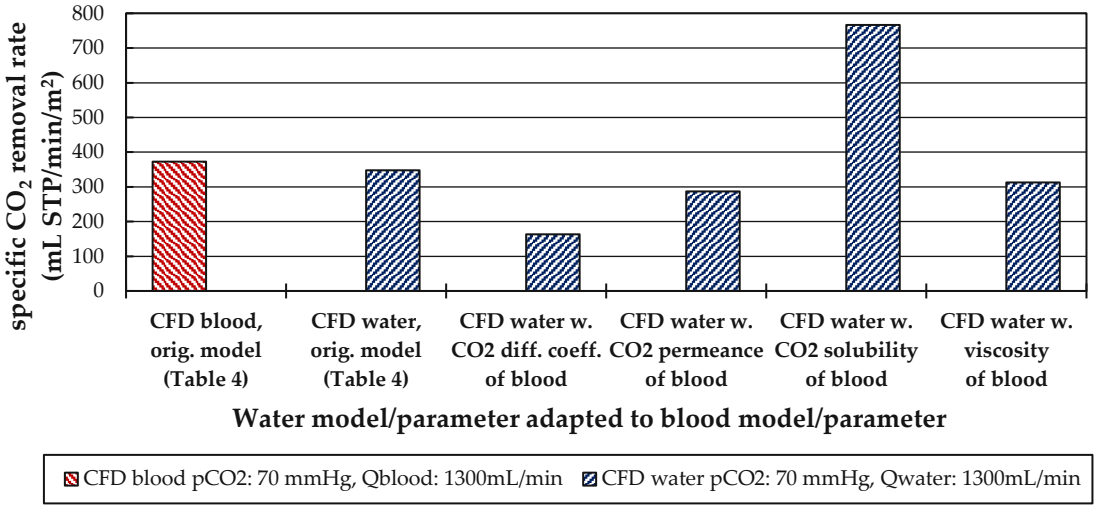

Figure 4.14. Influence of CO_2 diffusion, CO_2 permeance CO_2 solubility, and viscosity model on the CO_2 removal rate. By Lukitsch et al. [**Journal Publication VIII**] (CC BY 4.0).

It can be concluded that the different material properties of water and blood result in differently pronounced mass transport characteristics. Therefore, experimental studies investigating the p_{CO2} boundary layer should not be carried out with water as a blood model. However, the opposing influences of the material properties on the CO_2 removal rate compensate each other and therefore allow a reasonable agreement of the macroscopic CO_2 removal rate of water and blood. Consequently, for the determination of the macroscopic CO_2 removal rate, water can be considered suitable [**Journal Publication VIII**].

The fact that both, the CO_2 removal rate of water and that of blood, could be satisfactorily reproduced with the developed CFD model indicates that the CFD model – which is characterized by the consideration of the membrane resistance and the use of the up-scaling method – is a sound basis for further numerical investigation of oxygenators and the p_{CO2} boundary layer located therein.

4.2.6 Alternative Modeling Approaches – Computation of Sherwood Number

Computation of the Sherwood number by considering the CO_2 transport in blood as the transport of a passive scalar is an inexpensive numerical approach to predict the CO_2 removal performance of oxygenators (**CFD Objective VI**). This work used this simplified CFD approach to assess different hollow fiber geometries (Table 4.2 - cross-section) in crossflow mode.

Die approbierte gedruckte Originalversion dieser Dissertation ist an der TU Wien Bibliothek verfügbar.
The approved original version of this doctoral thesis is available in print at TU Wien Bibliothek.
TU Bibliothek Your knowledge hub WIEN

Table 4.2. Overview of the five microstructured fiber shapes investigated. [**Journal Publication V**].

Name	Dimensions	Sinus 3	Sinus 6, 50 µm	Sinus 6, 25 µm	Sinus 9, 50 µm	Sinus 9, 25 µm
Cross-section	-					
Average Diameter	µm	400	400	400	400	400
Nr. of Periods	-	3	6	6	9	9
Amplitude	µm	50	50	25	50	25
Specific Area	m^2/m^3	3810	4976	3920	5962	4482

As shown in Table 4.3, the increase in CO_2 flux is not proportional to the increase in the specific area. This behavior is caused by cavities formed by the microstructured fiber shape. They facilitate the occurrence of low-velocity zones. The latter leads to an increased formation of concentration polarization and an increased risk of thrombus formation. Based on the CFD model prediction, the best performing fiber shape (Sinus 6, 50 µm) allows for a potential CO_2 flux improvement of 48 % [**Journal Publication V**].

Table 4.3. Comparison of the expected and actual component flux increase. [**Journal Publication V**].

Geometry	Expected increase based on area [%]	Actual increase based on Sh [%]	Difference [%]
Sinus 3	15	1	-14
Sinus 9, 50 µm	79	21	-58
Sinus 9, 25 µm	35	9	-26
Sinus 6, 50 µm	**50**	**48**	**-2**
Sinus 6, 25 µm	18	12	-6

However, the simplified CFD model cannot consider that an inhomogeneous wall thickness must be assumed for both a cylindrically shaped lumen and a microstructured lumen. However, inhomogeneous wall thickness would lead to an inhomogeneous distribution of CO_2 transfer along the fiber circumference. Therefore, it can be assumed that the increase in CO_2 flux predicted by the simplified CFD model is undercut in practice [**Journal Publication V**].

To conclude, the simplified model has advantages due to the lower complexity than the proposed multi-region CFD model (Section 2.2.5) and the independence of empirical parameters required by Sherwood correlations (Section 2.3.1). However, it only allows for a qualitative assessment of transmembrane flux since the membrane resistance is neglected and a total CO_2 removal is assumed at the membrane wall (c_{CO2} of zero at the membrane wall – Section 2.3.2).

Die approbierte gedruckte Originalversion dieser Dissertation ist an der TU Wien Bibliothek verfügbar.
The approved original version of this doctoral thesis is available in print at TU Wien Bibliothek.
TU Bibliothek Your knowledge hub WIEN

5 Conclusion and Outlook

Within the scope of this work, standard experimental and numerical methods for optimizing oxygenators were evaluated. Based on the results obtained, recommendations can be made to increase the reliability, accuracy, and efficiency of the reviewed methods. The suggested improvements apply in particular to the early phase of oxygenator development.

Our studies show that water-glycerol is a suitable rheological model for blood, provided that increased shear rates (> 200 1/s) can be assumed. In both blood pumps [**Journal Publication VII**] and membrane packings [104], this threshold is exceeded in wide ranges (Section 4.1.1). Xanthan gum could be added to the water-glycerol mixture [94] to model the shear rate dependence of blood viscosity. Then, similar to studies in [**Journal Publication V**], the effect of the shear rate-dependent blood viscosity on the velocity distribution could be investigated experimentally, using a 2D micro PIV. For further validation of CFD results, experimental preparations with an extended 3D micro PIV are planned.

Water can be recommended as a simple blood model to determine the CO_2 removal rate of an oxygenator. While water is commonly used in in vitro tests, there is no systematic quantification of the associated error in the literature. Furthermore, no application limits for in vitro water tests have been determined to date. In this work, the deviation between the macroscopic CO_2 removal rate in in vitro water tests and in vivo porcine blood tests was systematically determined. It is on average 10 % (Section 4.1.2). With the help of CFD simulations, application limits for in vitro water tests were determined. They show that the use of water to investigate the concentration polarization in the boundary layer experimentally is not suitable (Section 4.2.5). Nevertheless, due to the similarity of the macroscopic removal rate, water allows a reliable and efficient prototype development with a significant reduction of the required workload.

Furthermore, viscosity models for blood have been developed based on data from human volunteers, pigs, horses, and sheep. They allow considering the dependence of viscosity on hematocrit, temperature, and shear rate (Section 4.1.3). While numerous viscosity models for human blood can be found in the literature, viscosity models for the blood of animal models are scarce [**Journal Publication VII**]. However, an accurate representation of viscosity is essential for reliable CFD models and when selecting a suitable animal model in experimental studies. Since cows are a common animal model, a viscosity model comparable to [**Journal Publication VII**] should also be developed for bovine blood. Furthermore, due to its inherent properties as a suspension, the measured viscosity of blood depends on the measurement method used. Thus, a dependency of the measured blood viscosity on the surface condition of the measurement equipment can be assumed. This behavior is currently being investigated in a follow-up study.

While in literature, the CO_2 removal rate is determined in equal measures on the blood side and the gas side, a clear recommendation for the gas side determination can be made based on the findings of this work. An evaluation of our measurement data of the in vitro and in vivo studies shows that the measurement error of the gas-side CO_2 removal rate determination (3 % of reading) is significantly smaller than that of the blood-side determination (16 % of reading – Section 4.1.5). Regarding the influence of the test animal

Die approbierte gedruckte Originalversion dieser Dissertation ist an der TU Wien Bibliothek verfügbar.
The approved original version of this doctoral thesis is available in print at TU Wien Bibliothek.
TU Bibliothek Your knowledge hub WIEN

species on the CO_2 removal rate, there are relatively small differences in the results obtained. A difference of 14 % between the CO_2 removal rates of bovine and porcine blood can be observed (Section 4.1.4). However, we have to point out that the test procedures differed between species. While bovine blood tests were performed in vitro, porcine blood tests were performed in vivo. Consequently, porcine blood tests were subject to stronger physiological variations and experimental interventions.

Furthermore, a CO_2 solubility model suitable for bovine and porcine blood could be determined (Section 4.2.1). Accurate CO_2 solubility models are of great importance for developing accurate CFD models and a reliable blood-side determination of the CO_2 removal rate (Section 2.1.6). Nevertheless, an evaluation of CO_2 solubility models is not found in the current literature, except for the review done in this work.

In addition, follow-up work is currently evaluating the suitability of CO_2 solubility models for human blood in clinical studies. The commercial oxygenators used for this purpose have a larger membrane area than the prototype oxygenator investigated. Due to the associated higher CO_2 removal rate, a lower scatter of the CO_2 removal rate measured on the blood side can be assumed. Consequently, a more reliable evaluation of the CO_2 solubility models and the blood-side CO_2 removal rate measurement can be conducted.

Based on our measurement data, it can be deduced that through contact with blood, a drop in the CO_2 permeance of commercial hollow fiber membranes to 22 % of their original CO_2 permeance is possible (Section 4.1.6). Further CFD studies showed that the CO_2 removal rate is approximately linearly dependent on the CO_2 permeance (Section 4.2.3). Therefore, in contrast to current scientific practice, the consideration of membrane resistance could be essential for a reliable prediction of the CO_2 removal performance of an oxygenator.

The studies conducted here are currently limited to CO_2 permeance measurements of commercial hollow fiber membranes installed in an oxygenator prototype. In this respect, follow-up studies should quantify if commercial hollow fiber membranes in commercial oxygenators show a comparable drop in permeance. In this context, attention should be paid to whether and how quickly a drop in permeance occurs.

In the course of this work, a CFD solver for mass transport in membrane oxygenators was developed – membraneFOAM. Similar to comparable codes in literature, the solver resolves the blood region within the membrane packing. In addition, the membrane wall and the sweep gas region in the fiber lumen can be resolved, providing a high level of detail of the gas transport phenomena.

However, the future development of oxygenators via CFD simulations is limited due to the high numerical effort, especially for mass transfer simulations. Consequently, a gap between the geometric scale of CO_2 transport simulations (single fibers) and hydrodynamic simulations (representative packing segments) can be observed in the current literature [**Journal Publication II**]. The upscaling method developed in this work (Section 2.2.6) bridges this gap and thus allows us to predict the macroscopic CO_2 removal rate of an oxygenator using CFD simulations. The deviation in experimentally and numerically determined CO_2 removal is 3 % for in vitro water tests and 6 % for in vivo porcine blood tests (Section 4.2.4).

Die approbierte gedruckte Originalversion dieser Dissertation ist an der TU Wien Bibliothek verfügbar.
The approved original version of this doctoral thesis is available in print at TU Wien Bibliothek.
TU Bibliothek Your knowledge hub WIEN

Based on the available literature review, experimental data, and simulation results, we make the following recommendation for future oxygenator prototypes:

i. New devices should integrate the blood pump into the oxygenator. An integrated pump could reduce the total circuit priming volume and concentration polarization at the membrane and improves the handling of the equipment.
ii. When selecting hollow fiber membranes, special consideration should be given to the resistance against pore wetting, which can cause a significant drop in gas exchange performance.
iii. CFD simulations should be used to identify stagnation zones in the blood flow. Stagnation zones must be prevented to minimize the risk of thrombosis.

With the help of the reviewed and developed experimental and numerical methods, commercial extracorporeal oxygenators can be investigated and improved, and future intracorporal oxygenators efficiently developed.

Die approbierte gedruckte Originalversion dieser Dissertation ist an der TU Wien Bibliothek verfügbar.
The approved original version of this doctoral thesis is available in print at TU Wien Bibliothek.
TU Bibliothek Your knowledge hub WIEN

References

[1] J. E. Hansen, E. P. Ampaya, G. H. Bryant, and J. J. Navin, "Branching pattern of airways and air spaces of a single human terminal bronchiole," *J. Appl. Physiol.*, vol. 38, no. 6, pp. 983–989, Jun. 1975, doi: 10.1152/jappl.1975.38.6.983.

[2] L. P. Perepechkin and N. P. Perepechkina, "Hollow fibres for medical applications. A review," *Fibre Chem.*, vol. 31, no. 6, pp. 411–420, Nov. 1999, doi: 10.1007/BF02358251.

[3] W. J. Federspiel and K. A. Henchir, "Lung, Artificial: Basic Principles And Current Applications," in *Encyclopedia of Biomaterials and Biomedical Engineering, Second Edition*, 0 vols., CRC Press, 2008, pp. 1661–1672. doi: 10.1081/E-EBBE2-120007349.

[4] D. Brodie and M. Bacchetta, "Extracorporeal Membrane Oxygenation for ARDS in Adults," *N. Engl. J. Med.*, vol. 365, no. 20, pp. 1905–1914, Nov. 2011, doi: 10.1056/NEJMct1103720.

[5] E. Fan *et al.*, "An Official American Thoracic Society/European Society of Intensive Care Medicine/Society of Critical Care Medicine Clinical Practice Guideline: Mechanical Ventilation in Adult Patients with Acute Respiratory Distress Syndrome," *Am. J. Respir. Crit. Care Med.*, vol. 195, no. 9, pp. 1253–1263, May 2017, doi: 10.1164/rccm.201703-0548ST.

[6] J. R. Beitler, A. Malhotra, and B. T. Thompson, "Ventilator-induced Lung Injury," *Clin. Chest Med.*, vol. 37, no. 4, pp. 633–646, Dec. 2016, doi: 10.1016/j.ccm.2016.07.004.

[7] R. Passos, R. Oliveira, M. Trabuco, R. Rodrigues, S. Souza, and P. Batista, "Barriers to providing lung-protective ventilation to patients with ALI/ARDS," *Crit. Care*, vol. 14, no. Suppl 1, p. P189, 2010, doi: 10.1186/cc8421.

[8] M. Kaushik *et al.*, "Extracorporeal Carbon Dioxide Removal: The Future of Lung Support Lies in the History," *Blood Purif.*, vol. 34, no. 2, pp. 94–106, 2012, doi: 10.1159/000341904.

[9] J. Reeb *et al.*, "Vascular access for extracorporeal life support: tips and tricks," *J. Thorac. Dis.*, vol. 8, no. Suppl 4, pp. S353–S363, Apr. 2016, doi: 10.21037/jtd.2016.04.42.

[10] W. J. Federspiel and R. G. Svitek, "Lung, Artificial: Current Research and Future Directions," *Encycl. Biomater. Biomed. Eng.*, May 2008, doi: 10.1201/b18990-162.

[11] L. K. Von Segesser, "8 - Coatings for cardiovascular devices: extracorporeal circuits," in *Coatings for Biomedical Applications*, M. Driver, Ed. Woodhead Publishing, 2012, pp. 251–263. doi: 10.1533/9780857093677.2.251.

[12] J. Li *et al.*, "Transient adhesion of platelets in pump-oxygenator systems: influence of SMA and nitric oxide treatments," *J. Biomater. Sci. Polym. Ed.*, vol. 10, no. 2, pp. 235–246, Jan. 1999, doi: 10.1163/156856299X00153.

[13] R. W. Melchior, S. W. Sutton, W. Harris, and H. J. Dalton, "Evolution of membrane oxygenator technology for utilization during pediatric cardiopulmonary bypass," *Pediatr. Health Med. Ther.*, vol. 7, pp. 45–56, Jun. 2016, doi: 10.2147/PHMT.S35070.

[14] S. A. Conrad, A. Bagley, B. Bagley, and R. N. Schaap, "Major findings from the clinical trials of the intravascular oxygenator," *Artif. Organs*, vol. 18, no. 11, pp. 846–863, Nov. 1994, doi: 10.1111/j.1525-1594.1994.tb03334.x.

[15] S. A. Conrad, J. M. Eggerstedt, V. F. Morris, and M. D. Romero, "Prolonged intracorporeal support of gas exchange with an intravenacaval oxygenator," *Chest*, vol. 103, no. 1, pp. 158–161, Jan. 1993, doi: 10.1378/chest.103.1.158.

Die approbierte gedruckte Originalversion dieser Dissertation ist an der TU Wien Bibliothek verfügbar.
The approved original version of this doctoral thesis is available in print at TU Wien Bibliothek.
TU Bibliothek Your knowledge hub WIEN

[16] S. A. Conrad, J. B. Zwischenberger, J. M. Eggerstedt, and A. Bidani, "In vivo gas transfer performance of the intravascular oxygenator in acute respiratory failure," *Artif. Organs*, vol. 18, no. 11, pp. 840–845, Nov. 1994, doi: 10.1111/j.1525-1594.1994.tb03333.x.

[17] J. Mortensen and G. Berry, "Conceptual and Design Features of a Practical, Clinically Effective Intravenous Mechanical Blood Oxygen/Carbon Dioxide Exchange Device (Ivox)," *Int. J. Artif. Organs*, vol. 12, no. 6, pp. 384–389, Jun. 1989, doi: 10.1177/039139888901200607.

[18] H. J. Eash, S. G. Budilarto, B. G. Hattler, and W. J. Federspiel, "Investigating the effects of random balloon pulsation on gas exchange in a respiratory assist catheter," *ASAIO J. Am. Soc. Artif. Intern. Organs 1992*, vol. 52, no. 2, pp. 192–195, Apr. 2006, doi: 10.1097/01.mat.0000199752.89066.83.

[19] W. J. Federspiel *et al.*, "Ex vivo testing of the intravenous membrane oxygenator," *ASAIO J. Am. Soc. Artif. Intern. Organs 1992*, vol. 46, no. 3, pp. 261–267, Jun. 2000, doi: 10.1097/00002480-200005000-00004.

[20] B. G. Hattler *et al.*, "A respiratory gas exchange catheter: In vitro and in vivo tests in large animals," *J. Thorac. Cardiovasc. Surg.*, vol. 124, no. 3, pp. 520–530, Sep. 2002, doi: 10.1067/mtc.2002.123811.

[21] R. G. Jeffries, B. J. Frankowski, G. W. Burgreen, and W. J. Federspiel, "Effect of Impeller Design and Spacing on Gas Exchange in a Percutaneous Respiratory Assist Catheter," *Artif. Organs*, vol. 38, no. 12, pp. 1007–1017, Dec. 2014, doi: 10.1111/aor.12308.

[22] K. M. Mihelc, B. J. Frankowski, S. C. Lieber, N. D. Moore, B. G. Hattler, and W. J. Federspiel, "Evaluation of a Respiratory Assist Catheter that Uses an Impeller Within a Hollow Fiber Membrane Bundle," *ASAIO J.*, vol. 55, no. 6, p. 569, Dec. 2009, doi: 10.1097/MAT.0b013e3181bc2655.

[23] A. J. Makarewicz, L. F. Mockros, and R. W. Anderson, "A pumping intravascular artificial lung with active mixing," *ASAIO J. Am. Soc. Artif. Intern. Organs 1992*, vol. 39, no. 3, pp. M466-469, Sep. 1993, doi: 10.1097/00002480-199307000-00063.

[24] A. J. Makarewicz, L. F. Mockros, and R. W. Anderson, "A Dynamic Intravascular Artificial Lung.," *ASAIO J.*, vol. 40, no. 3, p. M747, Sep. 1994.

[25] S. N. Vaslef, L. F. Mockros, and R. W. Anderson, "Development of an intravascular lung assist device," *ASAIO Trans.*, vol. 35, no. 3, pp. 660–664, Sep. 1989, doi: 10.1097/00002480-198907000-00160.

[26] K. M. High, T. Nicholson, R. B. Richard, G. R. Panol, K. Shelley, and M. T. Snider, "Effects of blood phase oscillation on gas transfer in a microporous intravascular lung," *ASAIO J. Am. Soc. Artif. Intern. Organs 1992*, vol. 40, no. 3, pp. M735-739, Sep. 1994, doi: 10.1097/00002480-199407000-00096.

[27] V. Nodelman, H. Baskaran, and J. S. Ultman, "Enhancement of O2 and CO2 transfer through microporous hollow fibers by pressure cycling," *Ann. Biomed. Eng.*, vol. 26, no. 6, pp. 1044–1054, Dec. 1998, doi: 10.1114/1.115.

[28] M. T. Snider *et al.*, "Small intrapulmonary artery lung prototypes: design, construction, and in vitro water testing," *ASAIO J. Am. Soc. Artif. Intern. Organs 1992*, vol. 40, no. 3, pp. M533-539, Sep. 1994, doi: 10.1097/00002480-199407000-00057.

[29] G. Cattaneo, A. Strauß, and H. Reul, "Compact intra-and extracorporeal oxygenator developments," *Perfusion*, vol. 19, no. 4, pp. 251–255, Jul. 2004, doi: 10.1191/0267659104pf748oa.

[30] G. F. M. Cattaneo, H. Reul, T. Schmitz-Rode, and U. Steinseifer, "Intravascular Blood Oxygenation Using Hollow Fibers in a Disk-Shaped Configuration: Experimental Evaluation of the Relationship Between Porosity and Performance," *ASAIO J.*, vol. 52, no. 2, pp. 180–185, Apr. 2006, doi: 10.1097/01.mat.0000204151.56591.28.

Die approbierte gedruckte Originalversion dieser Dissertation ist an der TU Wien Bibliothek verfügbar.
The approved original version of this doctoral thesis is available in print at TU Wien Bibliothek.
TU Bibliothek Your knowledge hub WIEN

[31] G. F. Cattaneo and H. Reul, "New fiber configuration for intravenous gas exchange," *Int. J. Artif. Organs*, vol. 28, no. 3, pp. 244–250, Mar. 2005, doi: 10.1177/039139880502800309.
[32] B. Flörchinger *et al.*, "Pumpless extracorporeal lung assist: a 10-year institutional experience," *Ann. Thorac. Surg.*, vol. 86, no. 2, pp. 410–417; discussion 417, Aug. 2008, doi: 10.1016/j.athoracsur.2008.04.045.
[33] T. Müller *et al.*, "Extracorporeal pumpless interventional lung assist in clinical practice: determinants of efficacy," *Eur. Respir. J.*, vol. 33, no. 3, pp. 551–558, Mar. 2009, doi: 10.1183/09031936.00123608.
[34] A. Aravantagi, K. P. Patra, S. Shekar, and L. K. Scott, "Pumpless arteriovenous carbon dioxide removal: A novel simplified strategy for severe asthma in children," *Indian J. Crit. Care Med. Peer-Rev. Off. Publ. Indian Soc. Crit. Care Med.*, vol. 15, no. 4, pp. 224–226, 2011, doi: 10.4103/0972-5229.92078.
[35] D. Wang *et al.*, "Toward Ambulatory Arteriovenous CO2 Removal: Initial Studies and Prototype Development," *ASAIO J.*, vol. 49, no. 5, pp. 564–567, Oct. 2003, doi: 10.1097/01.MAT.0000084116.78848.0C.
[36] N. K. Burki *et al.*, "A Novel Extracorporeal CO2 Removal System," *Chest*, vol. 143, no. 3, pp. 678–686, Mar. 2013, doi: 10.1378/chest.12-0228.
[37] H. Peperstraete, S. Eloot, P. Depuydt, F. De Somer, C. Roosens, and E. Hoste, "Low flow extracorporeal CO2 removal in ARDS patients: a prospective short-term crossover pilot study," *BMC Anesthesiol.*, vol. 17, no. 1, p. 155, Nov. 2017, doi: 10.1186/s12871-017-0445-9.
[38] S. Fischer *et al.*, "Bridge to Lung Transplantation With the Extracorporeal Membrane Ventilator Novalung in the Veno-Venous Mode: The Initial Hannover Experience," *ASAIO J.*, vol. 53, no. 2, pp. 168–170, Apr. 2007, doi: 10.1097/MAT.0b013e31802deb46.
[39] S. Livigni *et al.*, "Efficacy and safety of a low-flow veno-venous carbon dioxide removal device: results of an experimental study in adult sheep," *Crit. Care*, vol. 10, no. 5, p. R151, Oct. 2006, doi: 10.1186/cc5082.
[40] F. Ruberto *et al.*, "Extracorporeal removal CO2 using a venovenous, low-flow system (Decapsmart) in a lung transplanted patient: a case report," *Transplant. Proc.*, vol. 41, no. 4, pp. 1412–1414, May 2009, doi: 10.1016/j.transproceed.2009.03.048.
[41] R. Borchardt *et al.*, "Description of a Flow Optimized Oxygenator With Integrated Pulsatile Pump," *Artif. Organs*, vol. 34, no. 11, pp. 904–910, 2010, doi: 10.1111/j.1525-1594.2010.01123.x.
[42] R. Borchardt, P. Schlanstein, I. Mager, J. Arens, T. Schmitz-Rode, and U. Steinseifer, "In Vitro Performance Testing of a Pediatric Oxygenator With an Integrated Pulsatile Pump," *ASAIO J.*, vol. 58, no. 4, pp. 420–425, Aug. 2012, doi: 10.1097/MAT.0b013e318251dc70.
[43] R. Kopp *et al.*, "A Miniaturized Extracorporeal Membrane Oxygenator with Integrated Rotary Blood Pump: Preclinical In Vivo Testing," *ASAIO J.*, vol. 57, no. 3, pp. 158–163, Jun. 2011, doi: 10.1097/MAT.0b013e31820bffa9.
[44] R. G. Jeffries, L. Lund, B. Frankowski, and W. J. Federspiel, "An extracorporeal carbon dioxide removal (ECCO2R) device operating at hemodialysis blood flow rates," *Intensive Care Med. Exp.*, vol. 5, no. 1, p. 41, Sep. 2017, doi: 10.1186/s40635-017-0154-1.
[45] D. Wang *et al.*, "Short Term Performance Evaluation of a Perfluorocopolymer Coated Gas Exchanger for Arteriovenous CO2 Removal," *ASAIO J.*, vol. 49, no. 6, pp. 673–677, Dec. 2003, doi: 10.1097/01.MAT.0000093967.27012.5A.

Die approbierte gedruckte Originalversion dieser Dissertation ist an der TU Wien Bibliothek verfügbar.
The approved original version of this doctoral thesis is available in print at TU Wien Bibliothek.
TU Bibliothek Your knowledge hub WIEN

[46] D. T. Arazawa *et al.*, "Immobilized carbonic anhydrase on hollow fiber membranes accelerates CO2 removal from blood," *J. Membr. Sci.*, vol. 403, pp. 25–31, Jun. 2012, doi: 10.1016/j.memsci.2012.02.006.
[47] M. Zhang *et al.*, "Anti-thrombogenic Surface Coatings for Extracorporeal Membrane Oxygenation: A Narrative Review," *ACS Biomater. Sci. Eng.*, vol. 7, no. 9, pp. 4402–4419, Sep. 2021, doi: 10.1021/acsbiomaterials.1c00758.
[48] M. F. Maitz, "Applications of synthetic polymers in clinical medicine," *Biosurface Biotribology*, vol. 1, no. 3, pp. 161–176, Sep. 2015, doi: 10.1016/j.bsbt.2015.08.002.
[49] K. Nakata *et al.*, "Development of a new silicone membrane oxygenator for ECMO," *Ann. Thorac. Cardiovasc. Surg.*, vol. 6, no. 6, pp. 373–377, Dec. 2000.
[50] J. Santos *et al.*, "Toward Development of a Higher Flow Rate Hemocompatible Biomimetic Microfluidic Blood Oxygenator," *Micromachines*, vol. 12, no. 8, Art. no. 8, Aug. 2021, doi: 10.3390/mi12080888.
[51] M. Dabaghi *et al.*, "An ultra-thin highly flexible microfluidic device for blood oxygenation," *Lab. Chip*, vol. 18, no. 24, pp. 3780–3789, Dec. 2018, doi: 10.1039/C8LC01083H.
[52] D. M. Hoganson, H. I. P. Ii, E. K. Bassett, I. D. Spool, and J. P. Vacanti, "Lung assist device technology with physiologic blood flow developed on a tissue engineered scaffold platform," *Lab. Chip*, vol. 11, no. 4, pp. 700–707, Jan. 2011, doi: 10.1039/C0LC00158A.
[53] M. Cressoni *et al.*, "Decreasing pulmonary ventilation through bicarbonate ultrafiltration: an experimental study," *Crit. Care Med.*, vol. 37, no. 9, pp. 2612–2618, Sep. 2009, doi: 10.1097/CCM.0b013e3181a5668a.
[54] A. G. May, A. Sen, M. E. Cove, J. A. Kellum, and W. J. Federspiel, "Extracorporeal CO2 removal by hemodialysis: in vitro model and feasibility," *Intensive Care Med. Exp.*, vol. 5, Apr. 2017, doi: 10.1186/s40635-017-0132-7.
[55] M. E. Cove, G. MacLaren, W. J. Federspiel, and J. A. Kellum, "Bench to bedside review: Extracorporeal carbon dioxide removal, past present and future," *Crit. Care*, vol. 16, no. 5, p. 232, 2012, doi: 10.1186/cc11356.
[56] ISO 7199:2016, "Cardiovascular implants and artificial organs — Blood-gas exchangers (oxygenators)," *ISO/TC 150/SC 2*, no. 3, p. 13, Nov. 2016.
[57] K. M. Mihelc, B. J. Frankowski, S. C. Lieber, N. D. Moore, B. G. Hattler, and W. J. Federspiel, "Evaluation of a Respiratory Assist Catheter that Uses an Impeller Within a Hollow Fiber Membrane Bundle," *ASAIO J.*, vol. 55, no. 6, p. 569, Dec. 2009, doi: 10.1097/MAT.0b013e3181bc2655.
[58] B. G. Hattler *et al.*, "A respiratory gas exchange catheter: In vitro and in vivo tests in large animals," *J. Thorac. Cardiovasc. Surg.*, vol. 124, no. 3, pp. 520–530, Sep. 2002, doi: 10.1067/mtc.2002.123811.
[59] S. Kawahito *et al.*, "Gas Transfer Performance of a Hollow Fiber Silicone Membrane Oxygenator: Ex Vivo Study," *Artif. Organs*, vol. 25, no. 6, pp. 498–502, 2001, doi: 10.1046/j.1525-1594.2001.06706-4.x.
[60] A. Kaesler *et al.*, "In-Vitro Visualization of Thrombus Growth in Artificial Lungs Using Real-Time X-Ray Imaging: A Feasibility Study," *Cardiovasc. Eng. Technol.*, Sep. 2021, doi: 10.1007/s13239-021-00579-y.
[61] T. Maeda *et al.*, "Preclinical Evaluation of a Hollow Fiber Silicone Membrane Oxygenator for Extracorporeal Membrane Oxygenator Application," *ASAIO J.*, vol. 46, no. 4, pp. 426–430, Aug. 2000.
[62] T. Motomura *et al.*, "Development of Silicone Rubber Hollow Fiber Membrane Oxygenator for ECMO," *Artif. Organs*, vol. 27, no. 11, pp. 1050–1053, 2003, doi: 10.1046/j.1525-1594.2003.07077.x.

Die approbierte gedruckte Originalversion dieser Dissertation ist an der TU Wien Bibliothek verfügbar.
The approved original version of this doctoral thesis is available in print at TU Wien Bibliothek.
TU Bibliothek Your knowledge hub WIEN

[63] J. F. Golob *et al.*, "Acute In Vivo Testing of an Intravascular Respiratory Support Catheter," *ASAIO J.*, vol. 47, no. 5, pp. 432–437, Oct. 2001.
[64] H. P. Wendel, A. Philipp, N. Weber, D. E. Birnbaum, and G. Ziemer, "Oxygenator thrombosis: worst case after development of an abnormal pressure gradient - incidence and pathway," *Perfusion*, vol. 16, no. 4, pp. 271–278, Jul. 2001, doi: 10.1177/026765910101600402.
[65] E. Akoumianaki, A. Jonkman, M. C. Sklar, D. Georgopoulos, and L. Brochard, "A rational approach on the use of extracorporeal membrane oxygenation in severe hypoxemia: advanced technology is not a panacea," *Ann. Intensive Care*, vol. 11, no. 1, p. 107, Jul. 2021, doi: 10.1186/s13613-021-00897-3.
[66] H. J. Eash, B. J. Frankowski, K. Litwak, W. R. Wagner, B. G. Hattler, and W. J. Federspiel, "Acute In Vivo Testing of a Respiratory Assist Catheter: Implants in Calves Versus Sheep," *ASAIO J. Am. Soc. Artif. Intern. Organs 1992*, vol. 49, no. 4, pp. 370–377, 2003, doi: 10.1097/01.MAT.0000074991.94234.B6.
[67] A. G. May, R. G. Jeffries, B. J. Frankowski, G. W. Burgreen, and W. J. Federspiel, "Bench Validation of a Compact Low-Flow CO2 Removal Device," *Intensive Care Med. Exp.*, vol. 6, no. 1, p. 34, Sep. 2018, doi: 10.1186/s40635-018-0200-7.
[68] M. Hormes, R. Borchardt, I. Mager, T. S. Rode, M. Behr, and U. Steinseifer, "A validated CFD model to predict O_2 and CO_2 transfer within hollow fiber membrane oxygenators," *Int. J. Artif. Organs*, vol. 34, no. 3, pp. 317–325, Mar. 2011.
[69] L. Schraven *et al.*, "Effects of Pulsatile Blood Flow on Oxygenator Performance," *Artif. Organs*, vol. 42, no. 4, pp. 410–419, 2018, doi: 10.1111/aor.13088.
[70] W.-T. Wu, N. Aubry, M. Massoudi, J. Kim, and J. F. Antaki, "A numerical study of blood flow using mixture theory," *Int. J. Eng. Sci.*, vol. 76, pp. 56–72, Mar. 2014, doi: 10.1016/j.ijengsci.2013.12.001.
[71] N. A. Barrett, N. Hart, and L. Camporota, "In-vitro performance of a low flow extracorporeal carbon dioxide removal circuit," *Perfusion*, vol. 35, no. 3, pp. 227–235, Apr. 2020, doi: 10.1177/0267659119865115.
[72] A. S. Popel and P. C. Johnson, "Microcirculation and Hemorheology," *Annu. Rev. Fluid Mech.*, vol. 37, pp. 43–69, Jan. 2005, doi: 10.1146/annurev.fluid.37.042604.133933.
[73] P. W. Rand, E. Lacombe, H. E. Hunt, and W. H. Austin, "Viscosity of normal human blood under normothermic and hypothermic conditions," *J. Appl. Physiol.*, Jan. 1964, doi: 10.1152/jappl.1964.19.1.117.
[74] L. P. Chua and T. Akamatsu, "Measurements of gap pressure and wall shear stress of a blood pump model," *Med. Eng. Phys.*, vol. 22, no. 3, pp. 175–188, Apr. 2000, doi: 10.1016/S1350-4533(00)00027-8.
[75] S. Zhu *et al.*, "In vitro testing of an intra-ventricular assist device," *Comput. Assist. Surg.*, vol. 24, no. sup1, pp. 89–95, Oct. 2019, doi: 10.1080/24699322.2018.1560099.
[76] M. Pohl, M. O. Wendt, S. Werner, B. Koch, and D. Lerche, "In Vitro Testing of Artificial Heart Valves: Comparison Between Newtonian and Non-Newtonian Fluids," *Artif. Organs*, vol. 20, no. 1, pp. 37–46, 1996, doi: 10.1111/j.1525-1594.1996.tb04416.x.
[77] W. L. Lim, Y. T. Chew, T. C. Chew, and H. T. Low, "Pulsatile flow studies of a porcine bioprosthetic aortic valve in vitro: PIV measurements and shear-induced blood damage," *J. Biomech.*, vol. 34, no. 11, pp. 1417–1427, Nov. 2001, doi: 10.1016/S0021-9290(01)00132-4.
[78] T. T. Nguyen and, Y. Biadillah, R. Mongrain, and Brunette J., J.-C. Tardif, and O. F. Bertrand, "A Method for Matching the Refractive Index and Kinematic Viscosity of a Blood Analog for Flow Visualization in Hydraulic Cardiovascular Models," *J. Biomech. Eng.*, vol. 126, no. 4, pp. 529–535, Sep. 2004, doi: 10.1115/1.1785812.

Die approbierte gedruckte Originalversion dieser Dissertation ist an der TU Wien Bibliothek verfügbar.
The approved original version of this doctoral thesis is available in print at TU Wien Bibliothek.
TU Bibliothek Your knowledge hub WIEN

[79] S. Raz, S. Einav, Y. Alemu, and D. Bluestein, "DPIV prediction of flow induced platelet activation-comparison to numerical predictions," *Ann. Biomed. Eng.*, vol. 35, no. 4, pp. 493–504, Apr. 2007, doi: 10.1007/s10439-007-9257-2.
[80] M. Y. Yousif, D. W. Holdsworth, and T. L. Poepping, "A blood-mimicking fluid for particle image velocimetry with silicone vascular models," *Exp. Fluids*, vol. 50, no. 3, pp. 769–774, Mar. 2011, doi: 10.1007/s00348-010-0958-1.
[81] M. R. Najjari, J. A. Hinke, K. V. Bulusu, and M. W. Plesniak, "On the rheology of refractive-index-matched, non-Newtonian blood-analog fluids for PIV experiments," *Exp. Fluids*, vol. 57, no. 6, p. 96, May 2016, doi: 10.1007/s00348-016-2185-x.
[82] K. A. Brookshier and J. Tarbell, "Evaluation of Transparent Blood Analogue Fluids—Aqueous Xanthan Gum Glycerin," *Biorheology*, vol. 30, pp. 107–16, Mar. 1993, doi: 10.3233/BIR-1993-30202.
[83] J. A. Long, A. Undar, K. B. Manning, and S. Deutsch, "Viscoelasticity of pediatric blood and its implications for the testing of a pulsatile pediatric blood pump," *ASAIO J. Am. Soc. Artif. Intern. Organs 1992*, vol. 51, no. 5, pp. 563–566, Oct. 2005, doi: 10.1097/01.mat.0000180353.12963.f2.
[84] V. Deplano, Y. Knapp, L. Bailly, and E. Bertrand, "Flow of a blood analogue fluid in a compliant abdominal aortic aneurysm model: experimental modelling," *J. Biomech.*, vol. 47, no. 6, pp. 1262–1269, Apr. 2014, doi: 10.1016/j.jbiomech.2014.02.026.
[85] M. C. Brindise, M. M. Busse, and P. P. Vlachos, "Density and Viscosity Matched Newtonian and non-Newtonian Blood-Analog Solutions with PDMS Refractive Index," *Exp. Fluids*, vol. 59, no. 11, p. 173, Nov. 2018, doi: 10.1007/s00348-018-2629-6.
[86] ASTM International, *ASTM D445-17a, Standard Test Method for Kinematic Viscosity of Transparent and Opaque Liquids (and Calculation of Dynamic Viscosity)*. West Conshohocken, PA, 2017. [Online]. Available: www.astm.org
[87] J. T, T. T, S. O, S. Y, and M. T, "Species differences in erythrocyte mechanical fragility: comparison of human, bovine, and ovine cells," *ASAIO J.*, vol. 44, no. 5, pp. M452-5, Sep. 1998.
[88] J. Ding, S. Niu, Z. Chen, T. Zhang, B. Griffith, and Z. Wu, "Shear-Induced Hemolysis: Species Differences," *Artif. Organs*, vol. 39, May 2015, doi: 10.1111/aor.12459.
[89] U. Windberger, A. Bartholovitsch, R. Plasenzotti, K. J. Korak, and G. Heinze, "Whole Blood Viscosity, Plasma Viscosity and Erythrocyte Aggregation in Nine Mammalian Species: Reference Values and Comparison of Data," *Exp. Physiol.*, vol. 88, no. 3, pp. 431–440, 2003, doi: 10.1113/eph8802496.
[90] K. Tanishita, K. Nakano, Y. Sakurai, T. Hosokawa, P. D. Richardson, and P. M. Galletti, "COMPACT OXYGENATOR DESIGN WITH CURVED TUBES WOUND IN WEAVING PATTERNS," *ASAIO J.*, vol. 24, no. 1, pp. 327–331, Apr. 1978.
[91] M. S. Hout, B. G. Hattler, and W. J. Federspiel, "Validation of a Model for Flow-Dependent Carbon Dioxide Exchange in Artificial Lungs," *Artif. Organs*, vol. 24, no. 2, pp. 114–118, Feb. 2000, doi: 10.1046/j.1525-1594.2000.06465.x.
[92] W. J. Federspiel and B. G. Haulert, "Sweep Gas Flowrate and C02 Exchange in Artificial Lungs," *Artif. Organs*, vol. 20, no. 9, pp. 1050–1052, 1996, doi: https://doi.org/10.1111/j.1525-1594.1996.tb04593.x.
[93] R. G. Svitek and W. J. Federspiel, "A Mathematical Model to Predict CO2 Removal in Hollow Fiber Membrane Oxygenators," *Ann. Biomed. Eng.*, vol. 36, no. 6, pp. 992–1003, Jun. 2008, doi: 10.1007/s10439-008-9482-3.
[94] S. R. Wickramasinghe and B. Han, "Mass and momentum transfer in commercial blood oxygenators," *Desalination*, vol. 148, no. 1, pp. 227–233, Sep. 2002, doi: 10.1016/S0011-9164(02)00702-6.

Die approbierte gedruckte Originalversion dieser Dissertation ist an der TU Wien Bibliothek verfügbar.
The approved original version of this doctoral thesis is available in print at TU Wien Bibliothek.
TU Bibliothek Your knowledge hub WIEN

[95] H. Tabesh, M. H. Gholami, D. Torabi, and K. Mottaghy, "A pH-based experimental method for carbon dioxide exchange evaluation in cylindrical hollow fiber membrane oxygenators," *Asia-Pac. J. Chem. Eng.*, vol. 14, no. 4, p. e2337, 2019, doi: https://doi.org/10.1002/apj.2337.

[96] S. N. Vaslef, L. F. Mockros, R. W. Anderson, and R. J. Leonard, "Use of a Mathematical Model to Predict Oxygen Transfer Rates in Hollow Fiber Membrane Oxygenators," *ASAIO J.*, vol. 40, no. 4, p. 990, Dec. 1994.

[97] K. W. Q. Low, R. V. Loon, S. A. Rolland, and J. Sienz, "Formulation of Generalized Mass Transfer Correlations for Blood Oxygenator Design," *J. Biomech. Eng.*, vol. 139, no. 3, p. 031007, Mar. 2017, doi: 10.1115/1.4035535.

[98] B. Haddadi, C. Jordan, M. Miltner, and M. Harasek, "Membrane modeling using CFD: Combined evaluation of mass transfer and geometrical influences in 1D and 3D," *J. Membr. Sci.*, vol. 563, May 2018, doi: 10.1016/j.memsci.2018.05.040.

[99] R. Ghidossi, D. Veyret, and P. Moulin, "Computational fluid dynamics applied to membranes: State of the art and opportunities," *Chem. Eng. Process. Process Intensif.*, vol. 45, no. 6, pp. 437–454, Jun. 2006, doi: 10.1016/j.cep.2005.11.002.

[100] J. Zhang *et al.*, "Computational Study of the Blood Flow in Three Types of 3D Hollow Fiber Membrane Bundles," *J. Biomech. Eng.*, vol. 135, no. 12, pp. 121009-121009–11, Nov. 2013, doi: 10.1115/1.4025717.

[101] K. L. Gage, M. J. Gartner, G. W. Burgreen, and W. R. Wagner, "Predicting membrane oxygenator pressure drop using computational fluid dynamics," *Artif. Organs*, vol. 26, no. 7, pp. 600–607, Jul. 2002, doi: 10.1046/j.1525-1594.2002.07082.x.

[102] A. Funakubo, I. Taga, J. W. McGillicuddy, Y. Fukui, R. B. Hirschl, and R. H. Bartlett, "Flow vectorial analysis in an artificial implantable lung," *ASAIO J. Am. Soc. Artif. Intern. Organs 1992*, vol. 49, no. 4, pp. 383–387, Aug. 2003.

[103] H. Sato, I. Taga, T. Kinoshita, A. Funakubo, S. Ichiba, and N. Shimizu, "In vitro evaluation of a newly developed implantable artificial lung," *Acta Med. Okayama*, vol. 60, no. 2, pp. 113–119, Apr. 2006, doi: 10.18926/AMO/30728.

[104] J. Zhang, T. D. C. Nolan, T. Zhang, B. P. Griffith, and Z. J. Wu, "Characterization of membrane blood oxygenation devices using computational fluid dynamics," *J. Membr. Sci.*, vol. 288, no. 1, pp. 268–279, Feb. 2007, doi: 10.1016/j.memsci.2006.11.041.

[105] J. Zhang *et al.*, "Computational design and in vitro characterization of an integrated maglev pump-oxygenator," *Artif. Organs*, vol. 33, no. 10, pp. 805–817, Oct. 2009, doi: 10.1111/j.1525-1594.2009.00807.x.

[106] C. D'Onofrio *et al.*, "Three-dimensional computational model of a blood oxygenator reconstructed from micro-CT scans," *Med. Eng. Phys.*, vol. 47, pp. 190–197, Sep. 2017, doi: 10.1016/j.medengphy.2017.06.035.

[107] G. A. Fimbres-Weihs and D. E. Wiley, "Review of 3D CFD modeling of flow and mass transfer in narrow spacer-filled channels in membrane modules," *Chem. Eng. Process. Process Intensif.*, vol. 49, no. 7, pp. 759–781, Jul. 2010, doi: 10.1016/j.cep.2010.01.007.

[108] D. B. Dzhonova-Atanasova, I. H. Tsibranska, and S. P. Paniovska, "CFD Simulation of Cross-Flow Filtration," *Chem. Eng. Trans.*, vol. 70, pp. 2041–2046, Aug. 2018, doi: 10.3303/CET1870341.

[109] A. R. Mazaheri and G. Ahmadi, "Uniformity of the Fluid Flow Velocities Within Hollow Fiber Membranes of Blood Oxygenation Devices," *Artif. Organs*, vol. 30, no. 1, pp. 10–15, 2006, doi: 10.1111/j.1525-1594.2006.00150.x.

Die approbierte gedruckte Originalversion dieser Dissertation ist an der TU Wien Bibliothek verfügbar.
The approved original version of this doctoral thesis is available in print at TU Wien Bibliothek.
TU Bibliothek Your knowledge hub WIEN

[110] M. Hormes, R. Borchardt, I. Mager, T. S. Rode, M. Behr, and U. Steinseifer, "A validated CFD model to predict O_2 and CO_2 transfer within hollow fiber membrane oxygenators," *Int. J. Artif. Organs*, vol. 34, no. 3, pp. 317–325, Mar. 2011.
[111] A. Kaesler, M. Rosen, T. Schmitz-Rode, U. Steinseifer, and J. Arens, "Computational Modeling of Oxygen Transfer in Artificial Lungs," *Artif. Organs*, vol. 42, no. 8, pp. 786–799, 2018, doi: 10.1111/aor.13146.
[112] J. L. C. Santos, V. Geraldes, S. Velizarov, and J. G. Crespo, "Investigation of flow patterns and mass transfer in membrane module channels filled with flow-aligned spacers using computational fluid dynamics (CFD)," *J. Membr. Sci.*, vol. 1–2, no. 305, pp. 103–117, 2007, doi: 10.1016/j.memsci.2007.07.036.
[113] M. E. Taskin, K. H. Fraser, T. Zhang, B. P. Griffith, and Z. J. Wu, "Micro-scale Modeling of Flow and Oxygen Transfer in Hollow Fiber Membrane Bundle," *J. Membr. Sci.*, vol. 362, no. 1–2, pp. 172–183, Oct. 2010, doi: 10.1016/j.memsci.2010.06.034.
[114] H. Levene, in *In Contributions to Probability and Statistics: Essays in Honor of Harold Hotelling, I. Olkin et al. eds.*, Stanford University Press, 1960, pp. 278–292.
[115] B. Derrick, D. Toher, and P. White, "Why Welch's test is Type I error robust," *Quant. Methods Psychol.*, vol. 12, no. 1, Jan. 2016, Accessed: Jan. 14, 2021. [Online]. Available: https://uwe-repository.worktribe.com/output/915692
[116] P. A. Games and J. F. Howell, "Pairwise Multiple Comparison Procedures with Unequal N's and/or Variances: A Monte Carlo Study," *J. Educ. Stat.*, vol. 1, no. 2, pp. 113–125, 1976, doi: 10.2307/1164979.
[117] P. I. Energy And Environment, W. Y. Tey, Y. Asako, N. A. Che Sidik, and G. Rui-Zher, "Governing Equations in Computational Fluid Dynamics: Derivations and A Recent Review," Jun. 2017.
[118] B. van Leer, "Towards the ultimate conservative difference scheme. II. Monotonicity and conservation combined in a second-order scheme," *J. Comput. Phys.*, vol. 14, no. 4, pp. 361–370, Mar. 1974, doi: 10.1016/0021-9991(74)90019-9.
[119] J. Tu, G.-H. Yeoh, and C. Liu, "Chapter 4 - CFD Mesh Generation: A Practical Guideline," in *Computational Fluid Dynamics (Third Edition)*, J. Tu, G.-H. Yeoh, and C. Liu, Eds. Butterworth-Heinemann, 2018, pp. 125–154. doi: 10.1016/B978-0-08-101127-0.00004-0.
[120] A. Katz and V. Sankaran, "Mesh quality effects on the accuracy of CFD solutions on unstructured meshes," *J. Comput. Phys.*, vol. 230, no. 20, pp. 7670–7686, Aug. 2011, doi: 10.1016/j.jcp.2011.06.023.
[121] P. J. Roache, "Perspective: A Method for Uniform Reporting of Grid Refinement Studies," *J. Fluids Eng.*, vol. 116, no. 3, pp. 405–413, Sep. 1994, doi: 10.1115/1.2910291.
[122] J. H. Ferziger and M. Peric, *Numerische Strömungsmechanik*. Springer Berlin Heidelberg, 2008.
[123] B. M. Johnston, P. R. Johnston, S. Corney, and D. Kilpatrick, "Non-Newtonian blood flow in human right coronary arteries: steady state simulations," *J. Biomech.*, vol. 37, no. 5, pp. 709–720, May 2004, doi: 10.1016/j.jbiomech.2003.09.016.
[124] J. A. Loeppky, U. C. Luft, and E. R. Fletcher, "Quantitative description of whole blood CO2 dissociation curve and Haldane effect," *Respir. Physiol.*, vol. 51, no. 2, pp. 167–181, Feb. 1983, doi: 10.1016/0034-5687(83)90038-5.
[125] National Institute of Standards and Technology, "Isobaric Properties for Water," *NIST Chemistry WebBook*. https://webbook.nist.gov/cgi/fluid.cgi?P=1&TLow=20&THigh=40&TInc=1&Applet=on&Dig-

Die approbierte gedruckte Originalversion dieser Dissertation ist an der TU Wien Bibliothek verfügbar.
The approved original version of this doctoral thesis is available in print at TU Wien Bibliothek.
TU Bibliothek Your knowledge hub WIEN

its=5&ID=C7732185&Action=Load&Type=IsoBar&TUnit=C&PUnit=bar&DUnit=kg%2Fm3&HUnit=kJ%2Fkg&WUnit=m%2Fs&VisUnit=Pa*s&STUnit=N%2Fm&RefState=DEF (accessed Dec. 10, 2020).

[126] R. Sander, "Compilation of Henry's law constants (version 4.0) for water as solvent," *Atmospheric Chem. Phys.*, vol. 15, no. 8, pp. 4399–4981, Apr. 2015, doi: 10.5194/acp-15-4399-2015.

[127] D. M. Himmelblau, "Diffusion of Dissolved Gases in Liquids," *Chem. Rev.*, vol. 64, no. 5, pp. 527–550, Oct. 1964, doi: 10.1021/cr60231a002.

[128] J. Kestin, J. V. Sengers, B. Kamgar-Parsi, and J. M. H. Levelt Sengers, "Thermophysical Properties of Fluid H2O," *J. Phys. Chem. Ref. Data*, vol. 13, no. 1, pp. 175–183, 1984.

[129] W. Wagner and A. Pruss, "The IAPWS formulation 1995 for the thermodynamic properties of ordinary water substance for general and scientific use," *J. Phys. Chem. Ref. Data*, vol. 31, no. 2, pp. 387–535, 2002.

[130] W. Wagner and A. Pruß, "The IAPWS Formulation 1995 for the Thermodynamic Properties of Ordinary Water Substance for General and Scientific Use," *J. Phys. Chem. Ref. Data*, vol. 31, no. 2, pp. 387–535, Jun. 2002, doi: 10.1063/1.1461829.

[131] J. Kestin, J. V. Sengers, B. Kamgar-Parsi, and J. M. H. L. Sengers, "Thermophysical Properties of Fluid H2O," *J. Phys. Chem. Ref. Data*, vol. 13, no. 1, pp. 175–183, Jan. 1984, doi: 10.1063/1.555707.

[132] W. Sutherland, "The viscosity of gases and molecular force," *Lond. Edinb. Dublin Philos. Mag. J. Sci.*, vol. 36, no. 223, pp. 507–531, Dec. 1983, doi: 10.1080/14786449308620508.

[133] T. R. Marrero and E. A. Mason, "Gaseous Diffusion Coefficients," *J. Phys. Chem. Ref. Data*, vol. 1, no. 1, pp. 3–118, Jan. 1972, doi: 10.1063/1.3253094.

[134] F. J. Walburn and D. J. Schneck, "A constitutive equation for whole human blood," *Biorheology*, vol. 13, no. 3, pp. 201–210, Jun. 1976, doi: 10.3233/bir-1976-13307.

[135] D. Eckmann, S. Bowers, M. Stecker, and A. Cheung, "Hematocrit, Volume Expander, Temperature, and Shear Rate Effects on Blood Viscosity," *Anesth. Analg.*, vol. 91, pp. 539–45, Oct. 2000, doi: 10.1097/00000539-200009000-00007.

[136] A. S. Abednejad, G. Amoabediny, and A. Ghaee, "Surface modification of polypropylene membrane by polyethylene glycol graft polymerization," *Mater. Sci. Eng. C*, vol. 42, pp. 443–450, Sep. 2014, doi: 10.1016/j.msec.2014.05.060.

[137] C. Dornia *et al.*, "Analysis of thrombotic deposits in extracorporeal membrane oxygenators by multidetector computed tomography," *ASAIO J. Am. Soc. Artif. Intern. Organs 1992*, vol. 60, no. 6, pp. 652–656, Dec. 2014, doi: 10.1097/MAT.0000000000000133.

[138] M. J. Gartner, C. R. Wilhelm, K. L. Gage, M. C. Fabrizio, and W. R. Wagner, "Modeling Flow Effects on Thrombotic Deposition in a Membrane Oxygenator," *Artif. Organs*, vol. 24, no. 1, pp. 29–36, 2000, doi: 10.1046/j.1525-1594.2000.06384.x.

[139] T. He, J. He, Z. Wang, and Z. Cui, "Modification strategies to improve the membrane hemocompatibility in extracorporeal membrane oxygenator (ECMO)," *Adv. Compos. Hybrid Mater.*, May 2021, doi: 10.1007/s42114-021-00244-x.

[140] O. Siggaard-Andersen, P. D. Wimberley, N. Fogh-Andersen, and I. H. Gøthgen, "Measured and derived quantities with modern pH and blood gas equipment: Calculation algorithms with 54 equations," *Scand. J. Clin. Lab. Invest.*, vol. 48, no. sup189, pp. 7–15, Jan. 1988, doi: 10.1080/00365518809168181.

[141] J. R. Zierenberg, H. Fujioka, R. B. Hirschl, R. H. Bartlett, and J. B. Grotberg, "Oxygen and carbon dioxide transport in time-dependent blood flow past fiber rectangular arrays," *Phys. Fluids*, vol. 21, no. 3, p. 033101, Mar. 2009, doi: 10.1063/1.3056413.

Die approbierte gedruckte Originalversion dieser Dissertation ist an der TU Wien Bibliothek verfügbar.
The approved original version of this doctoral thesis is available in print at TU Wien Bibliothek.
TU Bibliothek Your knowledge hub WIEN

[142] R. Koller, *Suitability of water as a blood model for the quantitative determination of the CO2 separation rate of membrane oxygenators*. Wien: Wien, 2021. [Online]. Available: https://permalink.catalogplus.tuwien.at/AC16191912

Die approbierte gedruckte Originalversion dieser Dissertation ist an der TU Wien Bibliothek verfügbar.
The approved original version of this doctoral thesis is available in print at TU Wien Bibliothek.
TU Bibliothek Your knowledge hub WIEN

Appended Publications

Die approbierte gedruckte Originalversion dieser Dissertation ist an der TU Wien Bibliothek verfügbar.
The approved original version of this doctoral thesis is available in print at TU Wien Bibliothek.
TU Bibliothek Your knowledge hub WIEN

Journal Publication I

Fully resolved computational (CFD) and experimental analysis of pressure drop and blood gas transport in a hollow fibre membrane oxygenator module.

Harasek, M., Lukitsch, B., Ecker, P., Janeczek, C., Elenkov, M., Keck, T., Haddadi, B., Jordan, C., Neudl, S., Krenn, C., Ullrich, R., & Gfoehler, M.

Chemical Engineering Transactions ***2019***, *76*, 193–198.

DOI: 10.3303/CET1976033

Die approbierte gedruckte Originalversion dieser Dissertation ist an der TU Wien Bibliothek verfügbar.
The approved original version of this doctoral thesis is available in print at TU Wien Bibliothek.
TU Bibliothek Your knowledge hub WIEN

Journal Publication II

Computation of global and local mass transfer in hollow fiber membrane modules.

Lukitsch, B., Ecker, P., Elenkov, M., Janeczek, C., Haddadi, B., Jordan, C., Krenn, C., Ullrich, R., Gfoehler, M., Harasek, M.

Sustainability ***2020***.

DOI: 10.3390/su12062207

Die approbierte gedruckte Originalversion dieser Dissertation ist an der TU Wien Bibliothek verfügbar.
The approved original version of this doctoral thesis is available in print at TU Wien Bibliothek.
TU Bibliothek Your knowledge hub WIEN

Journal Publication III

Estimation methods for viscosity, flow rate and pressure from pump-motor assembly parameters.

Elenkov, M., Ecker, P., Lukitsch, B., Janeczek, C., Harasek, M., Gföhler, M.

Sensors ***2020***.

DOI: 10.3390/s20051451

Die approbierte gedruckte Originalversion dieser Dissertation ist an der TU Wien Bibliothek verfügbar.
The approved original version of this doctoral thesis is available in print at TU Wien Bibliothek.
TU Bibliothek Your knowledge hub WIEN

Journal Publication IV

Non-parametric dynamical estimation of blood flow rate, pressure difference and viscosity for a miniaturized blood pump.

Elenkov, M., Lukitsch, B., Ecker, P., Janeczek, C., Harasek, M., Gföhler, M.

International Journal of Artificial Organs ***2021***.

DOI: 10.1177/03913988211006720

Die approbierte gedruckte Originalversion dieser Dissertation ist an der TU Wien Bibliothek verfügbar.
The approved original version of this doctoral thesis is available in print at TU Wien Bibliothek.
TU Bibliothek Your knowledge hub WIEN

Journal Publication V

Microstructured hollow fiber membranes: Potential fiber shapes for extracorporeal membrane oxygenators.

Ecker, P., Pekovits, M., Yorov, T., Haddadi, B., Lukitsch, B., Elenkov, M., Janeczek, C., Jordan, C., Gfoehler, M., Harasek, M.

Membranes ***2021***.

DOI: 10.3390/membranes11050374

Die approbierte gedruckte Originalversion dieser Dissertation ist an der TU Wien Bibliothek verfügbar.
The approved original version of this doctoral thesis is available in print at TU Wien Bibliothek.
TU Bibliothek Your knowledge hub WIEN

Journal Publication VI

Suitable CO_2 solubility models for determination of the CO_2 removal performance of oxygenators.

Lukitsch, B., Ecker, P., Elenkov, M., Janeczek, C., Jordan, C., Krenn, C.G., Ullrich, R., Gfoehler, M., Harasek, M.

Bioengineering ***2021***.

DOI: 10.3390/bioengineering8030033

Die approbierte gedruckte Originalversion dieser Dissertation ist an der TU Wien Bibliothek verfügbar.
The approved original version of this doctoral thesis is available in print at TU Wien Bibliothek.
TU Bibliothek Your knowledge hub WIEN

Journal Publication VII

Animal blood in translational research: How to adjust animal blood viscosity to the human standard.

Ecker, P., Sparer, A., Lukitsch, B., Elenkov, M., Seltenhammer, M., Crevenna, R., Gföhler, M., Harasek, M., Windberger, U.

Physiological Reports ***2021***.

DOI: 10.14814/phy2.14880

Die approbierte gedruckte Originalversion dieser Dissertation ist an der TU Wien Bibliothek verfügbar.
The approved original version of this doctoral thesis is available in print at TU Wien Bibliothek.
TU Bibliothek Your knowledge hub WIEN

Journal Publication VIII

Water as a blood model for determination of CO_2 removal performance of membrane oxygenators.

Lukitsch, B., Koller, R., Ecker, P., Elenkov, M., Janeczek, C., Pekovits, M., Haddadi, B., Jordan, C., Gfoehler, M., Harasek, M.

Membranes ***2021***.

DOI: 10.3390/membranes11050356

Die approbierte gedruckte Originalversion dieser Dissertation ist an der TU Wien Bibliothek verfügbar.
The approved original version of this doctoral thesis is available in print at TU Wien Bibliothek.
TU Bibliothek Your knowledge hub WIEN

Reviewed Conference Publication I

Basic performance tests of the MILL intravascular CO_2 removal catheter.

Janeczek, C., Lukitsch, B., Huber-Dangl, F., Karabegovic, A., Jordan, C., Haddadi, B., Ullrich, R., Krenn, C., Gfoehler, M., Harasek, M.

Proceedings of the Annual International Conference of the IEEE Engineering in Medicine and Biology Society, EMBS ***2018***.

DOI: 10.1109/EMBC.2018.8512522

Die approbierte gedruckte Originalversion dieser Dissertation ist an der TU Wien Bibliothek verfügbar.
The approved original version of this doctoral thesis is available in print at TU Wien Bibliothek.
TU Bibliothek Your knowledge hub WIEN

List of Figures

Figure 1.1. Schematic overview of devices for oxygenator based CO_2 removal 4
Figure 1.2. Overview of experimental methods used for the development of oxygenators 9
Figure 1.3. Scheme for sweep flow- and blood-based CO_2 removal rate prediction method 10
Figure 1.4. Overview of CFD models used for the development of oxygenators 16
Figure 2.1. Prototype oxygenator 17
Figure 2.2. Scheme of pure gas permeation measurement. 18
Figure 2.3. Scheme of in vitro water tests. 19
Figure 2.4. Scheme of in vitro bovine blood tests. Oxygenator. 20
Figure 2.5. Scheme of in vivo porcine blood tests. 21
Figure 2.6. Prototype of the minimal invasive liquid lung (MILL) 23
Figure 2.7. Flow distribution test setup 24
Figure 2.8. Scheme of the viscosity estimation tests. 24
Figure 2.9. The geometry of the prototype oxygenator investigated 27
Figure 2.10. Coarse, medium, and fine computational mesh of a single hollow fiber membrane 28
Figure 2.11. Mesh for validation of the flow field via µPIV-Measurement data. 28
Figure 2.12. Workflow of the solving algorithm 29
Figure 2.13. Packing geometry 30
Figure 2.14. Workflow of the upscaling method. 31
Figure 2.15. Shear rate dependency of the whole blood viscosity of porcine blood. 31
Figure 4.1. Comparison of pump characteristics measured with water-glycerol and bovine blood 43
Figure 4.2. Comparison of experimentally determined CO_2 removal. 44
Figure 4.3. Shear rate dependency of whole blood viscosity (WBV) at physiological conditions 45
Figure 4.4. Comparison of experimentally determined CO_2 removal rate 46
Figure 4.5. Increase in CO_2 permeance during the follow-up gas permeation measurements. 47
Figure 4.6. Average prediction error of the different CO_2 solubility models 49
Figure 4.7. Average prediction error of the different solubility models 50
Figure 4.8. CFD mass transport simulations of a simplified geometry 51
Figure 4.9. Dependency of transmembrane CO_2 flux on permeance. Determined via CFD for water 52
Figure 4.10. Comparison of CO_2 removal determined with experiments and CFD simulations 53
Figure 4.11. Exemplary boundary profiles of CO_2 partial pressure 54
Figure 4.12. Dependency of boundary layer thickness 55
Figure 4.13. Sherwood correlations for porcine blood and water 55
Figure 4.14. Influence of CO_2 diffusion, CO_2 permeance CO_2 solubility, and viscosity model 56

Die approbierte gedruckte Originalversion dieser Dissertation ist an der TU Wien Bibliothek verfügbar.
The approved original version of this doctoral thesis is available in print at TU Wien Bibliothek.
TU Bibliothek Your knowledge hub WIEN

List of Tables

Table 1.1. Overview of the intravascular respiratory catheter. 5
Table 1.2. Overview of arteriovenous (AV) paracorporeal CO_2 removal devices. 6
Table 1.3. Overview of venovenous (VV) extracorporeal CO_2 removal (ECR) devices. 7
Table 2.1. Summary of material parameters required for the total diffusion coefficient ($D_{CO2,total}$). 33
Table 2.2. Summary of water material properties. 33
Table 4.1. Comparison of root mean square errors (RMSE) of the estimated parameters 43
Table 4.2. Overview of the five microstructured fiber shapes investigated. 57
Table 4.3. Comparison of the expected and actual component flux increase. 57

Die approbierte gedruckte Originalversion dieser Dissertation ist an der TU Wien Bibliothek verfügbar.
The approved original version of this doctoral thesis is available in print at TU Wien Bibliothek.
TU Bibliothek Your knowledge hub WIEN

List of Symbols

Latin Symbols

A	Membrane surface
a	Empirical parameter of Sherwood correlation
A_s	Empirical parameter of Sutherland's formula
b	Empirical parameter of Sherwood correlation
c_{CO2}	Concentration of physical dissolved CO_2
c_{CO2}	CO_2 concentration
$c_{CO2,b}$	Bulk flow value of CO_2 concentration
$c_{CO2,total}$	Total CO_2 concentration
c_{HCO3-}	Concentration of bicarbonate
c_i	Concentration of species i
c_p	Specific heat capacity
$c_{p,i}$	Specific heat capacity of species i
d	Characteristic length
D_{CO2}	Diffusion coefficient of physically dissolved CO_2
D_{CO2}	CO_2 diffusion coefficient
$D_{CO2,total}$	Total CO_2 diffusion coefficient of all CO_2 species
$D_{CO2,w}$	Diffusion coefficient of CO_2 in water
D_{eff}	Effective diffusion coefficient
D_f	Facilitated diffusion coefficient
d_{fiber}	Fiber diameter
D_{HCO3-}	Diffusion coefficient of bicarbonate
D_i	Diffusion coefficient species i
$H_{CO2,w}$	Henry´s law constant for CO_2 in water
H_i	Henry coefficient (solubility) of species i
j_{CO2}	Transmembrane CO_2 flux
k	Thermal conductivity
k_{CO2}	CO_2 mass transfer coefficient
n	Empirical parameter for power-law viscosity model of blood
n	Orthogonal vector component of the membrane wall
p	Pressure
p_{CO2}	CO_2 partial pressure
P_i	Permeance of species i
p_i	Partial pressure of species i
q	Empirical parameter of the Loeppky model (multiplier)
$\dot{Q}_{blood}$	Blood flow rate
$\dot{Q}_{CO2,blood}$	Blood-based CO_2 removal rate
$\dot{Q}_{sweep}$	Sweep gas-based CO_2 removal rate
$\dot{Q}_{sweep}$	Sweep flow rate
Re	Dimensionless Reynolds number
Sc	Dimensionless Schmidt number
Sh	Dimensionless Sherwood number
$S_{i,j}$	Ideal selectivity
S_m	Total transmembrane flux
$S_{m,i}$	Transmembrane flux of species i
T	Temperature
t	Empirical parameter of the Loeppky model (exponent)
T_s	Empirical parameter of Sutherland's formula
$\mathbf{u}$	Fluid velocity vector
V	Volume of cell of computational grid
$\dot{V}$	Permeate flow

Die approbierte gedruckte Originalversion dieser Dissertation ist an der TU Wien Bibliothek verfügbar.
The approved original version of this doctoral thesis is available in print at TU Wien Bibliothek.
TU Bibliothek Your knowledge hub WIEN

x_i	Mole fraction of species i
Y_i	Mass fraction of species i

Greek Symbols

α_{CO2}	Solubility of physically dissolved CO_2
$\dot{\gamma}$	Shear rate
$\Delta c_{CO2,blood}$	CO_2 concentration difference in blood flow
$\Delta c_{CO2,sweep}$	CO_2 concentration difference in the sweep flow
$\Delta h_{cond,i}$	Specific condensation enthalpy of species i
Δp	Pressure difference across the membrane
Δp_i	Partial pressure difference across the membrane
ε	Relative deviation of blood-based from sweep flow-based CO_2 removal rate
$\bar{\varepsilon}$	average prediction error
λ_{CO2}	Derivation of the total CO_2 concentration of blood by the partial pressure
μ	Dynamic viscosity
μ_0	Empirical parameter for power-law viscosity model of blood
μ_i	Dynamic viscosity of species i
μ_{max}	Newtonian viscosity at high shear rates for power-law viscosity model of blood
μ_{min}	Numerical limiter at low shear rates for power-law viscosity model of blood
μ_w	Dynamic viscosity of water
ν_{blood}	Kinematic viscosity of blood
ρ	Density
ρ_w	Density of water

Die approbierte gedruckte Originalversion dieser Dissertation ist an der TU Wien Bibliothek verfügbar.
The approved original version of this doctoral thesis is available in print at TU Wien Bibliothek.
TU Bibliothek Your knowledge hub WIEN

List of Abbreviations

Acronym	Description
AL	Artificial lung
ARDS	Acute respiratory distress syndrome
AV	Arteriovenous
AVCO2R	Arteriovenous carbon dioxide removal
BGA	Blood gas analyzer
CFD	Computational fluid dynamics
CO_2	Carbon dioxide
COPD	Chronic obstructive pulmonary disease
ECCO2R	Extracorporeal carbon dioxide removal
ECMO	Extracorporeal membrane oxygenation
GCI	Grid convergence index
LPV	Lung protective ventilation
LVAD	Left ventricular assist device
MFC	Mass flow controller
MILL	Minimal invasive liquid lung
N_2	Nitrogen
NDIR	Nondispersive infrared sensor
NO	Nitric oxide
O_2	Oxygen
PBS	Phosphate-buffered solution
PCV	Packed cell volume
PDMS	Polydimethylsiloxane
PISO	Pressure-Implicit with Splitting of Operators
PIV	Particle image velocimetry
PMP	Polymethylpentene
PP	Polypropylene
PR	Pressure registration
RBC	Red blood cells
RMSE	Root mean square error
STP	Standard temperature and pressure (273.15 K, 1 bar)
VA	Venoarterial
VV	Venovenous
WBV	Whole blood viscosity

Die approbierte gedruckte Originalversion dieser Dissertation ist an der TU Wien Bibliothek verfügbar.
The approved original version of this doctoral thesis is available in print at TU Wien Bibliothek.
TU Bibliothek Your knowledge hub WIEN

Benjamin Lukitsch

Date of birth: 02/03/1991 | **Nationality:** Austrian | **Gender:** Male | (+43) 6647942045 |

benjamin.lukitsch@gmx.at | Neustiftgasse 31/33, 1070, Vienna, Austria

WORK EXPERIENCE

01/07/2017 – CURRENT – Vienna, Austria

SCIENTIFIC EMPLOYEE - PROJECT ASSISTANT – INSTITUTE OF CHEMICAL, ENVIRONMENTAL AND BIOSCIENCE ENGINEERING, TU WIEN

As a scientific project assistant, I was responsible for the successful execution of two projects:

Development of an intracorporeal artificial lung

- Development of a computational fluid dynamic (CFD) simulation platform for a detailed in silico performance evaluation of the artificial lung (oxygenators).
- Modeling of species and hydrodynamic transport in the membrane packing of the oxygenator.
- Validation of the CFD platform and the models used via in vitro and in vivo experiments.
- Preparation and execution of the CFD simulations on high-performance computers.
- Evaluation and documentation of the CFD simulation results.

Planning and construction of a spinning plant for hollow fiber membranes with biomedical applications

- Design and planning of the spinning plant and the production plant for the preparation of the polymer solution (dope fluid).
- Commissioning of the plant.
- Production and testing of the hollow fiber membranes with regard to gas separation and ultrafiltration properties.

Dissemination of research results in journals and conferences. Compilation of project reports for funding agencies.

Biofluids Lab | Engineering Solutions for Organ Support | https://biofluidslab.tuwien.ac.at/mission/

01/11/2017 – 31/03/2020 – Vienna, Austria

DEVELOPMENT ENGINEER – CCORE TECHNOLOGY GMBH

Development of an intracorporeal artificial lung

- Conception, design, and construction of an intracorporeal artificial lung.
- Conception and planning of in vitro and in vivo tests to determine the carbon dioxide removal and oxygen supply of the intracorporeal artificial lung.
- Coordination and implementation of the tests described above at the Center for Biomedical Research at MedUni Vienna.
- Measurement data validation, evaluation, statistical analysis, and documentation of the test results.

CCCORE Technology | Minimally Invasive Blood Purification | https://ccore.at/en/home/

01/03/2015 – 30/06/2015 – Vienna, Austria

TUTOR – INSTITUTE FOR FLUID MECHANICS AND HEAT TRANSFER, TU WIEN

- Lecturing the fundamentals of fluid mechanics.
- Correcting exams.
- Conducting office hours and exam inspections.

01/03/2014 – 30/06/2014 – Vienna, Austria

TUTOR – INSTITUTE FOR FLUID MECHANICS AND HEAT TRANSFER, TU WIEN

- Lecturing the fundamentals of fluid mechanics.
- Correcting exams.
- Conducting office hours and exam inspections.

Die approbierte gedruckte Originalversion dieser Dissertation ist an der TU Wien Bibliothek verfügbar.
The approved original version of this doctoral thesis is available in print at TU Wien Bibliothek.
TU Bibliothek Your knowledge hub WIEN

01/07/2013 – 31/07/2013 – Vienna, Austria
PRODUCTION ENGINEER – HOERBIGER WIEN GMBH

- Adaptation of construction plans to enable more efficient machining.
- Inventory of production machinery for a relocation of the production facility.

EDUCATION AND TRAINING

01/08/2017 – CURRENT – Vienna, Austria
DOCTORAL PROGRAM - CHEMICAL ENGINEERING – TU Wien

Research and development of membrane oxygenators (artificial lungs)

The transport resistance for the respiratory gas exchange of artificial lungs is mainly characterized by the diffusive resistance in the boundary layer at the membrane. The resistance cannot be resolved experimentally. However, computational fluid dynamic (CFD) models developed in the course of my doctoral degree provide a detailed insight into the mass transfer problem and allow the diffusive resistance to be resolved. The model was experimentally validated. Design changes based on the simulations were tested in vitro.

Supervision: *Ao.Univ.Prof. Dipl.-Ing. Dr.techn. Micheal Harasek*

Field of study:

- Biomedical engineering
- Chemical engineering

01/10/2014 – 31/07/2017 – Vienna, Austria
MASTER OF SCIENCE - CHEMICAL ENGINEERING – TU Wien

Automated optimization on the basis of flow simulation
Computational fluid dynamics allows a detailed investigation of technical processes and thus provides a sound basis for process optimization. In the course of my master thesis, I developed a license-free framework that allows an automated optimization of process parameters based on flow simulations. Specifically, the optimization algorithm was developed to adjust the parameters of a turbulence model for the effective computation of convective heat transport.

https://repositum.tuwien.at/handle/20.500.12708/9815

Supervision: *Univ.Prof. Dipl.-Ing. Dr.techn. Jens-Uwe Repke*

Field of study:

- Chemical engineering

01/09/2010 – 30/09/2014 – Vienna, Austria
BACHELOR OF SCIENCE - CHEMICAL ENGINEERING – TU Wien

Parameter study of a fluid catalytic cracking plant

In the course of my bachelor thesis, I experimentally investigated the influence of process parameters on the product quality of a fluid catalytic cracking plant.

Supervision: *Ass.Prof. Dipl.-Ing. Dr.techn. Alexander Reichhold*

Field of study:

- Chemical engineering

Die approbierte gedruckte Originalversion dieser Dissertation ist an der TU Wien Bibliothek verfügbar.
The approved original version of this doctoral thesis is available in print at TU Wien Bibliothek.
TU Bibliothek Your knowledge hub WIEN

LANGUAGE SKILLS

Mother tongue(s): **GERMAN**

Other language(s):

	UNDERSTANDING		SPEAKING		WRITING
	Listening	Reading	Spoken production	Spoken interaction	
ENGLISH	C2	C2	C1	C1	C2

Levels: A1 and A2: Basic user; B1 and B2: Independent user; C1 and C2: Proficient user

DIGITAL SKILLS

Computational Fluid Dynamics (CFD)

OpenFOAM | Paraview | cfMesh | Gambit | SnappyHexMesh | Species distribution modeling | Turbulence modeling | Reaction modeling

Programming languages

C++ | Python | bash-script | MATLAB | VBA (Office)

Other

Microsoft Office | Catia V5 | Linux user-level | Good knowledge of graphic software (Gimp)

PUBLICATIONS

Animal blood in translational research: How to adjust animal blood viscosity to the human standard

https://www.ncbi.nlm.nih.gov/pmc/articles/PMC8157792/ – 2021
Ecker, P., Sparer, A., Lukitsch, B., Elenkov, M., Seltenhammer, M., Crevenna, R., Gföhler, M., Harasek, M., & Windberger, U. (2021). Animal blood in translational research: How to adjust animal blood viscosity to the human standard. *Physiological reports*, *9*(10), e14880. https://doi.org/10.14814/phy2.14880

Water as a blood model for determination of CO2 removal performance of membrane oxygenators

https://www.mdpi.com/2077-0375/11/5/356 – 2021
Lukitsch, B., Koller, R., Ecker, P., Elenkov, M., Janeczek, C., Pekovits, M., Haddadi, B., et al. (2021). Water as a Blood Model for Determination of CO2 Removal Performance of Membrane Oxygenators. *Membranes*, *11*(5), 356. MDPI AG. https://doi.org/10.3390/membranes11050356

Suitable CO2 Solubility Models for Determination of the CO2 Removal Performance of Oxygenators

https://www.mdpi.com/2306-5354/8/3/33 – 2021
Lukitsch, B., Ecker, P., Elenkov, M., Janeczek, C., Jordan, C., Krenn, C. G., Ullrich, R., et al. (2021). Suitable CO2 Solubility Models for Determination of the CO2 Removal Performance of Oxygenators. *Bioengineering*, *8*(3), 33. MDPI AG. https://doi.org/10.3390/bioengineering8030033

Die approbierte gedruckte Originalversion dieser Dissertation ist an der TU Wien Bibliothek verfügbar.
The approved original version of this doctoral thesis is available in print at TU Wien Bibliothek.
TU Bibliothek Your knowledge hub WIEN

Non-parametric dynamical estimation of blood flow rate, pressure difference and viscosity for a miniaturized blood pump

https://pubmed.ncbi.nlm.nih.gov/34399589/ – 2021
Elenkov, M., Lukitsch, B., Ecker, P., Janeczek, C., Harasek, M., & Gföhler, M. (2021). Non-parametric dynamical estimation of blood flow rate, pressure difference and viscosity for a miniaturized blood pump. The International Journal of Artificial Organs. https://doi.org/10.1177/03913988211006720

Microstructured Hollow Fiber Membranes: Potential Fiber Shapes for Extracorporeal Membrane Oxygenators

https://www.mdpi.com/2077-0375/11/5/374 – 2021
Ecker, P., Pekovits, M., Yorov, T., Haddadi, B., Lukitsch, B., Elenkov, M., Janeczek, C., et al. (2021). Microstructured Hollow Fiber Membranes: Potential Fiber Shapes for Extracorporeal Membrane Oxygenators. *Membranes*, *11*(5), 374. MDPI AG. https://doi.org/10.3390/membranes11050374

Computation of Global and Local Mass Transfer in Hollow Fiber Membrane Modules

https://www.mdpi.com/2071-1050/12/6/2207 – 2020
Lukitsch, B., Ecker, P., Elenkov, M., Janeczek, C., Haddadi, B., Jordan, C., Krenn, C., et al. (2020). Computation of Global and Local Mass Transfer in Hollow Fiber Membrane Modules. *Sustainability*, *12*(6), 2207. MDPI AG. https://doi.org/10.3390/su12062207

Fully Resolved Computational (CFD) and Experimental Analysis of Pressure Drop and Blood Gas Transport in a Hollow Fibre Membrane Oxygenator Module

https://www.cetjournal.it/index.php/cet/article/view/CET1976033 – 2019
Harasek, M., Lukitsch, B., Ecker, P., Janeczek, C., Elenkov, M., Keck, T., Haddadi, B., Jordan, C., Neudl, S., Krenn, C., Ullrich, R., & Gfoehler, M. (2019). Fully Resolved Computational (CFD) and Experimental Analysis of Pressure Drop and Blood Gas Transport in a Hollow Fibre Membrane Oxygenator Module. *Chemical Engineering Transactions*, *76*, 193-198. https://doi.org/10.3303/CET1976033

CONFERENCES AND SEMINARS

03/09/2019 – 07/09/2019 – Hannover, Germany
46th Annual Congress of the European Society for Artificial Organs (ESAO)

Fully Resolved CFD Simulation of the CO_2 Transport in a Hollow Fiber Membrane Oxygenator Packing

12/09/2018 – 15/09/2018 – Madrid, Spain
45th Annual Congress of the European Society for Artificial Organs (ESAO)

CFD Simulation of Blood Gas Transport in a Hollow Fiber Membrane Packing for Design Optimization of an Intracorporeal Membrane Oxygenator

15/11/2018 – 15/11/2018 – Vienna, Austria
17th Austrian OpenFOAM User Meeting (PFAU)

Challenges in Simulation of Blood Gas Transport in Hollow Fiber Membrane Oxygenators

DRIVING LICENCE

Driving Licence: B

Die approbierte gedruckte Originalversion dieser Dissertation ist an der TU Wien Bibliothek verfügbar.
The approved original version of this doctoral thesis is available in print at TU Wien Bibliothek.

VOLUNTEERING

01/09/2010 – 30/07/2016
Care for the Disabled - Visiting Service

Vienna, Austria
I made monthly day trips with a mentally disabled resident of an assisted living facility for six years.

Die approbierte gedruckte Originalversion dieser Dissertation ist an der TU Wien Bibliothek verfügbar.
The approved original version of this doctoral thesis is available in print at TU Wien Bibliothek.